PROPERTIES OF RECOMBINED MILK PROTEIN COMPOSITE GELS: EFFECTS OF PROTEIN SOURCE, PROTEIN CONCENTRATION AND PROCESSING TIME

A THESIS PRESENTED IN PARTIAL FULFILMENT OF THE REQUIREMENTS
FOR THE DEGREE OF
MASTER OF TECHNOLOGY
IN
FOOD TECHNOLOGY
AT MASSEY UNIVERSITY, PALMERSTON NORTH,
NEW ZEALAND

ROBYN ROSEMARY FINDLAY

2002

ABSTRACT

Increased knowledge of the interactions involved in the manufacture of Milk Protein Composite Gels (MPCGs) is essential for the further development of dairy-based analogue and recombined products and the advancement of novel product development. This study investigated MPCG manufacture using four protein sources (Rennet Casein, skim milk cheese (SMC), milk protein concentrate (MPC 85), calcium-depleted milk protein concentrate (IX MPC 85)), three protein to water (P/W) ratios (0.4, 0.5, 0.6) and four processing times (0, 4, 8, 16 minutes). The properties of the products were investigated using confocal and transmission electron microscopy, as well as rheological and functional tests.

Protein source was found to have the greatest impact on product characteristics, followed by P/W ratio with processing time having little, and often inconsistent, effects. Increased protein concentration resulted in a higher viscosity during manufacture, a decrease in fat droplet size, an increase in gel firmness, and a decrease in meltability. Increased processing time resulted in a decrease in fat droplet size, few significant changes in firmness (both small- and large-strain), and an increase in meltability.

Fracture property analysis showed that SMC produced softer, more elastic gels than Rennet Casein. The whey-containing samples produced softer, more brittle gels with little difference between them. Small-strain analysis showed that all samples were weak gels but the results did not follow the same trend as the fracture properties. The samples increased in firmness in the following order: SMC < Rennet Casein < IX MPC 85 < MPC 85.

Microstructure analysis showed the presence of whey protein aggregates in the MPC 85 and IX MPC 85 samples. These samples also demonstrated aggregation of the lipid droplets, which was attributed to the presence of whey proteins. Reduced levels of calcium resulted in lower levels of emulsification (larger lipid droplets) due to lower in-process viscosities.

Correlations between large- and small-strain testing showed that the correlation coefficient was dependent on the protein source being used and that although the level of correlation was not high, there was a general positive trend. The small-strain and UW Meltmeter tests did not agree on the order of increasing meltability except for the SMC samples, which were significantly more meltable than the other protein sources. The two tests were poorly correlated ($R^2 = 0.446$).

ACKNOWLEDGEMENTS

I would like to thank the Fonterra Research Centre (FRC) for providing this project and allowing me to write a Masters Thesis on work I have done as part of the Composite Gels group. I would like to thank my supervisors Prof. Harjinder Singh, Dr. Sheelagh Hewitt and Dr. Michael Whitton for their guidance and wisdom.

I would like to thank the following staff members at FRC for their input into this work. Mike Donkin for his suggestion and support for conducting a Masters degree through FRC. Gerhard Hoppe for allowing me to finish it. Dr. David Reid for his unrivalled enthusiasm, unwavering support and un-paid, after hours thesis editing. Andrew Saunders for all his assistance in planning and editing this work. Dr. Philip Watkinson for all his knowledge of fracture properties and meltabilty testing. Robbie Buwalda for all his assistance in the pilot plant and his knowledge of both equipment and processing techniques. Robyn Hirst for her expertise in microscopy techniques and results analysis. Dr. Siew Kim Lee for her assistance with the small-strain rheology equipment. Warren Fitzsimons for his assistance in sample production and processing advice early in the project.

I would also like to thank several Massey University staff members: Dr. Yacine Hemar for his expertise in small-strain rheology, Rod Bennet for his assistance in writing up, and Dr. Rogerio Pereira for his understanding of the equipment and manufacturing procedures.

I would also like to thank my colleagues for their support, encouragement and knowing when not to ask how it is going; Joanna Shepherd, Sophia Stathopolous, Janiene Gilliland, Arron Harford, Robert Hacking, Liz White, Satyendra Ram and Donald Love.

Thanks go to Emma Bermingham for her tales of PhD woes and also to Dave Thomas and Kane Champan for their encouragement.

Paul, thank you for your endless faith and your support over the last four and a half years that has helped to get me here today.

TABLE OF CONTENTS

LIST OF FIGURES

LIST OF TABLES

LIST OF EQUATIONS

NOMENCLATURE

ℓ	Length (mm)	(Rheology)
$\delta\ell$	Change in length (mm)	(Rheology)
ε	Strain (-)	(Rheology, normal)
σ	Stress (Pa)	(Rheology, normal)
γ	Shear strain (-)	(Rheology, tangential)
τ	Shear stress (Pa)	(Rheology, tangential)
H	Sample height at any time (mm)	(Compression testing)
H_o	Initial sample height (mm)	(Compression testing)
Δh_t	Displacement of crosshead at time *t* (mm)	(Compression testing)
v	Speed of compression (mm s^{-1})	(Compression testing)
F_t	Force during lubricated compression at time *t* (N)	(Compression testing)
r_o	Initial radius of sample (m)	(Compression testing)
σ_{max}	Maximum stress (Pa)	(Compression testing)
σ_∞	Infinite stress (Pa)	(Compression testing)
$\dot{\varepsilon}_o$	Initial strain rate (s^{-1})	(Compression testing)
ε_{max}	Maximum strain (-)	(Compression testing)
ε_c	Cauchy strain (-)	(Compression testing)
ε_H	Hencky strain (-)	(Compression testing)

σ_o	Maximum stress (Pa)	(Oscillatory rheology)
γ_o	Maximum strain (-)	(Oscillatory rheology)
$\sigma_{el.}$	Elastic material reaction stress (Pa)	(Oscillatory rheology)
$\sigma_{v.}$	Viscous material reaction stress (Pa)	(Oscillatory rheology)
$\dot{\gamma}$	Strain rate/Shear rate (s^{-1})	(Oscillatory rheology)
G'	Storage modulus (Pa)	(Oscillatory rheology)
G"	Loss modulus (Pa)	(Oscillatory rheology)
G*	Complex modulus (Pa)	(Oscillatory rheology)
G^*_{min}	Minimum complex modulus (Pa)	(Oscillatory rheology)
δ	Phase angle (°)	(Oscillatory rheology)
tan δ	Loss tangent	(Oscillatory rheology)
ω	Oscillation frequency (Hz)	(Oscillatory rheology)
η^*	Apparent viscosity	(Oscillatory rheology)

ABBREVIATIONS

AMF	Anhydrous milk fat
Ca	Calcium
C/P ratio	Calcium to protein ratio
CSA	Calcium sequestering agent
DSP	Disodium phosphate
EMC	Enzyme modified cheese
FRC	Fonterra Research Centre Limited
FTRC	Food Technology Research Centre
HPLC	High-performance liquid chromatography
IX MPC	Ion-exchanged MPC (calcium depleted)
MPC	Milk protein concentrate
MPCG	Milk protein composite gel
Na	Sodium
NaCl	Sodium chloride
NCN	Non-casein nitrogen
NPN	Non-protein nitrogen
NZDRI	New Zealand Dairy Research Institute
P/W ratio	Protein to water ratio
SALP	Sodium aluminium phosphate
SMC	Skim milk cheese

SMP	Skim milk powder
TEM	Transmission electron microscopy
TMP	Total milk protein
TN	Total nitrogen
TPA	Texture profile analysis
TSC	Trisodium citrate
TSP	Trisodium phosphate
WPC	Whey protein concentrate
WPI	Whey protein isolate

A copy of the Nomenclature and Abbreviations is given in a fold-out format at the back of this thesis.

1.0 INTRODUCTION

Milk protein composite gels (MPCGs) can be formed directly from milk, by recombining milk protein powders or via roux[1] formation with fat and milk protein powders. The two latter methods of forming milk protein gels are extremely versatile and products can be made to resemble a soft mousse-like product through to a hard cheese-like product through manipulation of the composition and processing methods (Saunders *et al.*, 1996c). These adaptable gels can be manufactured from a large range of stable intermediate protein products, such as Rennet Casein, milk protein concentrates (MPCs), calcium-depleted milk protein concentrates (IX MPCs[2]), skim milk powder, skim milk cheese (SMC) powder, sodium caseinate and calcium caseinate. These protein products influence the final flavour and texture of the product. The water content, amount and type of lipid, flavour and processing conditions can also be varied to produce a range of end products. Other ingredients may be used to influence texture and flavour, such as calcium chelating agents, salts, hydrocolloids, starches, enzyme modified cheese (EMC) and commercial flavour compounds.

Although milk protein gel products have been produced both commercially and for research purposes, the work has generally focused on emulating an existing product or investigating processed cheese. There has been little systematic work done to understand the chemical and physical interactions that affect the characteristics of the final product.

Composition, pH, shear, temperature, time, salt, emulsifiers, protein source, lipid, mixer design, mixing speed, cooling rate, order of addition, rate of addition, pH, acid type and level and the interactions between each of these affect the characteristics of the final product.

Increased knowledge of the mechanisms and outcomes of these interactions is essential for the further development of dairy-based analogue products and the advancement of novel product development (Saunders *et al.*, 1996c; Thompson and Hewitt, 2000). The work described in this thesis focuses on the effects of protein source, protein concentration and processing time on the product characteristics of recombined milk protein gels.

[1] Mixture of fat and protein powder
[2] IX MPCs are MPCs that are calcium depleted by ion exchange (IX)

2.0 LITERATURE REVIEW

2.1 Manufacture of Protein Products

The processes used in the manufacture of Rennet Casein, SMC, MPC 85 and IX MPC 85 are outlined in Figure 2.1.

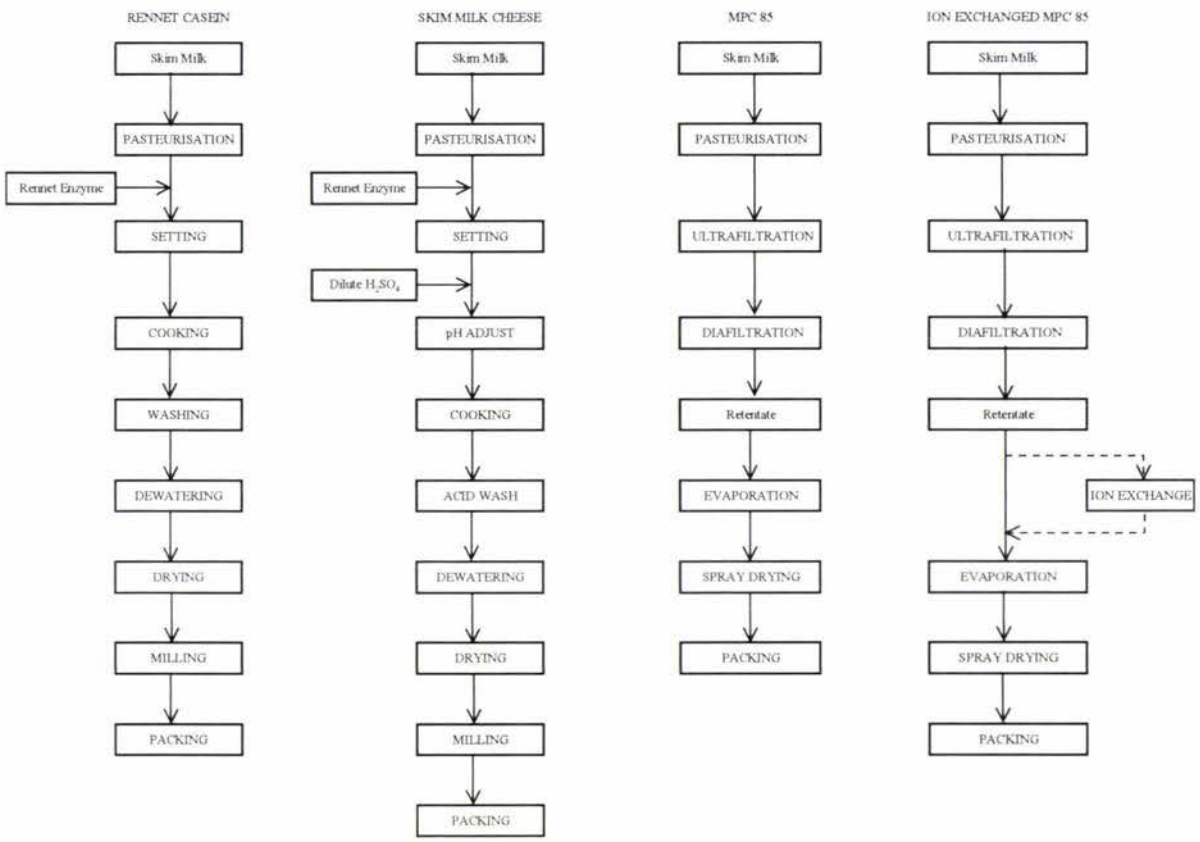

Figure 2.1: Manufacturing Processes for Rennet Casein, SMC, MPC 85 and IX MPC 85 (Bhaskar, V., 2002, personal communication; Elston, P., 2002, personal communication)

2.1.1 Casein Manufacture

There are four types of casein proteins α_{s1}-, α_{s2}-, β- and κ-. The phosphate groups of the caseins are capable of strongly binding polyvalent cations, causing charge neutralisation and precipitation of α_{s1}-, α_{s2}- and β-caseins. Conversely, κ-casein binds cations weakly and does not precipitate. Casein can be precipitated by either acid (lactic acid produced by the growth of bacteria, or addition of mineral acid) or enzymes (Fox *et al.*, 2000).

In milk, caseins are present as roughly spherical particles, called casein micelles. Acid addition causes colloidal calcium phosphate to dissolve, forming ionic calcium, which then enters the micelle and creates strong internal bonds. As the pH drops, the isoelectric point of the casein is approached and aggregation occurs. Addition of the enzyme chymosin results in cleavage of κ-casein and loss of the glycomacropeptide, leaving para-κ-casein at the surface of the micelle. The loss of the hydrophilic macropeptide causes the micelle to lose stability, hydrophobic sites on the protein begin to form bonds and the micelles aggregate to form curd (Fox *et al.*, 2000).

Rennet Casein is formed by taking skim milk, pasteurising it and adding the enzyme chymosin which cleaves the κ-casein proteins to produce para- κ-casein. Removal of κ-casein destabilises the casein micelles. The micelles aggregate and precipitate, leaving many of the minerals, lactose and whey proteins in the serum (Fox *et al.*, 2000). The curd is cooked to expel the whey and then washed, removing the serum before being dried with a ring-drier and milled (Elston, P., 2002, personal communication).

The SMC is manufactured in an analogous way, except that the pH is reduced after renneting and the washing is carried out with acidified water. The pH reduction removes calcium from the casein micelles. The calcium is then removed when the curd is washed (Elston, P., 2002, personal communication).

2.1.2 Manufacture of Milk Protein Concentrate

MPC powders contain both casein and whey proteins. Whey proteins are the proteins that are left in solution after caseins have been precipitated by either rennet coagulation or pH reduction (Mulvihill and Donovan, 1987; Pearce, 1989). There are four main whey proteins: β-lactoglobulin (β-lg), α-lactalbumin (α-la), blood serum albumin (BSA) and immunoglobulins (Ig). Whey proteins can be denatured by heat treatment, exposing sulphydryl groups that cause aggregation via disulphide bonding with other whey proteins (Anon., 1995; Fox *et al.*, 2000). The incorporation of whey proteins can therefore have a significant effect on the properties of product made from MPC powders.

MPC is made by pasteurising skim milk, followed by ultrafiltration and diafiltration to remove water, lactose and minerals. The retentate is evaporated before being spray dried. MPCs still contain whey proteins in their native state, some lactose and minerals, including

calcium. The casein micelles are believed to be intact and the κ-casein is not cleaved as in the case of Rennet Casein and skim milk cheese. Different protein concentrations can be achieved by varying the extent of ultra- and diafiltration. Typical commercial products are MPC 56, MPC 70 and MPC 85, where the number indicates the percentage of protein (Bhaskar, V., 2002, personal communication).

Ion exchanged MPC 85 follows the same process as the MPC 85 except part of the retentate is ion exchanged and re-blended to achieve the desired calcium level before being concentrated and spray dried. Reduction of calcium is carried out to aid reconstitution by improving the solubility of the MPC powder (Bhaskar, V., 2002, personal communication).

2.2 Rheological Testing

2.2.1 Introduction

Rheology is the science of deformation and flow of matter in food systems (Bourne, 1982). Generally, solid foods have two rheological aspects: they have a liquid-like (viscous) nature where they remain permanently deformed after the stress is removed and a solid-like (elastic) nature where they partially regain their original shape once the stress is removed. Viscoelasticity is the term used to describe the ratio of elasticity to viscosity, which is dependent on the time scale of deformation. On short time scales the behaviour is elastic, on long time scales the behaviour is viscous (Watkinson, 1993).

There are three main types of rheological tests: empirical, imitative and fundamental. Empirical tests are simple, rapid and do not require expensive equipment but give subjective textural measurements. Imitative tests are empirical tests that attempt to mimic the conditions that food is exposed to in the mouth during mastication and others, such as, spreading with a knife and cutting. These tests tend to give a good correlation with sensory values. Fundamental tests measure well-defined properties in the science of rheology or fracture mechanics (Watkinson, 1993). The advantages and disadvantages of these methods are discussed by Bourne (1982). In principle, if a well-defined fundamental rheological property is measured by different methods, the result is independent of the method used, provided the time scale is the same. The higher the stress and/or strain, the more the result may depend on the time scale of the measurement, measuring geometry and sample history (van Vliet *et al.*, 1991).

Stress can be applied in two ways (Figure 2.2):

a) stress (σ) in a normal, perpendicular direction resulting in compression or extension, or

b) shear stress (τ) parallel to the direction of the surface resulting in layers of the material sliding relative to each other.

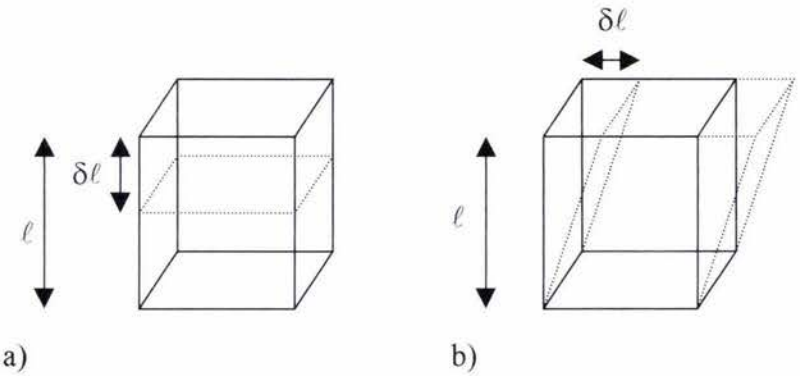

Figure 2.2: Application of stress to solid material a) normal b) tangential. [Adapted from Watkinson *et al.* (1993).]

The strain is the fractional change in a particular dimension, ℓ (height or length, m) and the nomenclature depends on whether the stress was applied perpendicular or tangentially:

a) for normal stress, the strain (ε) is the ratio of the height compressed to the original height,

$$\varepsilon = \delta\ell/\ell;$$

Equation 2.1: Normal strain calculation.

b) for tangential stress, the strain (γ) is defined as the ratio of the distance through which the point of application moves to the original height (Watkinson *et al.*, 1997)

$$\gamma = \delta\ell/\ell$$

Equation 2.2: Tangential strain calculation.

2.2.2 Large-Strain Testing (Compression Testing)

Uniaxial compression measures the force required to compress a sample, with a known geometry (usually a cylinder), at a constant rate. The advantages of this method are that the method is simple, fracture properties can be investigated and the rate of deformation can be easily varied. The main disadvantage associated with this method is that the undesirable friction between the sample and experimental apparatus can make calculation of the true stresses and strains difficult. In addition to the problem of friction, the rheological parameters are dependent on the size of the sample, fracture often starts before the maximum stress is reached and the test sample is not strained homogeneously during the test.

In general two fracture modes can be distinguished, fracture in tension and fracture in shear (Figure 2.3).

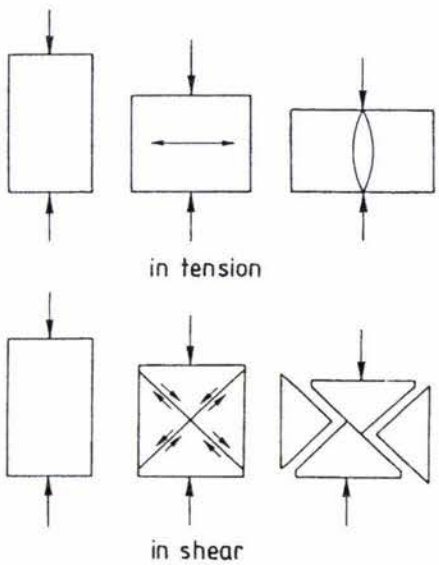

Figure 2.3: Possible fracture modes of a cylindrical test piece during uniaxial compression. [Taken from van Vliet *et al.* (1991).]

During uniaxial compression, the fracture starts at the outside if it occurs in tension, due to the increase in circumference of the sample during compression, whereas it usually starts inside the test piece if it occurs in shear.

Important factors to be considered in uniaxial testing are:

Sample Size: Ideal compression tests should be frictionless and the stress-strain relationship should be independent of the sample dimensions provided that the test piece is short enough to prevent buckling, the strain rate is kept constant and the test piece is free from structural defects (van Vliet and Peleg, 1991).

Sample Shape: In uniaxial compression the main effect of change in the height to diameter ratio is due to the influence of friction as the contact area between the sample and instrument changes. If friction between the compression plate and the sample prevents an increase in contact area, the centre of the sample will bulge. This can cause the sample to fracture in tension rather than shear (Figure 2.3), and if it fractures in tension it will do so at a lower Hencky compressive strain ε_H as defined in Section 2.2.2.2 (van Vliet and Peleg, 1991).

Sampling: A borer is used to obtain a cylindrical cheese sample for uniaxial compression. To minimise pre-test deformation due to friction, a borer with an internal diameter larger than the cutting edge is recommended (van Vliet and Peleg, 1991).

Strain Rate: As mentioned earlier, the results are dependent on the time scale of deformation: at short time scales the behaviour is elastic, at long time scales the behaviour is viscous.

The data provided by uniaxial compression is typically analysed by texture profile analysis (TPA) and/or fracture property analysis.

2.2.2.1 Texture Profile Analysis

TPA is an imitative test that generates parameters that are often used in sensory analysis.

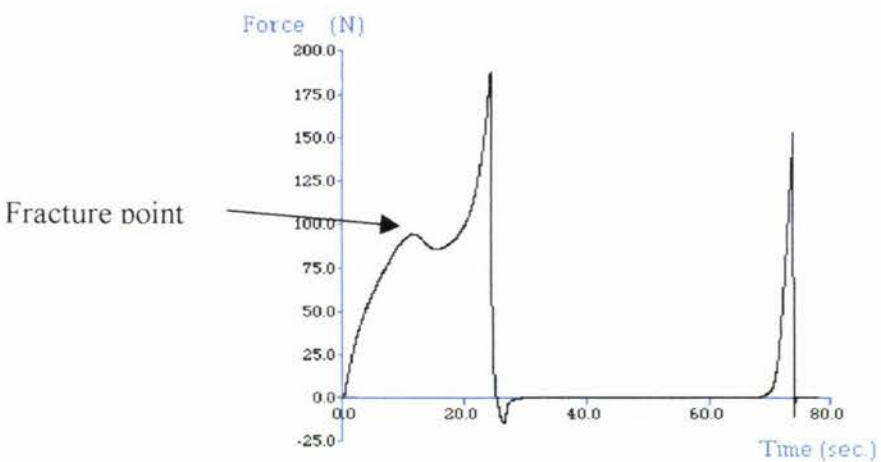

Figure 2.4: TPA curve for a Milk Protein Composite Gel sample (80% compression).

Figure 2.4 shows a typical force-time curve for a double-compression test of a Rennet Casein-based MPCG during which the sample is compressed twice to 80% of its original height.

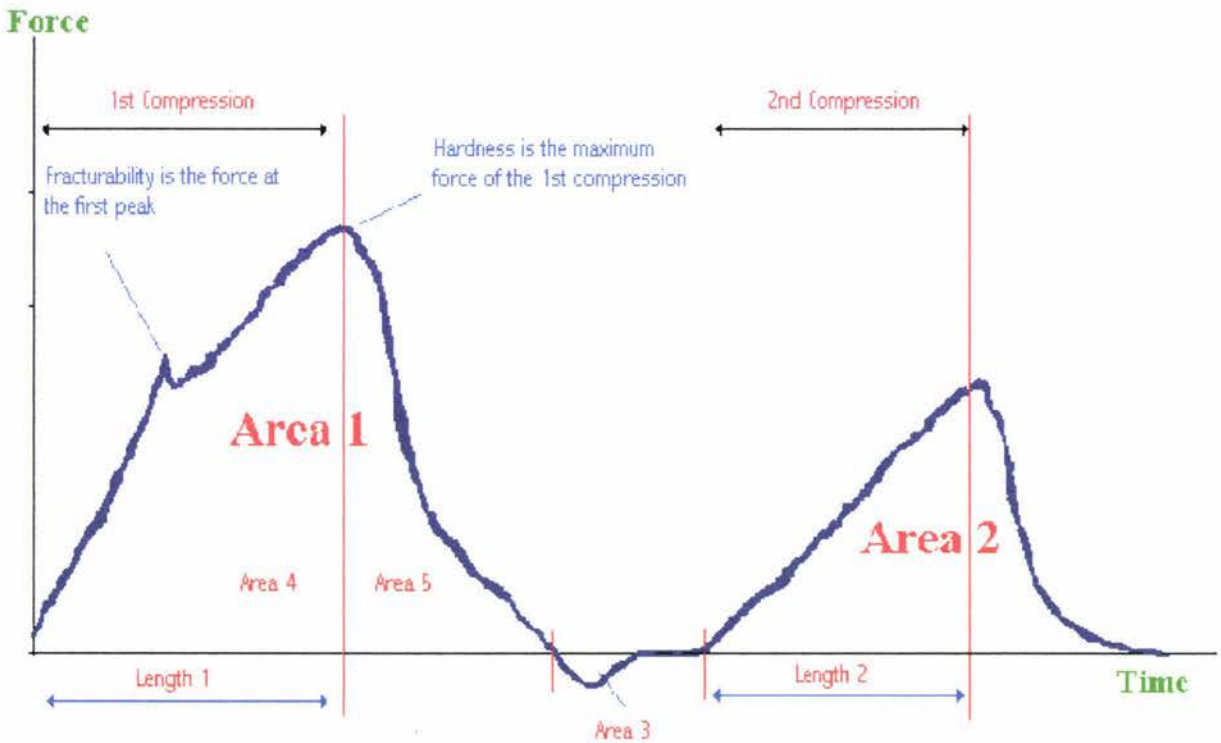

Figure 2.5: Texture profile analysis output indicating TPA parameters. [Adapted from Texture Technologies Corp. (2002).]

Hardness: The hardness value is the peak force of the first compression of the product. The peak force may occur before maximum compression. The point at which Hardness is measured can be seen in Figure 2.5.

Fracturability: When products fracture the Fracturability point occurs where the plot has its first significant peak before the peak force (as indicated in Figure 2.4 and seen as a small, sharp peak in Figure 2.5) during the probe's first compression of the product.

Cohesiveness: Cohesiveness is a measure of how well the product withstands a second compression compared to its behaviour during the first compression. It is measured as a ratio of the work done to deform the sample during the second compression to that during the first compression (refer to Area 2/Area 1 in Figure 2.5).

Springiness: Springiness is a measure of how well a product physically regains shape after it has been deformed during the first compression. Springiness is typically measured by the distance of the detected height of the product on the second compression (Length 2 in Figure 2.5), as divided by the original compression distance (Length 1 in Figure 2.5).

Gumminess: Gumminess only applies to semi-solid products and is given by Hardness *Cohesiveness.

Chewiness: Chewiness only applies for solid products and is calculated as Gumminess*Springiness. Chewiness is mutually exclusive with Gumminess since a product cannot be both a semi-solid and a solid at the same time.

Resilience: Resilience is how well a product "fights to regain its original position", a measure of "instant springiness". Resilience is measured on the withdrawal of the first penetration, before the waiting period is started. The calculation is the area during the withdrawal of the first compression, divided by the area of the first compression (Area 5/Area 4 in Figure 2.5). Resilience is not always measured with TPA calculations.

Adhesiveness: Adhesiveness is a measure of how sticky the sample is. It is the work done in removing the probe from the sample (Area 3 in Figure 2.5).

2.2.2.2 Fracture Property Analysis

Fracture property analysis involves comparison of the true stress and Hencky strain at the point of fracture. The parameters are fundamental mechanical properties of the material.

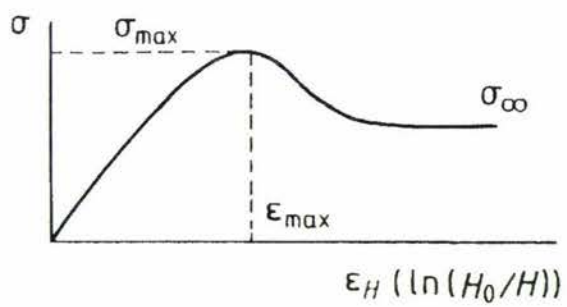

Figure 2.6: Compression stress as a function of Hencky strain. Where σ_{max} = maximum stress; σ_{∞} = infinite stress; ε_{max} = maximum strain [Taken from Van Vliet *et al.* (1991).]

$$\varepsilon_H = \ln (H_0/H)$$

Equation 2.3: Hencky strain.

$$\sigma = (F_t / \pi r^2_0) * H / H_0$$

Equation 2.4: True stress.

Where: H = Sample height at any time (mm)
H_o = Initial sample height (mm)
σ = Stress (Pa)
F_t = Force at time t (N)
r_o = Initial radius of sample (m)
[Taken from Watkinson *et al.* (1997)]

Force–distance data from the compression, the sample diameter and the distance the sample is compressed, are used to calculate the fracture stress (Pa) and fracture strain (-). This data can

then be compared using texture graphs by plotting fracture stress against fracture strain (Munro *et al.*, 2000).

2.2.3 Small-Strain Testing (Oscillatory Testing)

Large- and small-strain testing are different rheological techniques; large-strain testing has the advantage of better correlation to sensory evaluation, while small-strain testing has the advantage of the sample behaviour being described in physico-chemical and rheological terms. Because different information is gathered from each method, a complete rheological evaluation should include both small-strain and failure testing (Ziegler and Foegeding, 1990).

The three-dimensional structure of protein gels immobilizes liquid to impart rubber-like characteristics. The sections of the protein that are between the cross-links in the three-dimensional structure contribute to the ability of the gel to absorb stress. The following sections of the protein chain are not considered to contribute to stress absorption; the terminal end of the chain (bound by a cross-link at one end and free at the other end), intramolecular cross-links (when the protein cross-links with itself), and entanglements (sections not bound at fixed points as in the case of chemical cross-links) (Hsieh and Regenstein, 1992).

Depending on the type of protein involved, the transition from a dispersion of milk protein particles into a solid-like gel can be triggered by:

- lowering the pH toward the isoelectric point,
- heat denaturation,
- high pressure processing,
- enzyme treatment, or
- addition of divalent counterions (Dickinson and Hong, 1995).

Gels can be classified into strong gels, weak gels and entanglement gels using small-strain rheological test methods.

Dynamic measurement involves an applied stress, strain or strain rate that can be varied sinusoidally with time and the time scale changed by altering the frequency (ω) of oscillation. The oscillation stresses the sample in different directions in comparison to static measurement

in which the sample is constantly stressed in the same direction. By increasing the strain, the strain at which bonds begin to break can be determined.

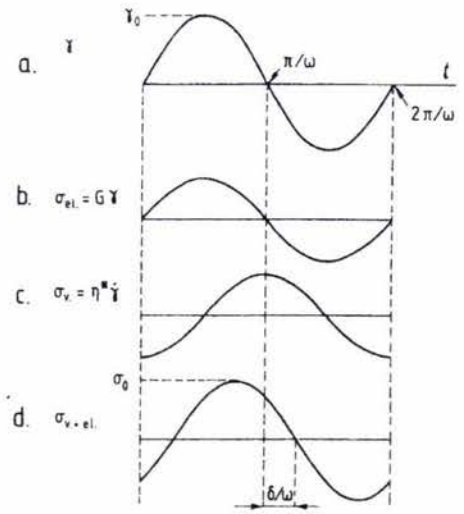

a. Oscillating frequency
(ω, rad s^{-1})

b. Elastic material reaction stress
(σ is in phase)

c. Viscous material reaction stress
(σ is $\pi/2$ rad out of phase)

d. Viscoelastic material reaction stress
(σ is out of phase by an angle δ)

Figure 2.7: Response stress (σ) in a material with time when an oscillating strain is applied. [Taken from van Vliet and Peleg (1991).]

Figure 2.7 shows the reaction stress (σ) of various types of materials to an oscillating strain (γ). A purely elastic material has a stress in phase with the strain being applied, while a purely viscous material has a stress that is $\pi/2$ out of phase with the applied strain. The viscoelastic material is between the two extremes, with a reaction stress between 0 and $\pi/2$ rad out of phase. The amount by which the stress is out of phase with the strain is called the phase angle, δ (van Vliet and Peleg, 1991).

Within the linear region, σ_0 is by definition proportional to γ. The elastic part of the stress is a measure of the energy stored and released per deformation cycle and corresponds to the storage modulus G' which is defined as:

$$G'(\omega) = (\sigma_0/\gamma_0) \cos \delta$$

Equation 2.5: Determination of storage modulus. [Taken from Watkinson and Jackson (1999)]

The parameters σ_0 and γ_0 can be seen in Figure 2.7.

The viscous part of the stress, which is a measure of the energy that is dissipated as heat per deformation cycle is out of phase and corresponds to the loss modulus G" which is defined as:

$$G''(\omega) = (\sigma_0/\gamma_0) \sin \delta$$

Equation 2.6: Determination of loss modulus. [Taken from Watkinson and Jackson (1999)]

The complex modulus is determined by:

$$G^* = G' + iG'' \quad \text{or} \quad G^* = \sqrt{(G'^2 + G''^2)}$$

Equation 2.7: Determination of complex modulus. [Taken from Watkinson and Jackson (1999)]

The strain rate at which the tests are carried is important in oscillatory testing. For a viscoelastic substance, part of the strain energy is stored in the material (elastic) and the remainder is dissipated (viscous) with the latter being time dependant, hence the behaviour of the material is dependent on strain rate, $\dot{\gamma}$ (van Vliet and Peleg, 1991).

Frequency sweeps enable differences in gel strength to be identified. The storage and loss moduli (G' and G") show power law dependencies on frequency: G' or G" $\propto \omega^p$ (Ziegler and Foegeding, 1990; Lapasin and Pricl, 1995).

$$G' = k\omega^p$$

Equation 2.8: Frequency dependence of the storage modulus. [Adapted from Rosenthal (1999).]

Using log calculus rules, this can be rewritten as:

$$\log (G') = p * \log (\omega) + \log (k)$$

where: ω = oscillation frequency (Hz)

k = G' at 1 Hz

p = degree of frequency dependence

G' = storage modulus (Pa)

Equation 2.9: Equation to describe a linear relationship between storage modulus and frequency derived from Equation 2.8.

Plotting log (G') versus log (ω) gives a straight line. The slope, p, is an indication of how frequency dependant the gel is. The intercept, k, is the storage modulus at a frequency of

1 Hz (Paulson and Tung, 1989). Using this p-value, gels can be classified as strong gels, weak gels and entanglement gels. Strong gels have a permanent covalent network and have a G' that is only slightly dependent on frequency (low p value). Entanglement network gels do not have strong cross-links, the gels flow like a liquid at low frequencies and G' and G" are highly frequency dependent (increases over several magnitudes resulting in a high p value) with a crossover occurring at some intermediate point. Weak gels have weak cross-links, are less frequency dependent than the entanglement network (increases within a magnitude) and do not have a crossover point (Clark and Ross-Murphy, 1987; Lee *et al.*, 1996; Bowland and Foegeding, 2001).

Many authors have compared product characteristics of milk protein gels, emulsions and products by taking G', G" and in some cases G* and tanδ at a frequency of 1 Hz (Cooney *et al.*, 1993; Dickinson and Hong, 1995; Gezimati *et al.*, 1996; Dickinson and Yamamoto, 1996; Marchesseau *et al.*, 1997; Zhou and Mulvaney, 1998; Chen and Dickinson, 1998b; Chen *et al.*, 1999; Drake *et al.*, 1999a; Drake *et al.*, 1999b; Everett and Olson, 2000).

Temperature sweeps are also common in processed cheese research. The storage modulus, loss modulus and loss tangent (tan δ) are measured at constant oscillation frequency, while the temperature is increased/decreased (Rao, 1999). The loss tangent, tan δ (Rüegg *et al.*, 1991), and mimimum complex modulus, G* (Ustanol *et al.*, 1994), have been suggested as a predictors for cheese meltability.

2.2.4 Melt and Flow Characterisation

Meltability is the ease with which a material flows upon heating (Muthukumarappan *et al.*, 1999). Methods for evaluating cheese meltability are described by Kosikowski (1977) (discussing the Schreiber test), Arnott *et al.* (1957), Olson and Price (1958) and Wang *et al.* (1998).

Park *et al.* (1984) compared four methods of cheese meltability evaluation and found a lack of correlation between the Arnott and Schreiber tests. The major issues with the Schreiber test are non-circular cheese spread and scorching (Muthukumarappan *et al.*, 1999) and puffing up of samples in the case of MPCGs (Thompson and Hewitt, S. A., 2000). Muthukumarappan *et al.* (1999) recommended modifying the Schreiber method by lowering the temperature to

90°C, placing the sample on an aluminium plate, heating for 5 minutes and using the area of spread of the sample as a method of melt measurement.

The Arnott, Schreiber, Olson and Price and modified Schreiber tests are empirical and cannot be represented by fundamental rheological parameters. Dynamic rheological testing of temperature dependence has been used on cheese (Nolan *et al.*, 1989; Tunick *et al.*, 1990; Ustanol *et al.*, 1994). Rüeg *et al.* (1991) stated that tan δ, could potentially be used as a predictor for cheese meltability, and Ustanol *et al.* (1994) suggested minimum complex modulus, G*, as a means of measuring cheese melt. The authors found that G^*_{min} was correlated to the Arnott test ($R^2 = -0.80$) for Cheddar cheeses (Ustanol *et al.*, 1994). Dynamic testing of cheese becomes difficult to perform at high temperatures due to sample slippage distorting the results. Slip and viscoelastic effects can be overcome by using squeezing flow rheometry to determine the viscosity of molten cheese (Kuo *et al.*, 2000) and has been has been used by several authors (Campanella *et al.*, 1987; Ak and Gunasekaran, 1995). Wang *et al.* (1998) modified the squeezing flow test. They developed the UW Meltmeter to evaluate the flow characteristics of melted cheese under constant force or constant deformation rate. The method can be used to calculate fundamental rheological parameters; the biaxial extensional strain rate (s^{-1}) and the biaxial stress growth coefficient (Pa.s).

2.2.5 Rheological Correlations

Rheology in the food industry is generally used to investigate variables that alter the structure and texture of the product. For consumable products it is important that the end use be considered and that the rheology results be related to sensory attributes.

Conflicting results have been reported for correlations between instrumental and sensory analysis of food products. Early investigations found that rheological oscillatory tests correlated poorly with sensory evaluation (Bourne, 1982). Subsequently, a number of sensory textural attributes of Rennet Casein based processed cheese analogues have been successfully correlated with compositional, microstructural and rheological information (Pereira, 2000). Instrumental and sensory correlations have been successfully made for Cheddar cheese (Hort and Le Grys, 2000), and a variety of commercial and experimental cheeses (Drake *et al.*, 1999a).

Small-strain and large-strain testing correlations have been attempted with varying results. Paulson and Tung (1989) attempted to correlate the penetration test results with dynamic shear testing results and found that while the puncture force correlated poorly with viscoelastic parameters, the slope of the deformation curve to the point of rupture correlated well with small-strain parameters, G' and G''. Drake *et al.* (1999a) found that G' and G" at 1 Hz correlated well with TPA hardness for a variety of commercial and experimental cheeses. Tang *et al.* (1995) studied WPC gels and found a reasonable agreement between the large-strain compression modulus and the small-strain storage modulus multiplied by a factor of three. The TPA results did not exhibit the same variation with pH as G' except for hardness at pH values > 5.5. The difference were attributed to the fact that the compression testing caused fracture while G' values were determined at relatively low strain. Large strain correlations have also been attempted; Gupta *et al.* (1984) found hardness to correlate with fracturability for commercial processed cheeses.

2.3 Milk Protein Composite Gels

Work done at the Food Technology Research Centre (FTRC), Massey University, showed that MPCGs products can emulate traditional products, from mousses to meat analogues (Saunders *et al.*, 1997; Sharma *et al.*, 1997a; Sharma *et al.*, 1997b). However the research has focussed on processing variables (particularly in processed cheese manufacture) rather than characteristics of the MPCGs themselves.

At Fonterra Research Centre Limited (FRC), Palmerston North, MPCGs are usually manufactured using typical processed cheese techniques (formulation, blending and processing - direct or indirect heating with optional vacuum) and equipment (Blentech and Stephan kettles). Temperature and shear are varied to suit the formulation and characteristics of the desired final product. Non-dairy ingredients may also be used, such as, gums, starches, vegetable oils. This is similar to the processed cheese methods outlined by Fox *et al.* (2000).

2.3.1 Protein Source

Table 1: Protein Sources for MPCG Manufacture

Caseins	Rennet Casein
	Acid Casein
	Calcium Caseinate
	Sodium Caseinate
	Skim Milk Cheese
Whey Protein Containing Powders	MPCs 85, 70 or 56
	Ion Exchanged MPCs
	Total Milk Protein (TMP[3])
	Whole Milk Powder
	Skim Milk Powder

There are a large number of potential protein sources for use in MPCGs (Table 1) and the impact of the different protein sources on gel properties is dependent on the formulation of the product as well as the processing conditions.

[3] TMP is made from skim milk that is heated at alkaline pH to denature the whey proteins before the protein is precipitated by acidification to pH 4.6, cooked and then dried and milled to form a powder product (New Zealand Dairy Research Institute, 2001)

Whey proteins can also be incorporated by adding whey protein powders such as whey protein concentrate (WPC) and whey protein isolate (WPI).

The effect of protein source is difficult to ascertain from literature due to the varied processing conditions and formulations used by various workers. In some cases, the results are reported but an explanation of the fundamental protein interactions are overlooked. Studies of acid and Rennet Casein composite gels used to investigate processed cheese, showed that the melting properties depended mainly on the type of casein used and on the type and dose of emulsifying salt (Savello *et al.*, 1989).

Lee *et al.* (1998) investigated several different protein sources (Rennet Casein, MPC 70, sodium caseinate, calcium caseinate) in MPCG formulations made in a Stephan cooker. It was found that a protein source with higher calcium resulted in a harder, thicker model processed cheese with lower meltability, which was in agreement with the results of Cavalier-Salou and Cheftel (1991).

MPCGs made from sodium caseinate did not reach a maximum viscosity (did not cream) even after prolonged cooking. This lack of structure formation during processing was attributed to the lack of calcium, which forms bridges between proteins. Lee *et al.* (1998) concluded that the form in which the calcium was present may have had an impact on the structural properties of the gels, as colloidal calcium phosphate is a more effective bridge-forming constituent than ionic calcium. The meltability (Arnott test) of the samples increased as follows: calcium caseinate < Rennet Casein < sodium caseinate/Rennet Casein < sodium caseinate. This indicates that the lower the calcium level, the more meltable the sample (Lee *et al.*, 1998). This work, however, did not compare proteins on a total protein basis so the different protein levels in the powders could have had a significant effect on the product characteristics.

2.3.1.1 Incorporation of Whey Proteins

Lee *et al.* (1998) found that MPC 70 produced a softer product than Rennet Casein, sodium caseinate and calcium caseinate. It was proposed that the presence of lactose lowered the total protein content of the MPC 70, thus decreasing compressive strength. Samples containing MPC 70 were observed to have irregular shaped lipid droplets, which was attributed to the low viscosity in the cooker during processing. It was proposed that higher the viscosity in the cooker results in greater shear stress leading to smaller lipid droplets being

formed. By inspection of the MPC 70 confocal images, it appeared that these irregular lipid droplets were aggregates of smaller fat droplets, but this was not discussed by the authors. The meltability (determined by the Arnott test) was higher than calcium caseinate, Rennet Casein, a calcium caseinate/MPC70 mixture and lower than a sodium caseinate/Rennet Casein mixture, a sodium caseinate/MPC 70 mixture and sodium caseinate. The effect of the whey proteins on the product characteristics was not discussed, the changes were discussed in terms of lactose, calcium and moisture levels.

Addition of whey protein containing powders such as TMP and MPC to processed cheese formulations have been investigated with similar results to MPCG work. Reduction in the meltability of Rennet Casein based MPCGs with increasing levels of TMP has been reported by several authors (Haylock and Avery, 1984; Abou El-Nour *et al.*, 1996). The same trend has been seen with increasing levels of MPC 85 (Abou El-Nour *et al.*, 1996; Abou El-Nour *et al.*, 1998). The effect of MPC was attributed to the binding of the denatured whey protein to the casein during the melting process particularly to para-κ-casein and possibly α_{s1}-casein, which caused a decrease in the meltability. Mleko and Foegeding (2001) proposed a 2-component model, consisting of a melting casein network and a non-melting whey protein network.

The firmness of the Rennet Casein MPCGs increased with increasing MPC 85 concentration. This was also attributed to binding of the denatured whey protein to the casein (Abou El-Nour *et al.*, 1998). Addition of WPC and WPI produced more brittle Rennet Casein-based MPCGs (Chang and Lloyd-Voss, 1994), a softer texture, lower adhesiveness, lower elasticity, lower chewiness and lower gumminess (Kaminarides and Stachtiaris, 2000).

Some authors have found an increase in firmness with particular combinations of whey proteins and casein-based protein powders. Combinations of WPC and SMP gave higher firmness than either of the two protein sources separately and it was assumed that there was a synergistic effect between the two proteins (Mleko and Foegeding, 2001). This synergistic effect has also been reported for a sodium caseinate and MPC 70 based MPCG (Lee *et al.*, 1998).

Aguilera and Kinsella (1991) found that addition of WPI to SMP gels increased compressive strength by reinforcing the protein network, while SMP addition to WPI gels disrupted the protein network, resulting in weaker gels. The WPI does not disrupt the SMP casein micelle

network, but forms a secondary network within it, reinforcing the matrix (Figure 2.8). The authors hypothesised that because the casein micelles form a "string-of-beads" arrangement, which require a minimum number of casein units to form a continuous network, that the undeveloped casein gel acts as a filler, disrupting the WPI network. Filled (emulsion) gels made with recombined cream had higher compression strengths than the mixed gels. It was proposed that casein micelles from the SMP formed a network that was associated with the protein coating on the lipid droplets and that the network was reinforced by a secondary WPI network (Aguilera and Kinsella, 1991). Contrary to this, Lee *et al.* (1999b) observed, using microscopy, that the whey proteins existed as separate domains within the casein network. The reason for the disagreement is probably due the different manufacturing temperatures used. The whey proteins would be in their native state in the work by Aguilera and Kinsella (1991) (60°C) and denatured in the work by Lee *et al.* (1999b) (85°C). High temperatures cause whey proteins to denature, exposing hydrophobic sulphydryl groups, which would cause the whey proteins to aggregate.

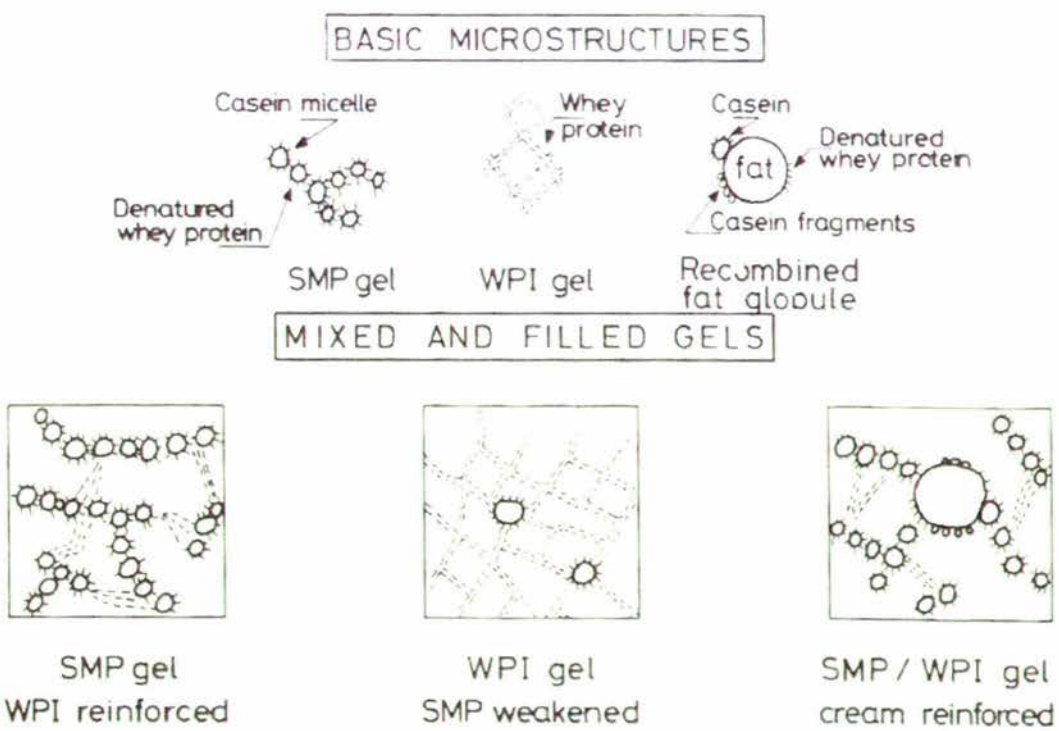

Figure 2.8: Proposed interaction between whey proteins and recombined fat globules in mixed and filled dairy gels. [Taken from Aguilera and Kinsella (1991).]

Processed cheese is a protein-gelled oil-in-water emulsion. The physical properties depend on composition (water, protein, fat, calcium sequestering agent (CSA), pH) and processing (thermal and mechanical energy input, time) variables. Processed cheese literature has been

used to gain an insight into MPCGs by Saunders *et al.* (1995) in addition to MPCGs being used to model processed cheese (Savello *et al.*, 1989; Lee and Klostermeyer, 1994a; Lee and Klostermeyer, 1994b; Lee and Klostermeyer, 1994c; Foegeding *et al.*, 1996; Lee *et al.*, 1996; Lee *et al.*, 1999a).

The decrease in meltabilty and increase in firmness due to whey protein incorporation has also been documented in processed cheese products (Ernstrom *et al.*, 1980; Savello *et al.*, 1989; Gupta and Reuter, 1993; Lee *et al.*, 1999b). The theory for the increase in firmness is that the unfolding of the whey protein molecules during heat processing exposes hydrophobic groups that can orient at the oil and water interface and improve emulsion stability, leading to an increase in firmness. The exposure of hydrophobic groups, and consequent interaction, is also thought to solidify the samples and inhibit melting (Gupta and Reuter, 1993). In contrast, Abd El-Salam (1996) found that addition of WPC to process cheese results in increased meltability, although the authors did not discuss the impact of a subsequent change in lipid and moisture content despite the fact that these variables have an impact on meltability.

While cheese and MPCGs do not share as many similarities as processed cheese and MPCGs, several theories have been proposed about the role of whey proteins in cheese that may be applicable to MPCGs. The observation that whey protein incorporation in cheese has also been observed to lower meltability and firmness is consistent with MPCG and processed cheese literature. One theory on the behaviour of whey proteins in cheese, processed cheese, and MPCGs is the "inert filler theory", where the whey protein does not interact with the gel network (Lawrence, 1989). In agreement with the inert filler hypothesis are reports of softer texture in various cheeses (Banks and Muir, 1985; Baldwin *et al.*, 1986; Delbeke, 1987; Spangler *et al.*, 1990; Everett and Jameson, 1993) Lawrence (1989) reported that whey protein addition gives a smoother texture and proposed two possible causes; either denatured β-lactoglobulin binding calcium or whey proteins increasing the water-holding capacity of the cheese matrix. This does not agree with the work of Green (1985), Green *et al.* (1981) and Creamer *et al.* (1987) who found that coarser, grittier structure was formed.

As with processed cheese literature, several authors have found contradicting results; that firmness of the cheese increases with higher levels of whey protein, accompanied by an increase in rubberiness and grittiness (Green *et al.*, 1981; Creamer *et al.*, 1987). Different apparatus and operating conditions employed by various researchers have lead to contradictory reports of the effects of whey proteins in cheeses (Lawrence, 1989). Denatured

whey proteins have been found to contribute to the texture of UF fresh cheese but native proteins do not, although denatured whey proteins contribute less to the texture than casein, giving lower rigidity and viscosity (Korolczuk and Mahaut, 1991; Mahaut and Korolczuk, 1992).

Lawrence (1989) also reviewed the melting quality of whey protein-containing cheese and identified several mechanisms for the reduction in meltablilty:

a) heat induced interaction of β-lactoglobulin with para-κ-casein and possibly α_{s2}-casein, reducing capacity for flow;

b) binding of free water by denatured whey proteins or casein complexes; and

c) calcium binding by denatured whey proteins.

2.3.2 Protein Concentration

The ratios of the main ingredients (protein, lipid and water) determine the final texture of the product with the protein-to-water ratio largely determining texture (Saunders *et al.*, 1996b). An increase in the P/W ratio results in an increase in hardness and firmness in both processed cheeses (Zuber *et al.*, 1987; Gupta and Reuter, 1993) and MPCGs (Saunders *et al.*, 1996b). Protein content also has an effect on lipid size distribution; lipid droplet size was seen to increase with increasing P/W ratio. Transmission electron microscopy (TEM) studies showed a more open structure in the protein phase in the low P/W ratio gels, as the P/W ratio increased the protein phase became more dense. The gels did not melt but "puffed up" and collapsed during the Schreiber test. The phenomenon had been related to a similar observation in MPCGs made from a skim milk cheese base. It was proposed that moisture inside the gel boiled and caused expansion; surface tension effects may be involved as a result of skin formation on the surface of the samples (Thompson and Hewitt, S. A., 2000). Maximum stress on compression and work to maximum stress increased as protein concentration increased (as a result of decreasing moisture content) for SMP/sodium caseinate MPCGs (Marshall, 1990). Decreasing protein concentration by increasing moisture decreases the strength of bonds between the casein fragments, leading to a product softening sooner during melting tests (Taneya *et al.*, 1979)

2.3.3 Lipid Content

The role of lipid in MPCGs is debatable; some authors believe that lipid does not play an active role in structure formation but rather increases the effective concentration of protein in the aqueous phase (Eymery and Pangborn, 1988) and others believe that it does play an active role, albeit by different mechanisms (van Vliet and Dentener-Kikkert, 1982; Jost *et al.*, 1986; Aguilera and Kessler, 1989). While others believe that lipid does not contribute to strength of the gels, but instead provides weak areas for fracture to pass through (Marshall, 1990).

Assuming lipid does impact on structure, two reinforcement theories for lipid-containing gels have been proposed:

a) the lipid droplet surface interacts with the protein network (van Vliet and Dentener-Kikkert, 1982); and,

b) a steric effect of the lipid droplets fitting in the porous structure of the protein matrix (Jost *et al.*, 1986).

Work by Aguilera and Kessler (1989) agrees with the above mechanism but also adds that larger lipid droplets can disrupt the protein network, adversely affecting structure and gel strength. The effect of lipid droplet size on the mechanism of interaction is illustrated in Figure 2.9.

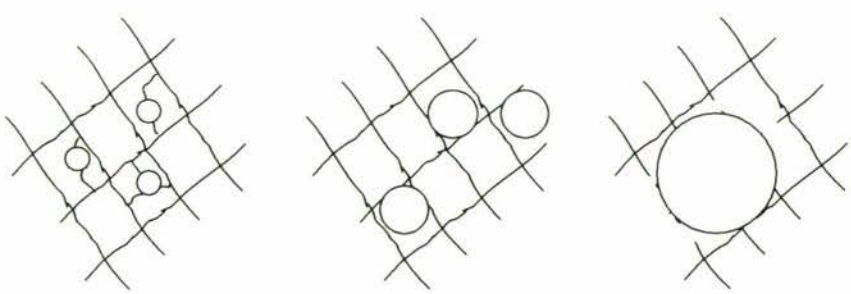

Figure 2.9: Proposed mechanisms of interactions between lipid droplets and protein matrix. [Taken from Aguilera and Kessler (1988).]

Increasing lipid content results in increased relative firmness of gels made with either sodium caseinate, SMP or WPC (Aguilera and Kessler, 1989). In agreement with these results, Emyery and Pangborn (1988) found that increasing lipid content increased the sensory parameters, such as, springiness, hardness, crumbliness and chewiness, in addition to

increasing all uniaxial compression parameters. This was not attributed to lipid reinforcing the protein network, but to a resultant increase in the effective concentration of protein in the aqueous phase. It was also noted that as the lipid content increased, the size of the lipid droplets decreased and they became more numerous.

Few papers discuss the effect of lipid on melting properties of MPCGs. It is well documented that for processed cheese, the size of the lipid droplets is important as it influences the firmness of the product and the "oiling off" properties. Some "oiling off" during heating is desirable as it prevents drying out, allowing flow and surface sheen. Generally for a given formulation, a smaller diameter of lipid droplets results in a firmer texture, a low tendency to oil off, and poor flowability on cooking (Fox *et al.*, 2000). The melting difficulties encountered by Thompson and Hewitt (2000) appear to be due to the lack of "oiling off" during the Schreiber test, resulting in "puffing up" of the samples and consequently, the inability to effectively measure melt properties. Similar problems, such as, case hardening and scorching have been reported by Drake *et al.*(1999b) and McMahon and Oberg (1998) for reduced fat processed cheese. Lee *et al.* (1999b) stated the effect of lipid droplet size on processed cheese meltability was coincidental, as various authors show contradictory results with no definite trend.

2.3.4 pH

The effect of pH varies, depending on the protein source and other ingredients used. For Rennet Casein based MPCGs, decreasing pH gave an increase in hardness, increased elasticity and a lower frequency dependency, indicating a higher degree of structural network (Lee *et al.*, 1996). Contrary to the work by Lee *et al.* (1996), it has also been observed that decreasing the pH of MPCGs resulted in lower instrumental elasticity, cohesiveness and chewiness. When the pH approached the casein isoelectric point, a more crumbly, chewy and sandy texture was produced (Eymery and Pangborn, 1988). The experimental conditions and acid used may be the cause of the discrepancy between the results. Lee *et al.* (1995) found that lipid droplet size decreased with increasing pH, which was attributed to the increased emulsifying capacity of the caseins.

In the manufacture of processed cheese, low pH tends to form crumbly, dry products that have a tendency toward oiling off. High pH value products tend to be soft and exhibit excessive flow when melted. Above pH 6.0 the product can become bitter and salty (Fox *et al.*, 2000)

and above 6.5 microbial growth can become an issue (Shimp, 1985). The pH affects protein conformation, protein solubility and the efficiency of CSAs to bind calcium. At the isoelectric point the opposite charges on the protein attract causing the protein molecule to aggregate, minimising its interaction with its environment. Above the isoelectric point, there is an excess of negative charge on the protein. As the pH approaches the isoelectric point the texture becomes more crumbly because external protein-protein interactions are minimised and the lipid begins to leak from the protein network. The type of acid used for pH adjustment can have secondary effects on the product. Acids such as fumaric, maleic, acetic and citric also bind calcium and at levels >1% may cause significant changes in the emulsifying ability of the protein (Shimp, 1985).

2.3.5 Calcium Sequestering Agents (CSAs)

Calcium concentration has been found to have a significant effect on MPCG characteristics (Lee *et al.*, 1998). Increased calcium concentration increases firmness of MPCGs (Cavalier-Salou and Cheftel, 1991; Lee *et al.*, 1998) and decreases meltability (Cavalier-Salou and Cheftel, 1991). The effect of calcium must be considered when using different protein sources, as in the work of Lee *et al.* (1998), as they contain different levels and forms of calcium (colloidal or ionic calcium phosphate). The amount and type of CSAs must be considered when formulating MPCGs made from different protein sources.

CSAs can assist in processed cheese (and MPCGs) by replacing calcium with other cations, binding calcium and affecting pH. Removing calcium increases the solubility of proteins and consequently the proteins are able to interact with aqueous and lipid phases (Shimp, 1985). CSAs are often called emulsifying salts, which is somewhat misleading as they are not emulsifiers. By removing the calcium cross-links that bind protein molecules together, they allow the protein to emulsify the lipid phase. Calcium sequestration involves the removal of calcium (Ca^{2+}) from the protein. The calcium is exchanged with monovalent sodium, breaking the inter- and intra-aggregate bonds that hold the structure together as shown (Figure 2.10).

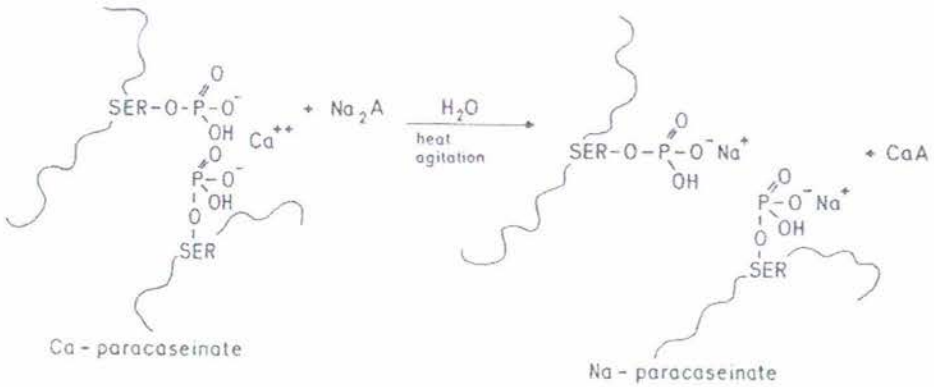

Figure 2.10: Effect of calcium removal on protein linkages. [Adapted from Caric and Kalab (1993).]

Commonly used CSAs or "emulsifying salts" are sodium citrates, sodium orthophosphates, sodium pyrophosphates, sodium tripolyphosphates, sodium polyphosphates, basic sodium aluminium phosphates and phosphate blends (Fox *et al.*, 2000). Emulsifying salts are used widely in the processed cheese industry and have been studied by many authors. Salts that weakly bind calcium, such as sodium citrate, sodium aluminium phosphate (SALP), disodium phosphate (DSP) and trisodium phosphate (TSP), have been found to give soft meltable processed cheeses. Effective calcium binders give good emulsification and hard, nonmelting processed cheeses (Shimp, 1985) for example, condensed phosphates impart nonmelting properties in processed cheese. DSP and TSC both produce processed cheese with good characteristics; with the DSP producing less meltable processed cheeses than the TSC. The theory proposed was that DSP and calcium cross link, creating a network that has sufficient rigidity to resist collapse and flow at the melting point of the lipid (Gupta *et al.*, 1984).

Cavalier-Salou and Cheftel (1991) investigated the effects of types and levels of emulsifying salts in MPCGs made from calcium or sodium caseinate. The decrease in firmness with increasing CSA concentration is due to a looser protein matrix, resulting from an increased pH and possible calcium release from protein components. The trend of a decrease in firmness was also observed by Thomas *et al.* (1980). Firmness was found to increase with the degree of phosphate polymerisation, which is in agreement with results of Swiatek (1964).

Cavalier-Salou and Cheftel (1991) found that the firmness and melting ability were inversely related, which is in agreement with results of Thomas *et al.* (1980) and Kalab *et al.* (1987) who studied the microstructure and texture properties of processed cheese. Increasing the CSA concentration increased meltability slightly (Thomas *et al.*, 1980). Cavalier-Salou and

Cheftel (1991) reported that sodium pyrophosphate, tripolyphosphate, or polyphosphate did not induce heat melting, while smaller chain CSAs such as sodium citrate and DSP did produce meltable products. This is in agreement with reports for processed cheese by Gupta *et al.*, (1984) and Shimp (1985). Savello *et al.* (1989) concluded that the type of casein used and the type and concentration of emulsifying salt had a large impact on the melting properties.

Increasing levels of DSP have been observed to change Rennet Casein-based MPCG samples from an unstable emulsion to a highly viscous macromolecular solution (entanglement network) to a weak gel as determined by small-strain rheology. Increasing DSP concentration also resulted in higher strain values at fracture, which was attributed to increased incorporation of protein into the gel network (Bowland and Foegeding, 2001).

Several workers have found different values for calcium binding capacity of several types of phosphates. However these variations may arise from workers using different ingredient and processing parameters (Zehren and Nusbaum, 1992).

2.3.6 Salt (NaCl) Concentration

Salt can also be used to assist in the emulsification process as it solubilises part of the colloidal calcium and can lead to improved meltability (Abou El-Nour *et al.*, 1996; Abou El-Nour *et al.*, 1998). It has been proposed that NaCl increases the solubility of calcium phosphate from the casein micelle and loosens its structure. This could be due to an increase in the ionic strength or the formation of sodium caseinate (Aoki *et al.*, 1999). A high ionic strength environment may have caused some protein precipitation ("salting out"). Protein precipitation results in insufficient hydrated protein being available to emulsify the oil and stabilise the emulsion (Ennis *et al.*, 1998). This agrees with the observation of aggregated protein areas during microstructural analysis in the work of Thompson and Hewitt (2000).

2.3.7 Lactose

Little work has been carried out to determine the effect of lactose content. Protein powders, such as MPC, contain significant levels of lactose and its effects on product characteristics must be considered. Browning and crystallisation are the problems most commonly associated with using lactose in processed cheese as a low cost filler. Crystal formation is avoided by maintaining lactose levels below the saturation concentration at the appropriate

temperature (16.9g lactose/100g water at 15°C). Lactose levels in processed cheese are usually maintained lower than the saturation concentration due to factors that increase the chance of crystallisation: the presence of other water-soluble components that compete for water, the presence of precipitating nuclei and low storage temperatures (Zehren and Nusbaum, 1992).

Lee *et al.* (1999a) proposed that lactose acts as a diluent due to the observation of decreased in-process viscosity with increasing lactose concentration. As the Maillard reaction occurs when lactose is heated, colour change is a potential adverse effect when processing at temperatures of 85°C. It was observed that there was little change in colour up to 7.5% lactose content. The firmness of the product decreases with increasing lactose concentration, possibly due to protein replacement.

Lee *et al.* (1999a) found that at levels greater than 5% lactose, the increase in lactose level resulted in an increase in lipid droplet diameter, which was thought to be due to lactose replacing the protein at the oil-water interface. Moisture content increased with increasing lactose concentration, but the effect of the Maillard reaction on the moisture method was not considered. The variation in moisture content was attributed to variation in steam quality and the amount of moisture introduced with the lactose. Meltability (Arnott test) appeared to be unaffected by lactose levels despite the dilution effect. An unusually high meltability result for 5% lactose was observed but could not be explained. Crystal formation was observed at concentrations greater than 5%. At 10%, the crystals that were formed were sufficiently large to induce grittiness in the final sample (Lee *et al.*, 1999a).

2.3.8 Processing

The manufacture of MPCGs usually follows similar procedures to processed cheese manufacture. The area of process manipulation is not well understood with reference to MPCGs and tends to be *ad hoc*, dependent on the ingredients and mixing equipment. Processing (thermal and mechanical input) of the ingredient blend can be carried out in either a double-jacketed vessel (batch) or a horizontal tube with mixing augers (continuous). Processing conditions cover the range 80 – 100°C for 4 – 15 minutes under partial vacuum (Saunders *et al.*, 1995). Unpublished work at FRC has shown that MPCGs can be produced at lower temperatures.

Cooling rate of the molten product has an effect on the structure and characteristics of the product. Rapidly cooled samples have reduced levels of protein-protein interaction and give a softer, more spreadable product. In particular, hydrophobic bonds are dependent on the rate of cooling since they are predominant in the temperature range 60 – 80°C (Guinee, 1987).

During manufacture of processed cheese, a phenomenon called "creaming" occurs, which is described as the shortening of body of the molten mass. It is attributed to the separation of large hydrophobic casein micelles into sub micelles, which then stabilise the emulsion (Zehren and Nusbaum, 1992). During manufacturing, this phenomenon is observed as an increase in viscosity with time at a constant rate of heat and shear input (Berger *et al.*, 1989). This has also been observed in the manufacture of MPCGs from calcium caseinate, MPC 70 and Rennet Casein, but was absent in a sodium caseinate MPCG. The low level of calcium in the sodium caseinate was determined to be the reason for lack of structure formation (Lee *et al.*, 1998). Lactose and type of CSA used affect creaming properties of processed cheese (BK Ladenburg, 1993). The type of manufacturing equipment must be selected to suit the product being made, as shear and heat input affect the structure development of MPCGs.

FTRC has carried out a considerable amount of work within the MPCG area. They initially followed the processing method outlined in the Analog cheese handbook (Cox-Smith, 1987). The order of addition recommended involved dissolving the salts in 82°C water, adding this solution to the casein in a Hobart mixer and mixing until a homogenous, viscous mixture was obtained. The molten fat (93°C) is added and when the mixture has thinned, citric acid added to adjust the pH to between 5.8 and 6.0.

It was found that the viscous mixture that formed using the previous method was difficult to manipulate and order of addition was altered to allow easier mixing and shorter processing times. The molten fat was added to the casein following by the dissolved salts and acid.

Increasing processing time has been observed to increase firmness (Saunders *et al.*, 1996c; Petley-Hibbs, 2001), fracture modulus and decrease fracture strain (Bowland and Foegeding, 1999), meltability (Saunders *et al.*, 1996c) and lipid droplet size (Saunders *et al.*, 1996c; Petley-Hibbs, 2001). Similar results have been seen in processed cheese manufacture (Harvey *et al.*, 1982; Fox *et al.*, 2000).

3.0 MATERIALS AND METHODS

3.1 Raw Materials

The ingredients used were Rennet Casein (Alaren 799, edible Rennet Casein 90 mesh, batch code 1251 1274 U9016) - Fonterra Co-operative Group Ltd. (Wellington, New Zealand), milk protein concentrate (ALAPRO 4850, batch code 1277 AL13 U0686) - Fonterra Co-operative Group Ltd. (Wellington, New Zealand), calcium-deplete milk protein concentrate (ALAPRO 4861, batch code 1575 AL06 X0020) - Fonterra Co-operative Group Ltd. (Wellington, New Zealand), skim milk cheese (NZDRI Product 010025065) – Fonterra Research Centre Ltd. (Palmerston North, New Zealand), fresh frozen milk fat for recombining (FFMR, 99.9% fat) - Fonterra Co-operative Group Ltd. (Wellington, New Zealand), sodium chloride (food grade) - Dominion Salt Ltd. (Blenheim, New Zealand), disodium hydrogenphosphate (food grade) - Interchem Agencies (Auckland, New Zealand), lactic acid (80% w/w) – Nutrinova (Auckland, New Zealand).

Table 2 shows the composition of the protein sources as determined by the Analytical Services Group, Fonterra Research Centre Ltd., using the methods outlined in Section 3.3.2.

Table 2: Composition of protein sources

Protein Source	Total Protein (%)	Whey Protein (%)	Moisture (%)	Fat (%)	Lactose (%)	Calcium (mg/kg)
Rennet Casein	80.3	0.1	10.8	0.3	0.05	26.9
MPC	82.8	10.9	5.4	1.5	2.59	20.9
IX MPC	82.8	9.5	5.5	1.5		14.2
SMC	84.9	0.5	9.0	6.4	1.21	12.8

Formulation targets were P/W ratios of 0.4, 0.5 and 0.6. The fat to protein ratio and salt to protein ratio were kept constant for all samples at 1.0 and 0.08 respectively. DSP levels were adjusted relative to the calcium level of the protein source and lactic acid was adjusted to maintain a final product pH of 5.6.

The SMC powder was manufactured to attain as close a calcium to protein (C/P) ratio as possible to the IX MPC 85. The SMC C/P ratio was slightly lower (0.15) than the IX MPC 85 C/P ratio (0.17).

3.2 Processing of Milk Protein Composite Gels

3.2.1 Processing Equipment

The development of a manufacturing procedure and the formulations for the MPCGs was an important part of the experimental work. Different pieces of processing equipment were studied to determine which was the easiest to use and produced the most consistent gels. The comparison of two typical pieces of equipment used in process cheese manufacture is discussed in Appendix 2.0. Different compositions were investigated to determine the P/W ratio range within which each piece of equipment could be operated.

3.2.2 Processing Method

A comparison of different processing conditions is discussed in Appendix 5.0 and Appendix 6.0.

Salt (NaCl), disodium phosphate, lactic acid and water were placed in the Blentech cooker (model # CC45 Blentech Corporation, Rohnert Park, CA, USA) and mixed at ambient temperature at a mixing speed of 50 rpm. The protein powder was added slowly over a period of 2 minutes. The cooker was stopped to add the chilled, size-reduced FFMR and then mixing continued for a further 3 minutes at ambient temperature.

The direct steam injection was initiated, while simultaneously increasing the mixing speed to 120 rpm and pulling a vacuum of 20 kPa. The inlet steam was adjusted to ensure the product conformed to a pre-set heating curve and the temperature was monitored at 30 second intervals. An example of the temperature profile is shown in Figure 3.1: the red lines are the limits within which the temperature was controlled. At 70°C, the vacuum was turned off and heating continued until 85°C.

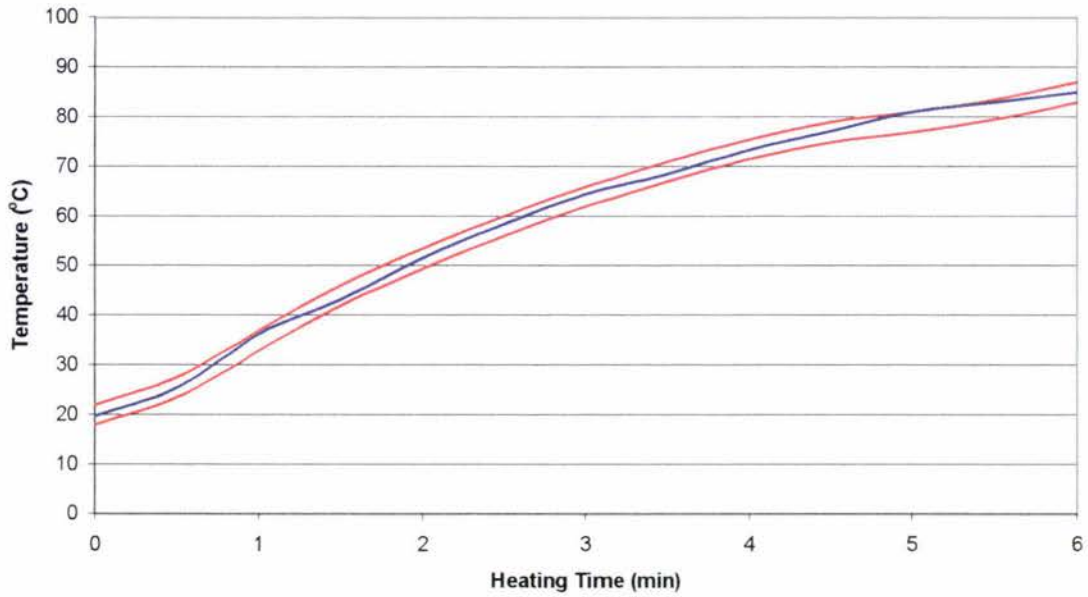

Figure 3.1: Temperature profile example for Blentech Cooker.

The sample timer was started and the 0 minute sample was collected in a 500 g container. The temperature was maintained via indirect heating and further samples were taken at 4, 8 and 16 minutes in 500 g containers. The samples were covered and allowed to cool for 15 minutes at room temperature before being placed in a 5°C storage room. The samples were left for 2 weeks to allow the pH and other physicochemical equilibrations to occur.

3.3 Analysis Methods for Milk Protein Composite Gels

3.3.1 Rheological Analysis

3.3.1.1 Dynamic Rheology

Dynamic rheology is a useful tool for determining the structure of the gel formed - entanglement network, weak or strong gel. Using a temperature sweep, the meltability of the sample can also be assessed. The dynamic oscillatory measurements were carried out using a Paar Pacifica UDS 200 rheometer (Physica Meβtechnik GmbH, Stuttgart, Germany) fitted with a 30 mm diameter serrated parallel plate with a gap of 2.0 mm. A Peltier serrated heating element was used as the bottom plate and set to a temperature of 5°C using a Viscotherm VT2 temperature controller (Physica Meβtechnik GmbH, Stuttgart, Germany). The data were collected using Physica software US 200 version 2.10 (Physica Meβtechnik GmbH, Stuttgart, Germany).

The gels were removed from the 500 g containers and cut into slices with a thickness of 2.0 mm using a drill press and a wire slicing attachment. The slices were stacked, then wrapped in polyethylene film, placed in airtight containers and stored at 5°C until required. The slices were unwrapped, cut into 30 mm diameter discs using a core borer, compressed between the two plates to a normal force of 1 N and left for 3 minutes to allow the sample to relax before commencement of the test. The exposed surface of the sample was coated in paraffin oil to prevent moisture loss.

Frequency Sweep: Frequency sweeps (0.0317 - 10 Hz) were carried out at a strain of 5×10^{-5}, which was within the linear viscoelastic region as determined by strain sweeps. The storage modulus (G'), loss modulus (G") and the complex modulus (G*) were recorded, where:

$$G' = (\sigma_0 / \gamma_0) \cos \delta$$

Equation 3.1: Calculation of storage modulus.

$$G'' = (\sigma_0 / \gamma_0) \sin \delta$$

Equation 3.2: Calculation of loss modulus.

$$G^* = G' + iG''$$

Equation 3.3: Calculation of complex modulus.

Where: σ_0 = stress (Pa)

γ_0 = strain (-)

δ = phase angle (°)

i = imaginary number $\sqrt{-1}$

The analysis of the small-strain parameters is discussed in the Results and Discussion Section 4.4.

Temperature Sweep: The storage modulus, loss modulus and complex modulus were recorded as the temperature of the sample was increased from 20°C to 80°C, at a rate of 1°C min^{-1}, with a constant frequency of 1 Hz and a constant strain of 5×10^{-5}.

3.3.1.2 Compression

Compression testing involves large strain, often resulting in fracture. This type of testing imitates the action in the mouth during sensory evaluation.

Two methods of large strain deformation testing were investigated to compare the standard New Zealand Dairy Research Institute (NZDRI) method with the method used by Food Technology Research Centre (FTRC) (Massey University, Palmerston North, New Zealand).

This work is discussed in Appendix 3.0 and Appendix 4.0. As a result of this investigation, the NZDRI method as outlined below, was adopted.

Six cylindrical samples were cut from the gels in the 500 g containers using a 20 mm internal diameter cork borer mounted on a drill press. The cylindrical samples were then sliced to a length of 25 mm using a wire cutter and a template. The cut samples were wrapped in polyethylene film, placed in airtight containers and held at 5 ± 1°C overnight.

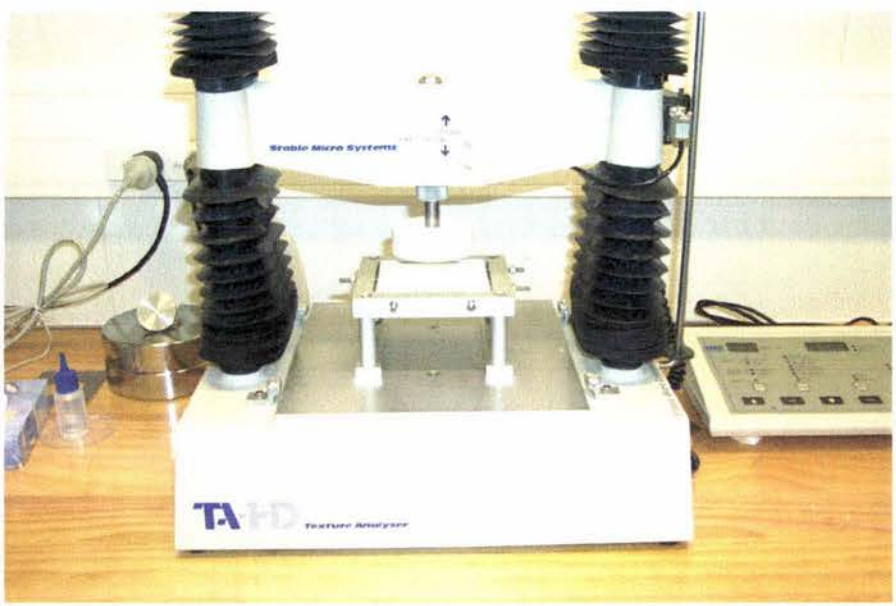

Figure 3.2: TA-HD Texture Analyser

The samples were compressed to 80% of their original height using a TA-HD Texture Analyser (Stable Micro Systems, Haslemere, UK) using a load cell of 500 N. The TA-HD used in this work is shown in Figure 3.2. The 60 mm diameter upper plate and the (95 x 105 mm) lower plate were made of Teflon and lubricated with paraffin oil (high viscosity) to minimise friction. Samples were tested at 5 ± 1°C and at a compression rate of 0.83 mm s^{-1}. The sample diameter used in calculations was the average of two measurements taken using a Digimatic micrometer (Mituoyo Corporation, Tokyo, Japan) prior to the beginning of the test. The fracture stress and fracture strain were calculated for each sample using a software package based on analysis methods outlined in draft standards for testing and analysis

protocol developed by the International Dairy Federation (IDF).[4] Details of the calculations are given in Appendix 1.0.

3.3.2 Chemical Analyses

The chemical analysis was undertaken to ensure that the product compositions matched the formulation target compositions. Each sample was held at 4 - 5°C before being tested 2 weeks after manufacture. All samples were tested for total nitrogen (TN), non-protein nitrogen (NPN), non-casein nitrogen (NCN), fat, moisture, pH, sodium, and calcium. The samples were analysed by the Analytical Services Group at Fonterra Research Centre Ltd.

3.3.2.1 Moisture

Aluminium containers, approximately 100 mm in diameter and 25 mm deep were placed in the oven and dried at 105°C for at least 30 minutes. The containers were cooled to room temperature in a desiccator and weighed (W_1). Approximately 10 g of shredded composite gel was placed in each container, before being weighed (W_2). The containers were placed in the oven at 105 ± 2°C for 16 hours. The containers were cooled to room temperature in a desiccator before being re-weighed (W_3). Moisture content was calculated as follows:

$$\text{Moisture (\%)} = (W_3 - W_1)/(W_2 - W_1) \times 100$$

Results are reported to the nearest 0.1% and duplicate determinations agreed to within 0.4% (American Public Health Association, 1985).

3.3.2.2 Protein

Total nitrogen content was determined using the Dumas method (International Dairy Federation, 2000). Samples of approximately 0.6 g were combusted using a Leco FP2000 instrument (Leco Corp., USA). Duplicates agreed to 0.4 % of the nitrogen content. The nitrogen content was converted to protein by multiplying by the factor 6.38.

[4] The draft standards were put together as a result of work done by the Joint Action Team on Rheological Tests for Milk Products, which is part of the IDF Standing Committee on Minor Components and Characterisation of Physical Properties.

3.3.2.3 Non-Casein Nitrogen

The sample preparation followed that of the total nitrogen before combustion, the casein was precipitated from the digested solution with acetic acid (International Dairy Federation, 1964) and the filtrate was then analysed by the Kjedahl method using a Tecator 2020 block digestor (Tecator, Sweden) as outlined in Section 3.3.2.4.

3.3.2.4 Non-Protein Nitrogen

The sample preparation was modified from the International Dairy Federation Method (1993). The filtrate was analysed for nitrogen by digesting with a Tecator 2020 block digestor (Tecator, Sweden), distilling and then titrating using a Tecator 1035 titration unit (Tecator, Sweden).

3.3.2.5 pH

The pH of the MPCG was measured using a Radiometer PHM 83 autocal pH meter (Radiometer, Denmark) with a Schott electrode (Germany). The probe was calibrated daily using Colourkey buffer solutions 4.0 and 7.0 (BDH Chemicals). The probe was cleaned daily by soaking in an acid pepsin solution. (British Standards, 1976)

3.3.2.6 Fat

The fat content was analysed using the Schmidt Bondzynski Ratzlaff method (International Dairy Federation, 1986). The sample was digested with hydrochloric acid, ethanol was added and subsequent extraction carried out of the acid-ethanol solution with diethyl ether and light petroleum. The solvents were removed by distillation and the mass of the fat remaining in the light petroleum was determined.

3.3.2.7 Calcium and Sodium

Samples were digested with nitric and hydrochloric acids using a commercial microwave system, then analysed by Inductively Coupled Plasma-Optical Emission Spectrometry (ICP-OES) (New Zealand Dairy Industry, 2001).

3.3.2.8 Salt (NaCl)

The salt content was determined with a Metrohm 702 Tritino and 730 Autosampler (Metrohm, Switzerland) (International Dairy Federation, 1988).

3.3.3 Determination of Microstructure

3.3.3.1 Confocal Microscopy

The microstructure analysis was conducted by Food Science section at the Fonterra Research Centre Ltd. The sample (approximately 5 mm x 5 mm x 5 mm) was frozen to –30°C in a Cryo-Cut Microtome (American Optical Company). The sample was allowed to equilibrate at –30°C for 30 minutes and was then sectioned into approximately 30 μm thick slices.

The frozen section was placed immediately on a glass microscope slide and stained with a solution containing the fluorescent dyes Nile blue (fat phase) and Fast Green FCF (protein phase). One drop of stain was placed on the cut surface and a cover glass placed on top, which spread the dye and prevented the section from drying out. The microscope slide containing the stained sample was kept at 5°C overnight to ensure maximum dye penetration before confocal examination the next day.

The two stains used to examine the protein and fat were:

Protein stain: Fast Green FCF "Gurr'Certistain' C.I. 42053, (BDH), prepared as a 0.33% solution in Citifluor (ALLTECH) a glycerol/PBS solution.

Fat stain: Nile Blue (hydrogen sulphate) "Gurr'Certistain' C.I. 51180, (BDH), prepared as a 0.33% solution in Citifluor (ALLTECH) a glycerol/PBS solution.

The samples were examined at 25°C with the 40X or 63X objective lens on using the TCS 4D Confocal Laser Scanning Microscope (Leica). The micrographs produced were combined images of the fat (red) and protein (green) phases.

3.3.3.2 Transmission Electron Microscopy

Fixation: The sample was cut into ~ 1 mm^3 cubes and put into a bijoux bottle containing 6.25% gluteraldehyde (Merck) in 0.2 M imidazole buffer (BDH). The imidazole buffer was adjusted to the pH of the sample and kept at 5°C over 2 days. The gluteraldehyde was rinsed twice with 0.2 M imidazole buffer at least 2 hours. The buffer was removed and the sample was then placed in 1% osmium tetroxide (Proscitech) in 0.2 M sodium cacodylate and kept overnight at room temperature. The sample was rinsed twice with distilled water (15 minutes each rinse). The sample was then placed in 1% uranyl acetate (Proscitech) for 30 minute and then rinsed twice with distilled water as before.

Dehydration: The dehydration process was carried out at 5°C in 25% acetone (BDH) for 15 minutes then in 50%, 70% and 90% acetone for 30 minutes each followed by 100% acetone (3 changes of solution over 90 minutes).

Embedding: The acetone was replaced with Procure 812 embedding resin (Proscitech) and put on rollers for 24 hours. A cube of the sample was placed into a BEEM embedding capsule (Proscitech) and this was cured at 60°C for 48 hours.

Sectioning: The embedded samples were then sectioned to a thickness of 80-90 nm using the Ultracut R microtome (Leica Microsystems, Vienna, Austria). These sections were then mounted on 3.05 mm copper/rhodium grids (Proscitech) and stained using lead citrate (BDH), before examination in a Transmission Electron Microscope (TEM) (Philips 201C, The Netherlands) at an accelerating voltage of 60 kV.

The grids containing the sections were filed and stored in a grid-box (Proscitech).

3.3.4 Meltability

3.3.4.1 UW Meltmeter Method

This method utilises a meltmeter (University of Wisconsin, Madison, USA) and is adapted from Wang *et al.* (1998). The gels were cut into cylinders using a 30 mm diameter cork borer on a drill press and cut into 7 mm thick slices using a wire cutter before being wrapped in polyethylene film and stored at 5°C overnight in airtight containers. The meltmeter was allowed to equilibrate to 60°C and the operating surfaces were cleaned, sprayed with silicone oil and then lubricated with paraffin oil. The sample was placed in the apparatus and allowed to equilibrate to the test temperature for 8 minutes after which the top plate was lowered instantaneously and height measurements recorded for 4 minutes. The data were analysed using Sigmaplot (version 4.01, SPSS Inc.) software to give an empirical ratio of final height to initial height. The software currently available to determine the fundamental parameters has been found to be inaccurate due to calculation errors and is currently being modified (Watkinson, P., 2002, personal communication).

4.0 RESULTS AND DISCUSSION

Four protein sources, three P/W ratios and four processing times were used to produce MPCG samples. The samples were analysed for microstructure (confocal microscopy, TEM), large- and small-strain rheological properties, and meltability. The processing times refer to the time spent in the Blentech cooker at the maximum temperature of 85°C.

4.1 Chemical Analysis

Chemical analysis was undertaken on the final products to ensure that formulation targets were met. The results shown in Table 3 (p 42) are the average of the two duplicates (except for SMC P/W 0.5 and 0.6). The targets for P/W ratio were 0.40, 0.50 and 0.60. The target for total protein to fat ratio was 1.0.

The calcium level of the SMC was manipulated during manufacture by lowering the pH of the curd. The aim was to achieve the same calcium:total protein ratio as the IX MPC 85, but it can be seen that the ratio was slightly lower (7%) than targeted. The calcium:total protein ratio in the MPC 85 was much lower (19%) than the Rennet Casein, probably due to calcium loss during diafiltration as part of the manufacturing process of MPC 85. As some authors feel that whey proteins may act as inert fillers (Spangler *et al.*, 1990), the calcium to casein ratio should be considered. The calcium to casein ratios for Rennet Casein and MPC 85 were close. The calcium to casein ratios of the calcium-depleted powders were significantly lower than Rennet Casein and MPC 85.

The chemical analysis results showed some discrepancies. As protein is the only source of calcium in the product, the calcium:protein ratio should be constant across all P/W ratios within each protein source, which was not the case for Rennet Casein and SMC. The first SMC P/W 0.6 sample had much lower sodium and calcium levels than expected (highlighted in blue in Table 3) although the ratio of Ca/Na is still in agreement with the other results. As the calcium and sodium samples are tested from the same solution, it is likely that there was a dilution error in the sample preparation.

In most cases, the F/P ratio and the P/W ratio were close to target except the P/W 0.5 and 0.6 SMC samples (highlighted in red in Table 3). The majority of the chemical analysis results show that the compositions are on target. The analytical results of the second P/W 0.6 sample were discarded because it is believed that errors in the analytical testing are the cause of the

discrepancy, as in the case of the low sodium and calcium results mentioned above. The texture data and confocal images indicate that there was no significant difference between the duplicates.

The SMC P/W 0.5 samples both have lower protein levels than the target and are close in composition. The samples do not demonstrate any appreciable differences from one another except for fat droplet size in the confocal microscopy. One of the SMC P/W 0.6 samples also had lower than expected protein levels. No explanation for the low protein contents could be found.

The whey protein levels of the Rennet Casein and SMC are much higher than expected (theoretically less than 0.05%). There were two abnormal IX MPC results P/W 0.4 IX MPC 85 had a higher whey protein level than expected (2.3%) and the P/W 0.5 lower than expected (2.6%), while the MPC 85 are all as expected. The expected values are calculated from analysis of the protein powders and the formulations. The calculation to determine whey protein levels is as follows: (NCN – NPN) x 6.38

The problem of higher apparent whey protein has been encountered previously in the analysis of processed cheese at FRC and is thought to be due to the emulsifying salts either hydrolysing the protein during sample manufacture or preventing some of the casein from precipitating during analytical testing (Conaghan, E., 2002, personal communication). The whey protein aggregates in the MPC 85 and IX MPC 85 samples would be expected to precipitate with the casein during NCN testing (Newstead, D., 2002, personal communication).

Some exploratory testing was carried out to determine the cause of the elevated whey protein levels. It was suggested that the enzyme, chymosin, may still be active in the SMC powder, causing elevated level of protein in the NCN test. The SMC and Rennet Casein powders were tested for residual rennet and it was found that SMC does have active chymosin in the powder, while Rennet Casein does not. The reason for this is SMC has a lower wash temperature during manufacturing, which is insufficient to deactivate the enzyme (Elston, P., 2002, personal communication). The variation in the IX MPC powder whey protein levels is not related to residual rennet and therefore this was considered not to have contributed to the elevated NCN results.

Electrophoresis gels run on the NCN and NPN samples of both the SMC powder and a P/W 0.4 SMC gel showed little whey protein compared to what was calculated from the NCN and NPN tests. The levels found from the SDS-PAGE gel were more consistent with the levels calculated via the formulation. Reverse phase high-performance liquid chromatography (HPLC) showed a small amount of PP5 (a segment of β-casein cleaved by pepsin) present and some small peptides, possibly from the breakdown of caseins by other proteases. These small protein fragments may be sufficient to cause higher than expected NCN levels. Small peptides, depending on their charge, may carry over to the NCN and NPN. These peptides were found to be at levels consistent with the apparent increase in the whey protein content (Elgar, D., 2002, personal communication).

As the amounts are small, inhomogeneity in the samples taken may have a large effect on the result. The reason for some powders being affected and others not was beyond the scope of this work. There is a need to develop a more accurate method of determining casein and whey protein levels in MPCG products.

Table 3: Chemical composition of samples (duplicates averaged except SMC P/W 0.5 and 0.6)

Protein Source	Target P/W ratio	P/W ratios for duplicates	Target Protein (%)	Total Protein (%)	Whey Protein (%)	Fat (%)	F/P Ratio	Moisture (%)	Calcium (mg/kg)	Ca/total protein (mg/kg)	Ca/ casein (mg/kg)	Na (mg/kg)	Ca/Na ratio
Rennet	0.4	0.40, 0.41	21	21.1	1.3	20.4	0.97	51.8	6490	308	327	10600	0.6
Casein	0.5	0.49, 0.50	23	23.3	-	23.2	1.00	47.3	7910	339	-	11900	0.7
	0.6	0.59, 0.60	25	25.4	-	25.5	1.00	42.3	8330	328	-	12700	0.7
SMC	0.4	0.40, 0.39	21	21.6	1.0	20.9	0.97	54.6	3270	151	159	8210	0.4
*	0.5	0.46	23	22.4	0.4	24.6	1.10	48.9	3570	167	159	8970	0.4
*	0.5	0.45	23	22.1	1.9	24.8	1.12	48.6	3420	155	169	9510	0.4
	0.6	0.59	25	25.4	1.4	26.2	1.03	43.4	2830	111	118	7160	0.4
*	0.6	0.54	25	23.2	0.6	27.4	1.18	43.0	4200	181	186	10100	0.4
MPC	0.4	0.40, 0.39	21	20.8	2.3	20.9	1.00	53.1	5580	268	302	9120	0.6
85	0.5	0.48, 0.49	23	23.0	3.0	22.0	0.96	47.5	6020	262	301	10350	0.6
	0.6	0.59, 0.60	25	25.3	3.3	25.5	1.01	42.6	6595	261	300	11300	0.6
IX	0.4	0.39, 0.38	21	20.3	3.2	21.3	1.05	52.7	3620	178	212	10900	0.4
MPC	0.5	0.49, 0.47	23	22.9	2.2	23.9	1.04	47.0	4050	177	196	12250	0.4
85	0.6	0.59, 0.57	25	24.6	3.1	25.9	1.05	42.3	4340	176	202	13000	0.4

* Both SMC 0.5 samples and one SMC 0.6 sample had low protein levels leading to low P/W and high F/P ratios.

4.2 Microstructure

When comparing confocal images between samples with different P/W ratios it must be remembered that the total fat content increased from approximately 21 – 26% (w/w). The image analysis software, which is used to automatically measure fat particle size, was unable to accurately distinguish fat/protein interfaces for the MPC 85 and IX MPC 85 samples due to areas of aggregated fat droplets. As a result, comparisons of confocal microscopy images were carried out visually to assess droplet size, shape and distribution.

The confocal images show the protein phases (green) and the fat phase (red), with black areas caused by air bubbles in the product. Because the confocal images are of a cross section of gel with a thickness of 30 μm, there may be areas where the top of a fat droplet or air bubble has been included in the section beneath a layer of protein, leading to a duller green area.

The nature of cross sectioning leads to projected areas that are not necessarily representative of the actual size of the fat droplet/air bubble. Figure 4.1 shows two different points at which a droplet or bubble may be sectioned and the resulting projected area that would be seen by confocal microscopy. The red and blue lines correspond to the red and blue projected areas respectively.

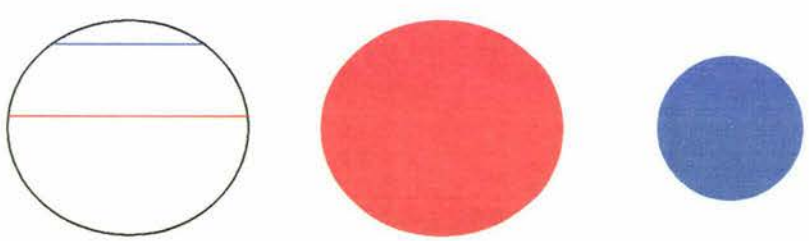

Figure 4.1: Effect of cross sectioning at different points in a fat droplet or air bubble.

The implication of this is that images with only a few droplets may not be representative of the actual size distribution, while images containing many fat droplets are more representative of the actual distribution. With hundreds or thousands of drops it is statistically unlikely that all the drops have been sectioned at the blue line, hence is still valid to compare size droplet distribution in the confocal images. As the TEM images show fewer fat droplets, the use of fat droplet size analysis is not suitable. Instead, the purpose of the TEM is to examine protein structures and the fat-protein interface. Consequently, the effect of sectioning must still be

considered in the case of a protein-coated particle being sectioned across the top, which would result in a dense area of protein being seen.

TEM was carried out on P/W ratios of 0.4 and 0.6 samples for all protein sources at 8 minutes, as this was the first processing time at which all the formulations had produced a gel.

4.2.1 Rennet Casein

The processing times refer to the time spent in the Blentech cooker at the maximum temperature of 85°C. Fat droplet size decreased with increased processing time for all P/W ratios (Figure 4.2, p 47). Rayan *et al.* (1980) found the same trend in processed cheese and Saunders *et al.* (1996c) in a Rennet Casein (P/W 0.3) composite gel. Increased processing time improved emulsification, resulting in a more continuous protein phase and smaller fat droplets. The heat and shear during mixing help hydrate and solubilise the protein and reduce the size of the fat droplets, with the soluble protein stabilising the fat droplets and preventing coalescence.

Increasing P/W ratio also resulted in decreased fat droplet size. In contrast, Thompson and Hewitt (2000) found an increase in fat droplet size with increasing P/W ratio, which was attributed to less protein being available for emulsification. The authors observed that the protein phase became denser with increasing P/W ratio and the trend was attributed to aggregated material (possibly undissolved protein). However, the result was most likely due to the inability of the equipment to adequately mix high viscosity samples. However, the authors found that gel strength increased with increasing protein concentration, which agrees with the current work and other literature discussing protein concentration. In most cases in the work of Thompson and Hewitt (2000), the P/W 0.4 and 0.5 samples were processed for approximately half the length of time than the P/W 0.3 samples, as these samples became too viscous for the equipment (a laboratory-scale Stephan cheese kettle) to mix.

A decrease in fat droplet size with increasing protein concentration was observed, seen in Figure 4.2. In theory, if protein hydration is not a limiting factor, the increase in protein concentration should assist emulsification, as more protein is available. This would support the observation of a decrease in fat droplet size. However, all ingredients are kept constant relative to the protein as P/W ratio increases, except for water. Efectively, an increase in P/W ratio is a decrease in moisture content. As a result, the amount of fat requiring emulsification increases proportionally as the protein concentration increases and the amount of water available to hydrate the protein decreases. Less water should result in more protein remaining unhydrated and therefore unable to emulsify the fat. Consequently, two observations should be made: the fat droplets would be expected to be larger, and; more unhydrated protein would be visible in the TEM images. Neither observation was made.

The decrease in fat droplet size with increasing protein concentration may be due to an increase in viscosity of the sample while in the cooker. At a constant shear rate, which is a function of the auger speed, the increase in viscosity results in an increase in shear thus producing smaller fat droplets.

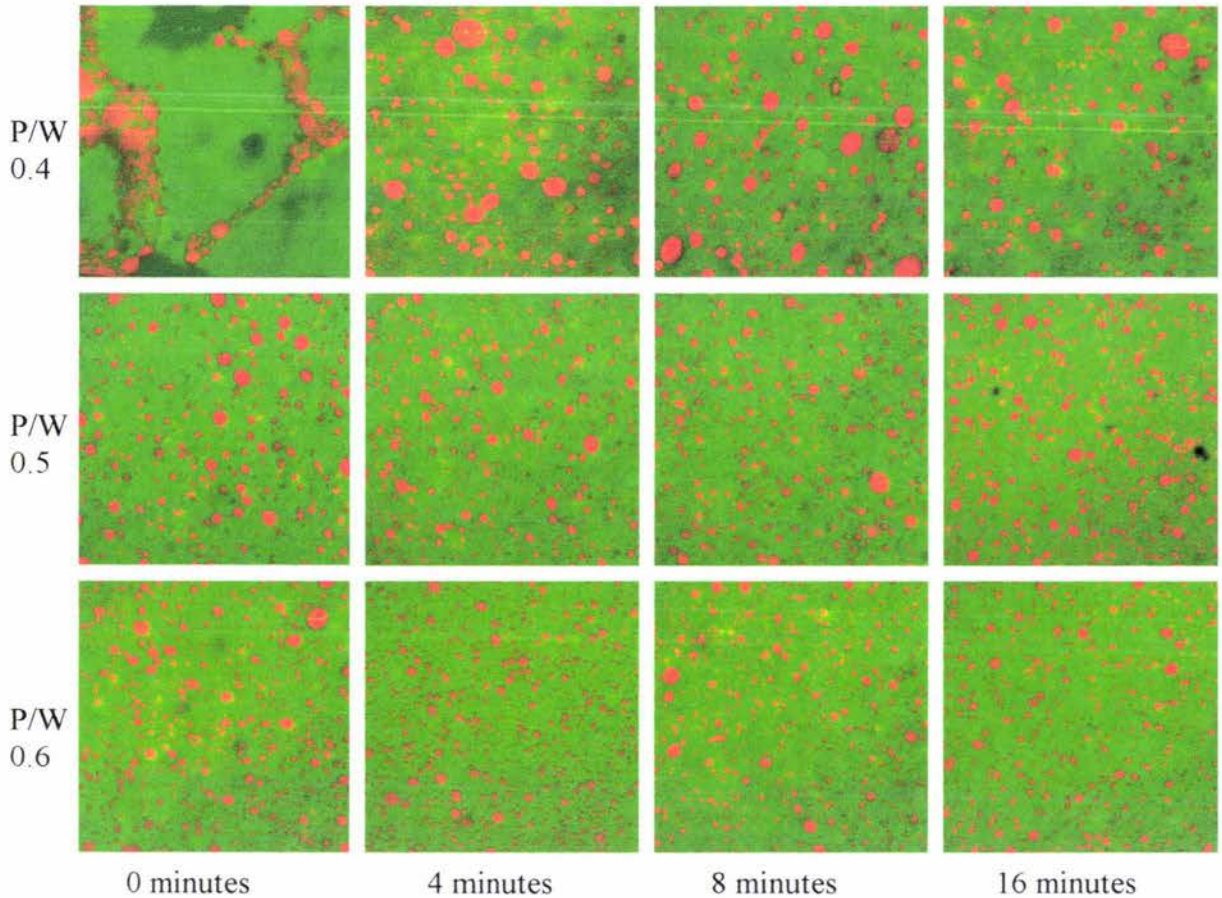

Figure 4.2: Confocal images of Rennet Casein composite gels (P/W 0.4, 0.5 and 0.6) with increasing processing time (400x magnification).

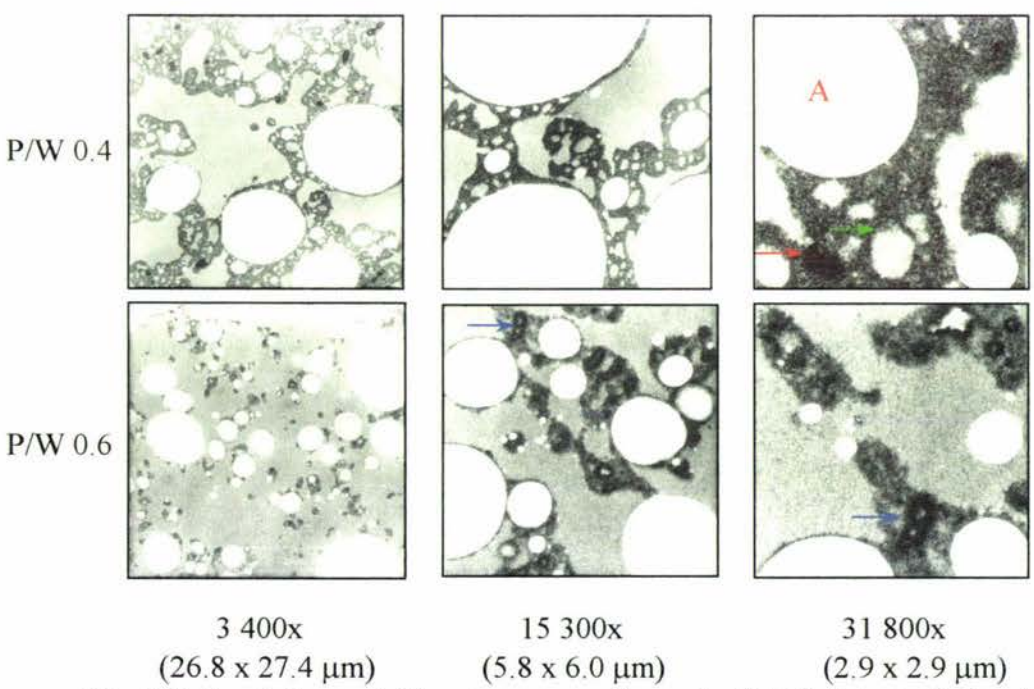

Figure 4.3: TEM of Rennet Casein composite gels (P/W 0.4 & 0.6) at 8-minutes processing time.

Figure 4.3 shows the TEM images of the P/W 0.4 & 0.6 samples processed for 8 minutes at increasing magnifications. The area labelled "A" indicates a fat droplet. Three different types of protein phase exist: 1) a homogenous dispersion of protein in the aqueous phase; 2) a more concentrated phase associated with the fat droplets that encapsulated small areas of the former phase (green arrow); and 3) small areas of very dense protein (red arrow), also encapsulated in the second phase. This observation has not been noted in prior work done at NZDRI[5] on Rennet Casein composite gels (Hirst, R., 2002, personal communication). This phenomenon has been seen previously in the TEM images of protein mixtures, such as dispersed egg-white particles in gelatin (Ziegler and Foegeding, 1990) and acid-heat-induced milk protein gels (Harwalker and Kalab, 1988), which have shown the presence of "capsules". These capsules occur in systems containing two different types of protein and have a dense outer protein coat that surrounds a protein gel network. The enclosed gel network is similar to the network that would usually be formed in the absence of the second protein.

There was no indication of intact micelle structure in Figure 4.3 or in any of the TEM images for other protein sources. The combination of processing conditions, pH and emulsifying salts probably resulted in significant dissociation of the casein micelles into their constituent proteins. Casein micelles would be expected to be visible at the magnifications used in this experimental work. Even at 72 000x magnification (not shown) there was no evidence of micelle or sub-micelle structures. For example, the 72 000x magnification images are 1260 nm wide, which would theoretically fit 2 – 6 micelles side by side. An example of a casein micelle in normal skim milk as viewed by TEM can be seen below in Figure 14.

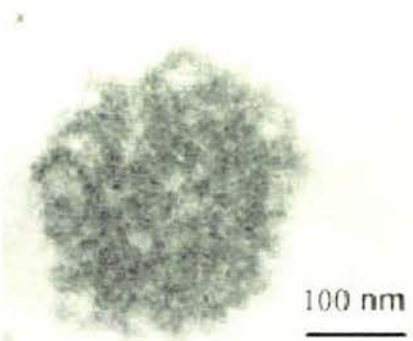

Figure 4.4: TEM image (85 000x) of a casein micelle. [Taken from McMahon and McMannis (1998).]

[5] Currently known as the Fonterra Research Centre Limited (FRC)

Electron dense areas (dark areas) were seen in all TEM images and may be the result of gluteraldehyde and osmium tetroxide, as described by Parnell-Clunies *et al.* (1986). Similar electron dense areas have also been noted by Petley-Hibbs (2001) and Aguilera *et al.* (1993). Aguilera *et al.* (1993), who studied whey proteins in an agar gel, found that the electron dense particles (<0.1 μm) were associated with the outer edge of fat droplets, but neither in the fat droplets, nor in the agarose phase and they were believed to be associated with the protein phase surrounding the fat gobules. Petley-Hibbs (2001) cited osmium artefacts and polyunsaturated fats as possible causes of the electron dense regions. Tamime *et al.* (1999) found electron dense particles in processed cheese analogues that were thought to be undissolved protein aggregates or fat-substitutes. They identified two kinds of electron dense particles. Against the background of fine-grained proteins, small dense dark spherical particles with sharp outlines of <1 μm were found, that were almost always associated with the fat droplets. A second kind of particle that was larger with a smooth texture was also seen. The TEM observations of Tamime *et al.* (1999) were complicated by the fact that two of the fat replacers used were protein based (electron dense) and one was carbohydrate based (electron translucent).

The electron dense particles (Type 3 protein phase) seen in this experimental work are thought to be undissolved protein powder particles. The particles are uniformly dispersed throughout the protein phase, indicating that they are probably not artefacts of the staining process. Many appear to have light areas in the centre, indicating less protein (blue arrow). The drying process of milk protein powders has been observed to result in a relatively insoluble shell of protein around a soluble protein centre. The dense particles shown in the TEM images in Figure 4.3 could be the remnants of milk protein powder particles that have not been dissolved during the manufacturing process. Previous authors have not found a conclusive explanation for the phenomenon of electron dense particles and further work should be carried out to determine the cause.

Figure 4.3 shows that there is less of the intermediate concentration protein phase (Type 2). As mentioned earlier, if water for hydration is not a limiting factor, the increase in protein concentration should assist emulsification, as more protein is available.

At 0-minutes processing time, the P/W 0.4 sample did not display a continuous protein phase. Protein particles surrounded by fat can be seen clearly in Figure 4.2. The protein was not hydrated sufficiently to allow the stabilisation of newly formed fat droplets before the

temperature reached 85°C, resulting in large areas of fat and protein. After 4 minutes of processing, the protein had formed a continuous phase; enclosing spherical fat particles. Further processing of up to 16 minutes reduced the number of larger fat droplets. It is also probable that the low protein level resulted in a low viscosity product, which at the given shear rate, resulted in insufficient shear stresses to adequately mix the fat into the protein network before the final temperature of 85°C was reached. Although the 0-minute processing time sample appears to be poorly emulsified on a microscopic scale, the sample did not appear to be different from the subsequent samples during large- and small-strain sample preparations. The TEM images in Figure 4.3 show that Type 1 and Type 2 protein phases are equally dominant. All the fat droplets are enclosed within the Type 2 protein phase. There does not appear to be any of the most concentrated protein phase (Type 3) associated with the more dilute aqueous phase (Type 1).

The mid-range protein level (P/W 0.50) consisted of a continuous protein network encapsulating fat droplets at all stages of processing. The 16-minute processing time sample showed several black areas indicating air bubbles in the product.

The TEM images in Figure 4.3 (P/W 0.6) show that the dominant protein phase is the more dilute aqueous phase (Type 1), although some of the Type 2 phase is still evident and associated with the fat droplets. A higher P/W ratio sample may be expected to exhibit more of the concentrated protein phase, due to less water available to hydrate the protein, but this is not the case. The greater viscosity of the high P/W ratio samples in the Blentech cooker, leading to greater shear stresses, may allow better mixing between the water, protein and fat, resulting in better hydration and smaller fat droplets. Improved hydration would lead to more of the concentrated protein phase being incorporated into the aqueous protein phase and the lipid-water interface. The smaller fat droplets provide increased area of the lipid-water interface for the hydrated proteins to become associated with, also decreasing the extent of the concentrated protein phase. Decreasing fat droplet size with increasing P/W ratio may also be due to the higher total fat concentration, leading to more fat-auger contact, which breaks the fat up into smaller droplets.

4.2.2 Skim Milk Cheese

As in the case of Rennet Casein, the fat droplet size decreased with increasing processing time and increasing P/W ratio (Figure 4.5) as discussed in Section 4.2.1.

The fat droplets in the SMC P/W 0.40 sample were larger than those of the corresponding Rennet Casein sample. Removing calcium from the renneted micelles was expected to dissociate the micelles into their soluble constituent proteins, which would then be available to adsorb at the new lipid-water interfaces. As a result, the emulsification ability of these proteins was expected to be higher than that of Rennet Casein, leading to smaller fat droplets. The reduction in calcium may have limited the amount of cross-linking in the protein network and formed a softer melt with lower in-process viscosity. As discussed in Section 4.2.1, higher viscosity leads to smaller fat droplets. As seen in the TEM images, there is no evidence of micelle or sub-micelle structure in either the SMC or Rennet Casein gels. This means that all of the individual proteins were available to play an active role in network formation and fat stabilisation for both protein source-based gels. Both protein sources are renneted to the same level (Elston, P., 2002, personal communication) so renneting should have little influence on the differences in properties between the two protein sources. The fat droplets for both were spherical, with little or no aggregation, but the fat droplets in the SMC samples appeared to decrease in size with processing time to a greater extent than in the Rennet Casein samples. This could be due to the Rennet Casein samples reaching a higher level of emulsification more quickly, with little change afterwards, while SMC required more heat and shear energy input to achieve the same level of emulsification. This was a surprising result as SMC has more soluble protein and this should to migrate quickly to the fat surface, increasing emulsification.

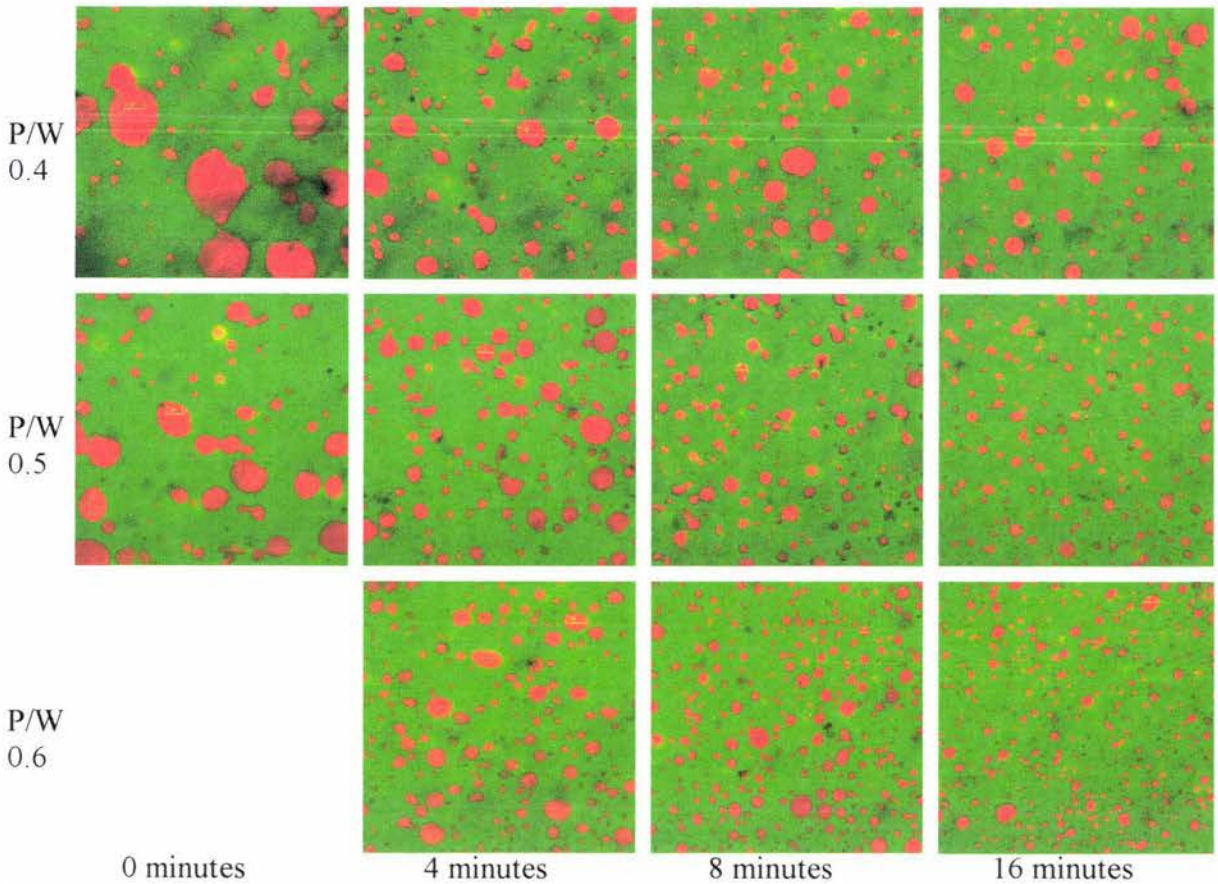

Figure 4.5: Confocal images of SMC composite gels (P/W 0.4, 0.5 and 0.6) with processing time (400x magnification).

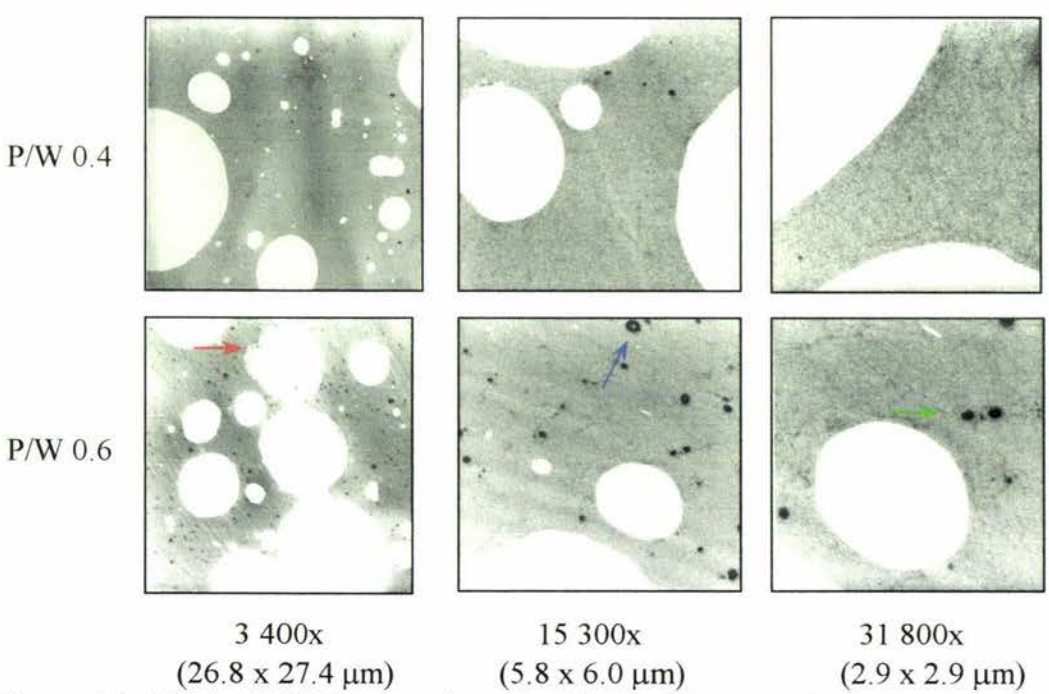

Figure 4.6: TEM of SMC composite gels (P/W 0.4 & 0.6) at 8-minutes processing time.

The duplicates had different fat droplet sizes at each P/W ratio, although there was little effect in terms of texture as determined by large-strain testing (refer to Section 4.3.3).

The SMC P/W 0.4 (Figure 4.5) had large fat droplets at 0-minutes processing time, with smaller droplets that did not appear to change significantly with time after 4-minutes processing. The duplicate sample had small fat droplets for all processing times, with only the 16-minute sample being visibly different, showing more of the smaller fat droplets. There appears to be little difference between the two duplicates with respect to chemical analysis (Table 3, p 42). Although the SMC P/W 0.4 0-minutes processing time sample shows large fat droplets, the protein in the TEM images appears to be much more evenly dispersed than the corresponding Rennet Casein sample.

The P/W 0.5 sample seen in Figure 4.5 (first duplicate in Table 3) had larger fat droplets than the duplicate. The chemical analysis shows that both the duplicates had lower than expected protein levels, although there is little difference between the two duplicates. The difference in microstructure did not appear to greatly alter the texture, so the practical implications of such a difference is small (refer to Section 4.3.3).

The P/W 0.6 duplicate (second duplicate in Table 3), which is not shown in Figure 4.5, appears to be the same except for the 16-minute processing time sample, which has a greater number of small fat droplets. This sample had a lower protein content according to chemical analysis.

Unlike Rennet Casein, the P/W 0.6 samples did not form gels at 0-minutes processing time. The lower calcium level in SMC should allow the micelles to disintegrate into their constituent proteins and form a network. The evenly dispersed appearance of the protein in the TEM images is in agreement with this theory. Lee *et al.* (1998) found that lower calcium contents lead to thinner melts while processing MPCGs. As all ingredients are kept constant with respect to protein, increasing the P/W ratio effectively decreases the amount of water available for hydration of the protein. The reduction of calcium was expected to improve solubility of the protein, allowing it to hydrate quickly and subsequently form a protein network. During processing, visual observations of the molten mass showed that the protein network appeared to form first with free fat being slowly incorporated into this network as the processing time increased. The network may have formed quickly with the available water,

excluding fat, and then required more shear stress and heat input than the other samples to incorporate the fat.

Figure 4.6 shows the 8-minute processing time sample at increasing magnification. The sample consists of a continuous aqueous protein phase with dark, electron dense areas evident. The intermediate (Type 2) and dense protein phases (Type 3) seen in the Rennet Casein gels are not present, indicating that all the protein (except the protein in the electron dense particles) is involved in either network formation or lipid-water interface adsorption. There is no accumulation of protein around the fat droplets, as seen in Rennet Casein.

The TEM images shown in Figure 4.6 displayed evenly dispersed electron dense particles, indicating they are unlikely to be artefacts of the staining technique. The same phenomenon of light areas (blue arrow) inside the particles, as seen in the Rennet Casein samples, is also present in the SMC samples and attributed to the insoluble powder particles as discussed in Section 4.2.1. The number of particles is much greater for the P/W 0.6 samples, supporting the theory that the particles are most likely protein-based.

Dark "strands" appeared to radiate from many of the electron dense particles (green arrow, Figure 4.6). This can be seen to a greater extent in the 0.6 P/W ratio samples (Figure 4.7).

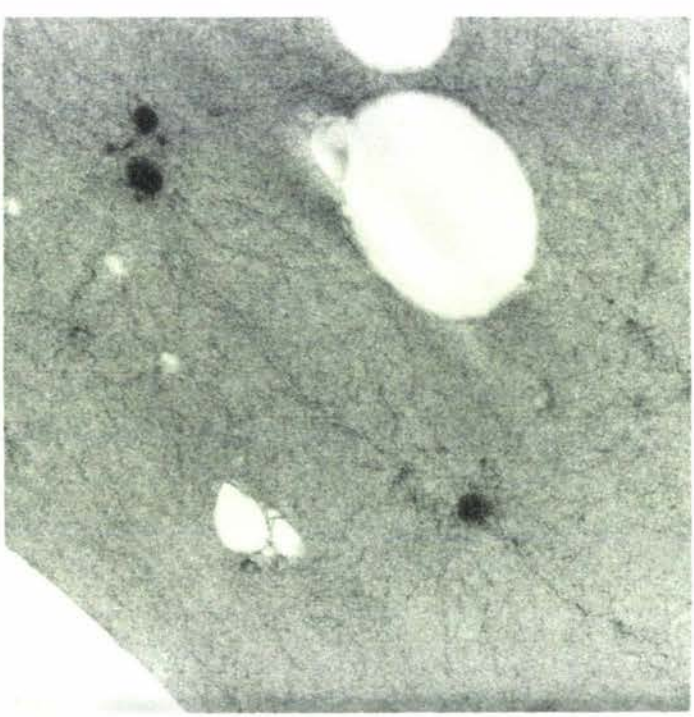

Figure 4.7: Enlarged TEM image of SMC illustrating the presence of electron-dense "strands".

This behaviour has not been noted in work by other authors citing electron dense particles present (Parnell-Clunies *et al.*, 1986; Aguilera *et al.*, 1993; Tamime *et al.*, 1999; Petley-Hibbs, 2001). This phenomenon was not seen in the Rennet Casein TEM images (Figure 4.3). The removal of calcium is thought to make the SMC soluble compared with Rennet Casein (Elston, P., 2002, personal communication). This phenomenon may be the highly soluble protein slowly dissolving from the powder particles, possibly during cooling and storage, into the aqueous phase.

The crystal (red arrow) (Figure 4.6) is thought to be a calcium phosphate crystal, as seen in Kalab *et al.* (1980). The calcium phosphate crystals grow during storage (Hirst, R., 2002, personal communication). Kalab *et al.* (1980) reported seeing calcium sequestering agent crystals in processed cheese after 10 minutes of processing at 82°C. It may be possible that other samples also contained some calcium phosphate crystals but were not observed in other images due to the small sample area involved in TEM.

Visual observations during processing indicated a stretchy product, similar to mozzarella. The samples could be stretched for several metres during packing at 85°C. This product may have potential in the analogue mozzarella market. It was difficult to match the heating profile once the temperature exceeded 70°C as the product appeared to have formed a fibrous protein network that did not allow steam to easily pass through it, resulting in hot and cold spots rather than an evenly distributed heat. The viscosity appeared to be higher for the lower P/W ratio samples compared to the corresponding Rennet Casein samples. This is in contrast to the work by Lee *et al.* (1998), which noted that reduced calcium resulted in lower in-process viscosities. The difference in ingredients and experimental procedure are most likely the cause of this is discrepancy.

4.2.3 Milk Protein Concentrate 85

The fat droplets appeared to decrease in size with increased processing time and increased P/W ratio (Figure 4.8). This agrees with the trends seen in the Rennet Casein and SMC samples. The MPC 85 samples showed considerable differences from the Rennet Casein and SMC samples with respect to the appearance of the fat. The fat phase consisted of aggregates of small fat droplets, rather than independent spherical fat droplets. Consequently, there appeared to be a continuous protein phase randomly interrupted by fat aggregates as opposed to the more evenly dispersed appearance of the Rennet Casein and SMC samples. With increasing mixing time, the fat droplets appeared to decrease in size and link together. This aggregation phenomenon has been seen in emulsions (30% oil, 3% protein) stabilised with MPC 85 (Hemar, Y., 2002, personal communication) and in work by Lee *et al.* (1998). A theory proposed by Yost and Kinsella (1992) for whey protein emulsions states that if there is insufficient protein available for fat surface coverage, fat droplets can share protein aggregates and a decrease in the size of protein aggregates and an increase in the number of fat droplets in a given area interfacial area is observed. During mixing, the shear stresses on the product break up the fat droplets into smaller ones, creating new interfacial area of the fat. In this system, there probably was sufficient protein available to cover the newly formed interfaces.

Dalgleish *et al.* (2002) stated that although the general belief is that caseins adsorb more readily due to their higher proportion of hydrophobic residues and the more flexible, open structure, the experiments that support this theory have mostly been conducted at room temperature with the maximum temperature being approximately 40°C. Dalgliesh *et al.* (2002) found that whey proteins have the ability to adsorb at the oil-water interface and displace casein. This exchange is almost undetectable at ambient temperatures, slow at 40°C and occurs within 2 minutes at 80°C. The workers found that α_{s1}- and β-caseins were replaced at the oil-water interface by α-lactalbumin and β-lactoglobulin and that the reaction was temperature dependent. At room temperature, the reaction was almost undetectable but at 80°C the reaction was complete after 2 minutes. Denaturation is not a prerequisite for adsorption but the whey proteins do become surface denatured. Gupta and Reuter (1993) found that unfolding of the whey protein molecules during heat processing improves emulsion stability by exposing hydrophobic groups that can orient at the oil and water interface. In solely whey protein systems, protein coated fat droplets have been observed to act as active

fillers in the protein network (McClements *et al.*, 1993; Aguilera *et al.*, 1993; Chen and Dickinson, 1998a; Chen and Dickinson, 1998b; Rosenberg, 2000). This was confirmed by the observation of fat droplets that were closely associated with the protein matrix using Scanning Electron Microscopy (SEM) (Yost and Kinsella, 1992). Most literature deals with dilute model protein systems, which are often at ambient temperature, and it should be noted that such theories may be not be transferable to a complex, high concentration, high temperature, and high shear system.

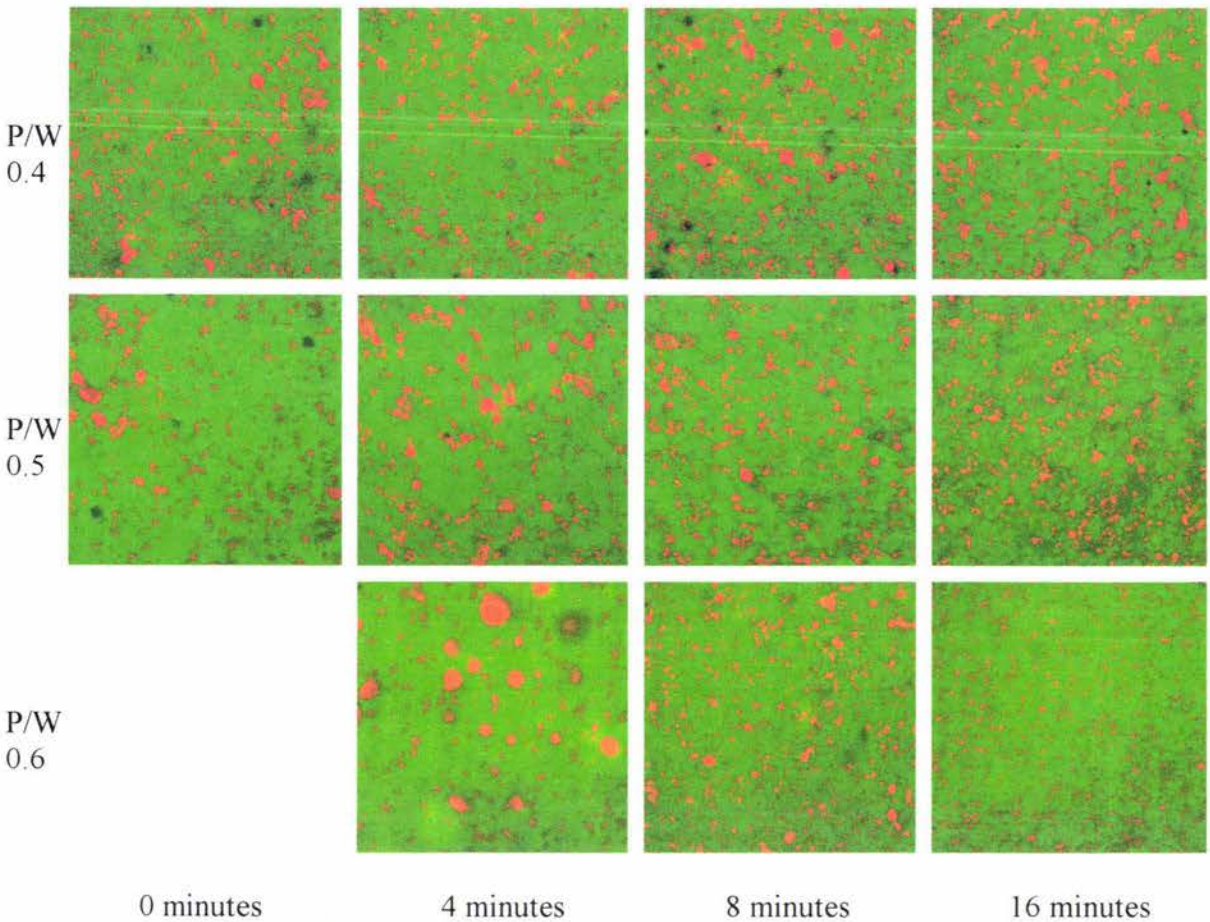

Figure 4.8: Confocal Image of MPC 85 composite gels (P/W 0.4, 0.5 & 0.6) with increasing Processing Time (400x magnification).

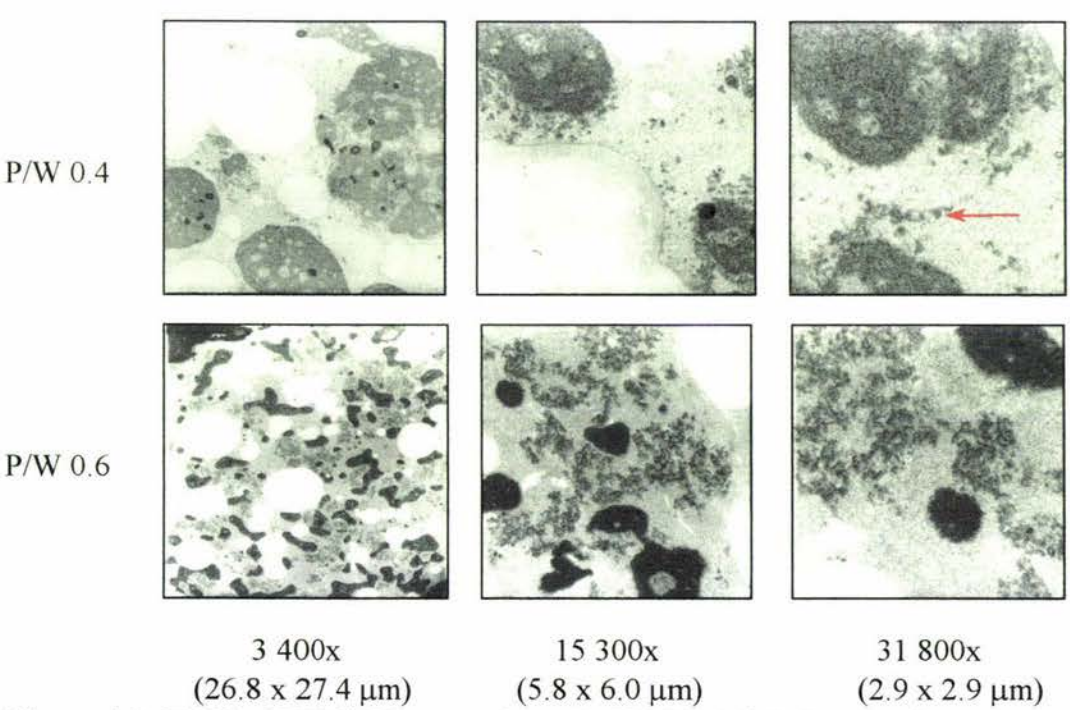

Figure 4.9: TEM of MPC 85 composite gels (P/W 0.4 & 0.6) at 8-minute processing time.

Processes that may be competing are:

- displacement of casein by whey proteins at the oil-water interface beginning at temperatures above 40°C (involving surface denaturation).
- denaturation of whey proteins at temperatures > 70°C, exposing hydrophobic and sulphydryl groups that may:
  - (i) aggregate with other denatured whey proteins and form clusters in the casein matrix;
  - (ii) adsorb at the oil-water interface; or
  - (iii) attach to hydrophobic residues of other whey proteins attached to fat globules.

At 0-minutes processing time, most of the whey proteins are likely to have been denatured.

Unlike in SMC gels, the fat droplets appeared to be surrounded by a layer of protein that was more concentrated than the protein phase surrounding it (Figure 4.9, p58). This may be whey protein as mentioned earlier with regard to the work of Dalgleish *et al.* (2002). It is thought that the aggregation is caused by whey proteins at the oil-water interface interacting with those attached to other fat droplets as they are brought into contact to one another via mixing in the kettle.

The MPC 85 sample contained the three distinct types of protein phase, as seen in Rennet Casein samples (Figure 4.9: P/W 0.4, 3 400x): the homogeneous, aqueous-based protein phase (Type 1); the highly concentrated protein phase (Type 2); and the intermediate concentration phase that encapsulates smaller areas of the two former phases (Type 3). The MPC 85 intermediate phase was not associated with the fat phase, as it was seen in the Rennet Casein samples. Again, there was no evidence of micelle-like structures, indicating that the constituent proteins had been released.

The red arrow (Figure 4.9) points to protein aggregates that were not present in Rennet Casein or SMC samples. It is thought that these were denatured whey protein aggregates as seen in work by Lee *et al.* (1999b). Few whey protein aggregates are near the oil-water interface in the MPC 85 gels (Figure 4.9), although there may have been individual whey proteins adsorbed. In the highest magnification image (31 800x), there appeared to be whey protein aggregates in the intermediate protein phase. The presence of these hydrophilic proteins in the intermediate phase may prevent this phase from associating with the fat droplet, as

previously seen in the Rennet Casein samples. Shimp (1985) observed that as whey proteins are the most water-soluble dairy proteins, they tend to stay in the bulk of the water phase and not concentrate at the water/lipid phase interface.

Aguilera and Kinsella (1991) proposed 3 ways that whey proteins could interact with casein in the formation of a network:

1. a casein gel, reinforced with whey proteins
2. a whey protein gel, disrupted by caseins
3. an emulsion gel with both proteins, reinforced by the lipid droplets

It appears that the whey proteins existed as separate domains within the casein network (Figure 4.9) as seen by Lee *et al.* (1999b).

In pure whey protein systems, the whey proteins are able to adsorb to the lipid-water interface, and in mixed protein systems, in which whey protein-coated fat droplets are added, the whey protein adsorbed to the interface is able to interact with the network (Aguilera *et al.*, 1993). In the MPC 85 samples, it does not appear that the whey protein aggregates (red arrow) have adsorbed to the interface, this was initially thought to be due to being less competitive than casein as a result of their hydrophilic nature. The results of Dalgleish *et al.* (2002) suggest that the fat/water interface (Figure 4.9) should consist of α-lactalbumin and β-lactoglobulin, which have displaced caseins and some remaining caseins (mostly α_{s2}- and κ-caseins). Not all of the whey protein available displaces the caseins and the exchange does not appear to be an equilibrium, and denaturation does not appear to be a prerequisite. As the TEM technique used in this experimental work does not distinguish between types of protein, this theory cannot be proven.

The work at Massey University was conducted at ambient temperature (Hemar, Y., 2002, personal communication) and from the work of Dalgleish *et al.* (2002), it would appear that the Massey work would most likely have predominantly casein adsorbed at the oil-water interface. The present work would be expected to have a significant proportion of whey protein at the interface, yet they both present microstructures involving fat droplet aggregation. The current work also involves a much higher level of protein, consequently introducing significant viscosity effects, as well as the effect of denatured whey proteins. It is recommended that this phenomenon be investigated in future work, as it expected to have an impact on the texture and possibly meltability of MPCGs.

The intermediate protein phase was diminished compared to the lower P/W ratio sample. This trend was also seen in the Rennet Casein samples. The existence of several different protein concentration phases is commonly seen in MPC 85-based composite gels and is attributed to insufficient hydration of the protein (Hirst, R., 2002, personal communication). The P/W 0.4 and 0.6 MPC 85 duplicates appeared similar in microstructure. However, the P/W 0.5 duplicate (not shown) had much larger fat droplets at 0-, 4- and 8-minute processing times, but the reason for the difference is unknown.

The P/W 0.6 MPC 85 sample did not form a gel at 0 minutes. MPC 85 powder has less casein than Rennet Casein and, in a low moisture content product, the amount of hydrated casein may be insufficient to emulsify the fat phase without additional heat and shear input. At 4-minutes processing time, a continuous protein phase had formed, enclosing large spherical fat droplets. After 8-minutes processing time, the fat droplets had been reduced in size to be equivalent to the lower P/W samples, but the degree of aggregation was much lower. At 16 minutes, the fat droplet size was reduced even further and the degree of aggregation was still very low.

4.2.4 Ion-Exchanged Milk Protein Concentrate 85

IX MPCs were developed to improve solubility of the powder, which should lead to better and faster hydration of the protein. Johns and Ennis (1981) found complete or partial replacement of calcium with sodium via ion exchange significantly increased WPC solubility, which affected the textural characteristics of the gels.

The IX MPC 85 samples showed a protein matrix containing areas of concentrated protein (lighter green areas, as indicated by the red arrow) as seen in the MPC 85 samples discussed in Section 4.2.3. The samples appeared to be like SMC at early processing times with large fat droplets, but become more like MPC 85 at longer processing times.

The P/W ratio 0.6 sample did not form a gel for the first two processing times (0- and 4-minutes processing time). It is thought that the combination of calcium reduction combined with whey proteins, resulted in a lower viscosity product with less hydrated protein capable of emulsifying the fat phase.

The three phases of protein concentration were evident in the TEM images (Figure 4.11). Denatured whey protein aggregates were present and appeared to be associated with some of the smaller fat droplets (red arrow). The whey protein aggregates may have been associated with the intermediate protein phase, although the stain is too dark to discern variations in protein density. There did not appear to be a thick layer of protein around the fat droplets, as seen in the case of Rennet Casein, although there will be some form of interfacial protein. The images did not show the same protein particles that are evident in the other protein sources.

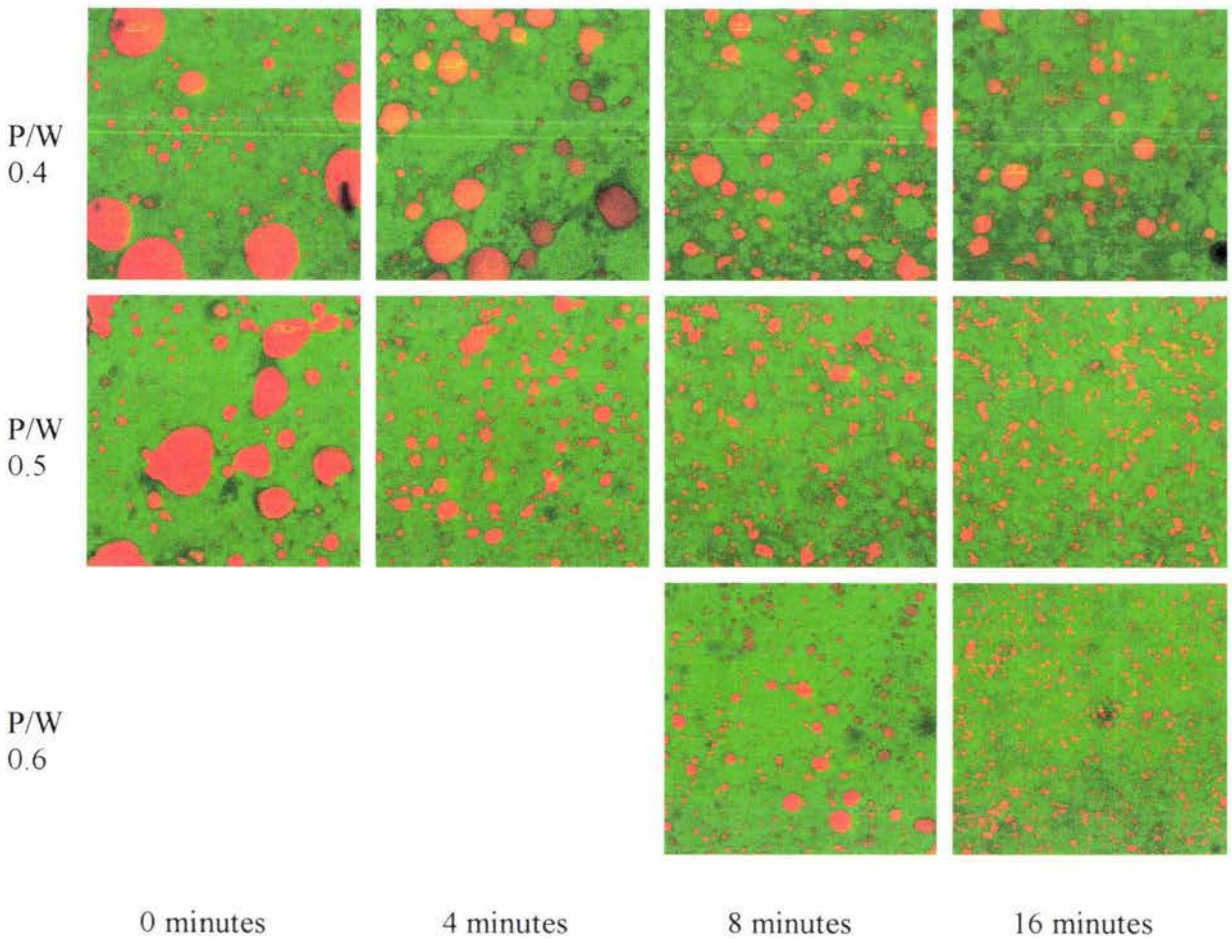

Figure 4.10: Confocal images of IX MPC 85 composite gels (P/W 0.4, 0.5 & 0.6) with processing time (400x magnification).

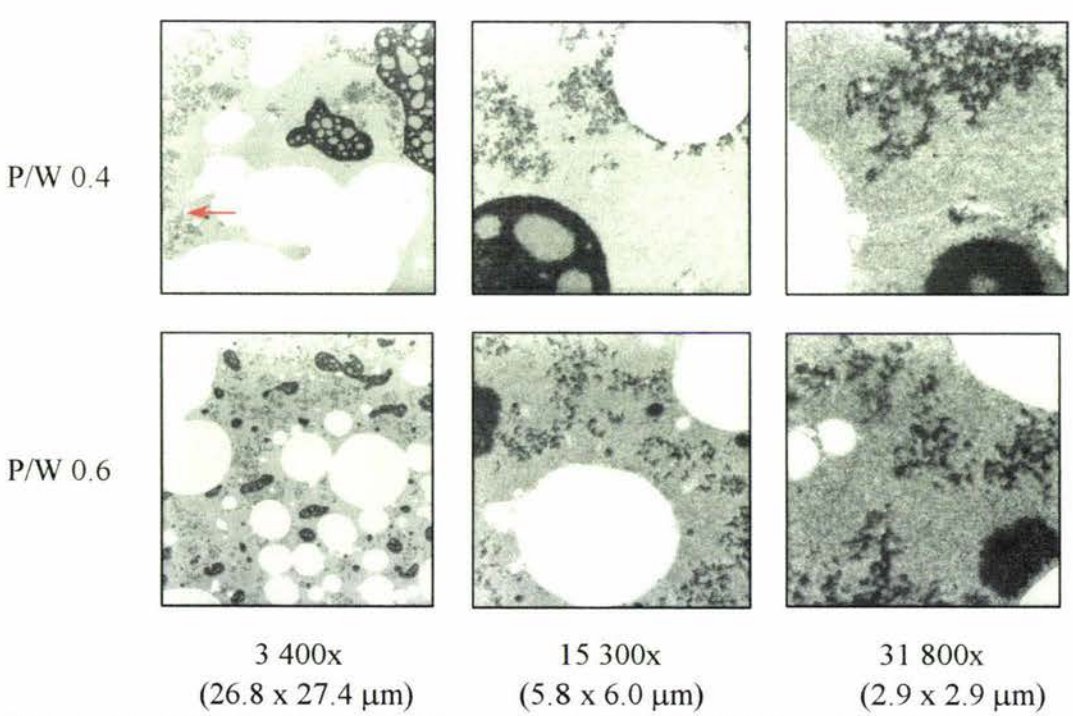

Figure 4.11: TEM of IX MPC 85 composite gels (P/W 0.40) at 8-minutes processing time.

All IX MPC 85 samples showed much larger fat droplets than the MPC 85 samples, which decreased in size and began to aggregate with increased processing time. The fat droplet size decreased with increasing P/W ratio, as with all of the other protein sources. The emulsification of the fat did not appear to be as good as in the MPC 85 samples, analogous to SMC not being as well emulsified as Rennet Casein. It is thought that the lower calcium level reduced shear stresses in the Blentech, resulting in larger fat droplets.

In the P/W 0.4 sample, the smaller fat droplets began to aggregate at 8 minutes. The P/W 0.50 4-minute processing time sample contained smaller fat particles that were beginning to aggregate. The size reduction and aggregation led to the 16-minute processing time sample resembling the MPC 85 samples.

No 0- and 4-minute processing time samples were produced for the P/W 0.6 samples because the fat had not been incorporated into the network at those times. From earlier samples, it was observed that a reduction in calcium or increase in whey protein content led to the requirement for extra shear and heat input in order to incorporate the fat. It is thought that, in the case of IX MPC 85, the calcium reduction and lower casein level had a cumulative effect, increasing the required shear and heat input to 8-minutes processing time. The size of the fat droplets decreased greatly from 4- to 16-minutes processing and the small fat droplets become aggregated (Figure 4.10).

4.3 Large Strain Rheology

Large strain rheological testing was carried out on all of the protein sources, P/W ratios and processing times. (The processing times were the length of time that samples were agitated in the Blentech kettle once they had reached the maximum cook temperature of 85°C.)

Fracture stress-fracture strain graphs have been used by Munro *et al.* (2000) to illustrate textural differences. This experimental work has adopted the use of textural indicators, as used by Truong and Daubert (2001) to investigate vane rheometry. The textural indicators show relative changes in texture:

- Brittle – high fracture stress, low fracture strain
- Mushy – low fracture stress, low fracture strain
- Rubbery – low fracture stress, high fracture strain
- Tough – high fracture stress, high fracture strain

For example, if the trend with increasing processing time is towards a higher fracture stress and lower fracture strain, the sample is considered to develop a more brittle texture.

4.3.1 Statistical Analysis Issues

Statistical analysis was complicated by the fact that much of the data were found to be non-normal in addition to having unequal variances.

Table 4: Non-normal data sets.

Protein Source	P/W ratio	Parameter
Rennet Casein	0.4	fracture Strain
	0.5	fracture stress
SMC	0.4 & 0.5	fracture stress & fracture strain
MPC 85	0.4	fracture strain
IX MPC 85	0.5	fracture strain

The Rennet Casein P/W 0.4 fracture strain was expected to be non-normal due to the crumbly nature of the product. The SMC P/W 0.4 and 0.5 samples were also expected to be non-normal as the results were at the limits of the testing procedure as discussed in Section 4.3.3.

Although analysis of variance (ANOVA) can be a powerful tool for analysing data, it is based on the assumptions of normality and equal variances. The data did not fit other probability distributions and no single transformation could be used to make the data conform to the assumptions. A non-parametric method was required to determine whether P/W ratio, protein source or processing time affected the rheological properties. The non-parametric tests do not rely on the assumption of normality but they cannot be relied upon for post-hoc multiple comparisons. The Kruskal-Wallis procedure tests whether there is a difference among several treatment groups, but does not identify where the difference lies. The method was used and as a result overall differences were identified, but no indication of the magnitude of the difference could be obtained. As a result, it was suggested that ANOVA be used and that the data be interpreted, bearing in mind that the assumptions underlying the method are violated (Crawford, R., 2002, personal communication). The statistics are included only as indicators of possible differences and as a result, expert opinion is required to interpret what the statistics suggest.

4.3.2 Rennet Casein

The fracture stress and fracture strain results for Rennet Casein composite gels in Table 5 are the averages for duplicate samples. The significant differences between samples at different processing times were determined by using ANOVA within each P/W ratio.

Figure 4.12 illustrates the changes in fracture stress and fracture strain with increased processing time for both duplicates at each P/W ratio. The differences described are with respect to changes relative to the textural indicators. The textural indicators are not absolute values but relative terms.

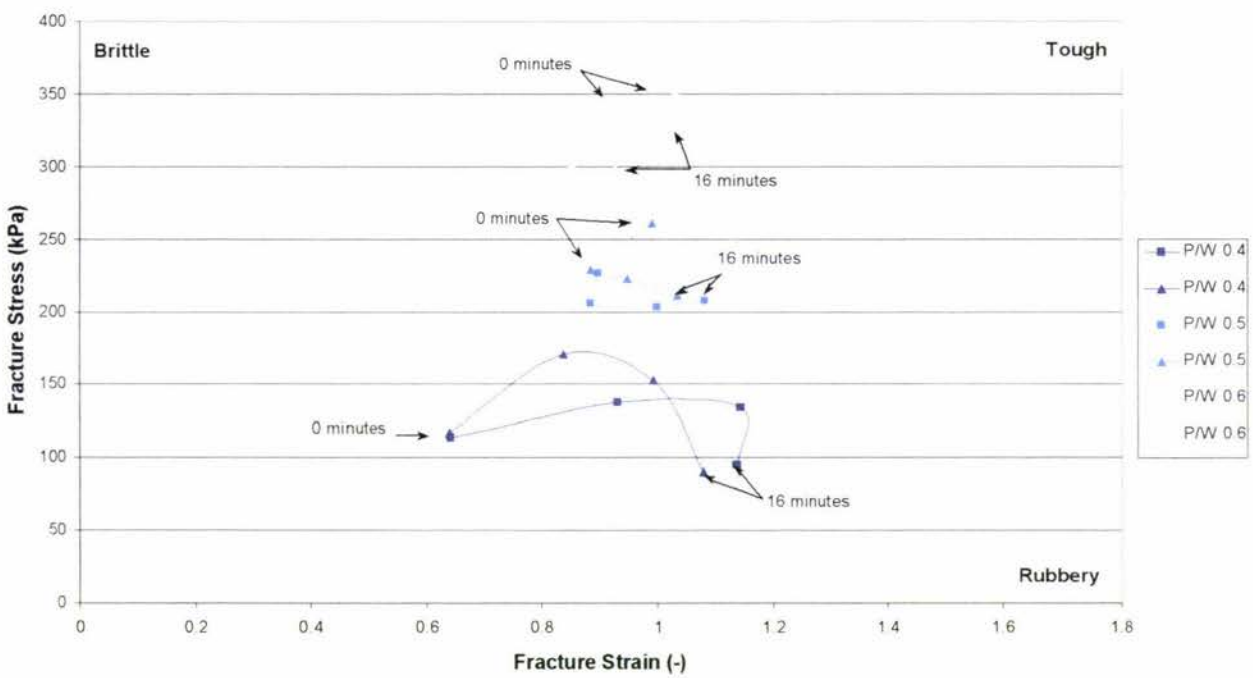

Figure 4.12: Fracture stress and fracture strain for Rennet Casein composite gel samples.

Table 5: Fracture properties for Rennet Casein composite gel samples (n = 2).

P/W	Processing Time (min)	Fracture Stress (kPa)	Fracture Strain (-)
0.4	0	115^{ab}	0.640^{a}
	4	155^{c}	0.886^{b}
	8	144^{bc}	1.068^{c}
	16	93^{a}	1.105^{c}
	All	**127^{a}**	**0.921^{a}**
0.5	0	242^{b}	0.941^{ab}
	4	218^{ab}	0.885^{a}
	8	211^{ab}	0.980^{ab}
	16	202^{a}	1.004^{b}
	All	**218^{b}**	**0.952^{a}**
0.6	0	344^{a}	0.982^{a}
	4	307^{a}	0.890^{a}
	8	321^{a}	0.984^{a}
	16	314^{a}	0.986^{a}
	All	**322^{c}**	**0.960^{a}**

For each parameter, superscripts with no letters in common denote significant differences between samples at $\alpha = 0.05$.
Significant differences were calculated within each P/W ratio.

The fracture stress decreased with increasing processing time, except for P/W 0.4 0-minute sample, while the fracture strain trend was dependent on P/W ratio. Increasing P/W ratio resulted significant increases in fracture stress, but little change in fracture strain.

The trend of fracture strain with processing time appeared to be dependent on the P/W ratio. The fracture strain for the P/W ratio 0.4 samples increased significantly, the P/W 0.5 samples demonstrated a minimum at 4-minutes processing time while the P/W 0.6 samples did not change significantly with increasing processing time.

During manufacture of process cheese, a phenomenon called creaming occurs as discussed in Section 2.3.8. The action of overcreaming processed cheese results in undesirable crumbly, brittle products due to the network proceeding beyond a desirable structure because of levels of ingredients or extent of processing. An overcreamed network would be reflected in increased torsional fracture stress and decreased fracture strain (Bowland and Foegeding, 1999). If plotted on a texture map, this would indicate a shift towards the brittle indicator (top

left corner). It appears that the samples were not overcreamed as the fracture properties did not move towards the brittle indicator.

The large change in fracture strain for the P/W 0.4 samples from 0-minutes to 4-minutes processing time may be attributed to the sample not being a continuous protein network at 0-minutes processing time. This can be seen in the confocal images in Section 4.2.1. The changes from 4- to 16-minutes processing time are not reflected by any obvious changes in the microstructure. The changes in texture after 4-minutes processing time may be due to changes occurring in the protein phase, such as, alignment of protein molecules or increased hydration.

The texture map (Figure 4.12) showed that the change of the P/W 0.4 samples with processing time was towards a more elastic nature, which agrees with the visible change of fracture during compression. During compression the change in texture was discernable to the eye: the 0-minute processing time sample crumbled, the 4-minute processing time sample broke into several large pieces, the 8-minute and 16-minute processing time samples remained intact. Walstra and van Vliet (1982) observed that fracture begins at the weakest point and that inhomogeneous samples lead to greater variability, which has implications for inadequately emulsified samples. Aguilera and Kessler (1988) noted that the size of the lipid droplets was found to be a critical factor in strengthening the matrix. If the lipid droplets are too large they disrupt the network, smaller droplets can sterically reinforce the network or the protein at the lipid-water interface can reinforce the network. Because the samples at 0-minutes processing time were not homogeneous, the lipid droplets disrupted the network and decreased gel strength. The difference between the P/W 0.4 duplicates is attributed to the "crumbly", inhomogeneous nature of the samples increasing the variability in the fracture data.

The increase in fracture stress with increased P/W ratio agreed with the TPA results of Thompson and Hewitt (2000), who investigated the effect of salt levels on Rennet Casein-based MPCGs at P/W ratios of 0.3, 0.4 and 0.5, and also with literature on increased protein levels in processed cheese (Zuber *et al.*, 1987; Gupta and Reuter, 1993) and MPCGs (Saunders *et al.*, 1996b).

The microstructure (Section 4.2.1) shows a decrease in fat droplet size with increased processing time, a trend also seen by Rayan *et al.* (1980) and Saunders *et al.* (1996c).

Contrary to the results of this experimental work, several authors have noted that decreasing fat droplet size coincides with an increase in firmness (Rayan *et al.*, 1980; Saunders *et al.*, 1996c; Fox *et al.*, 2000). Rayan *et al.* (1980) observed an increase in firmness from 0–5 minutes processing time, a smaller increase from 5-10 minutes and no change from 10-20 minutes processing time for processed cheese. Saunders *et al.* (1996c) attributed an increase in firmness with increased processing time (3 – 20 minutes) to a progressive increase in emulsification. The authors also found that increasing shear rate during processing led to an increase in firmness. An increase in firmness on the textural map would indicate a shift toward the "tough" indicator (an increase in fracture stress and strain). Most of the authors, however, have used TPA hardness, which would be more consistent with just the fracture stress.

According to the textural indicators, the P/W 0.5 and 0.6 samples became mushier from 0-minutes to 4-minutes and then started becoming more rubbery. The P/W 0.5 fracture strain values were not significantly different except the 4-minutes processing time sample, which was significantly lower. There were no significant differences in fracture stress or fracture strain between any P/W 0.6 samples.

4.3.2.1 Sensory Detection

Using the results of Pereira (2000) as a guide (minimum detectable difference in fracture stress of 18 kPa), the only difference in fracture stress for the P/W 0.4 in Table 5 that would not be detectable by sensory is the change from 4- to 8-minutes processing time. For P/W 0.5 the 4- to 16-minute processing time samples would not be different from each other but all the samples would be lower in fracture stress than the 0-minute processing time sample. The same trend occurred in the P/W 0.6 samples. While no limits to sensory detectable levels of strain have been determined in the literature, the work of Pereira (2000) may be used as a guide. The method used and the products tested were similar to the current work. No change in strain was detected by sensory methods, despite a change of 0.18 found using instrumental analysis. All the changes in fracture strain in this experimental work are within 0.18 except the P/W 0.4 0-minute samples, which are greater than 0.18 lower than the corresponding samples. It is unlikely that these changes would be detected by sensory evaluation and it is unknown whether the 0-minute processing time samples would be noticeably different when evaluated by sensory methods.

4.3.3 Skim Milk Cheese

The fracture stress and fracture strain results for SMC composite gels in Table 6 are the averages for duplicate samples. The significant differences between samples at different processing times were determined by using ANOVA for each P/W ratio. Figure 4.13 illustrates the changes in fracture stress and fracture strain with increased processing time for both duplicates at each P/W ratio. The fracture stress increased with increasing P/W ratio.

The fracture strains of many of the P/W 0.4 test plugs were not detected up to the 80% compression point. As a result, the Hencky strain reached a maximum of 1.60.

$$\text{Hencky strain } \varepsilon_H = -\ln (H_0 - H(t))$$
$$= -\ln (1.00 - 0.80)$$
$$= 1.6$$

Equation 4.1: Hencky strain. [Adapted from Watkinson *et al.* (1997)]

Because the samples did not fracture, no conclusions can be drawn about the results obtained. The P/W 0.4 sample may not fracture at any compression level, it may continue to flow rather than fracture. Because many of these samples did not fracture, the stress values were not stress at fracture but at rather stress at 80% compression. Although one of the samples appears to be lower than a fracture strain of 1.6, several of the replicates for each of the data points were at 1.6, but the average was lowered by the remaining data. The accuracy of the test at its upper limit is unknown especially given the amount of variation in the data. The P/W 0.5 samples also did not fracture, and as a result the stress and strain results were at maximum compression not at fracture.

The increase in stress with increased P/W ratio agrees with the Rennet Casein results (Section 4.3.2).

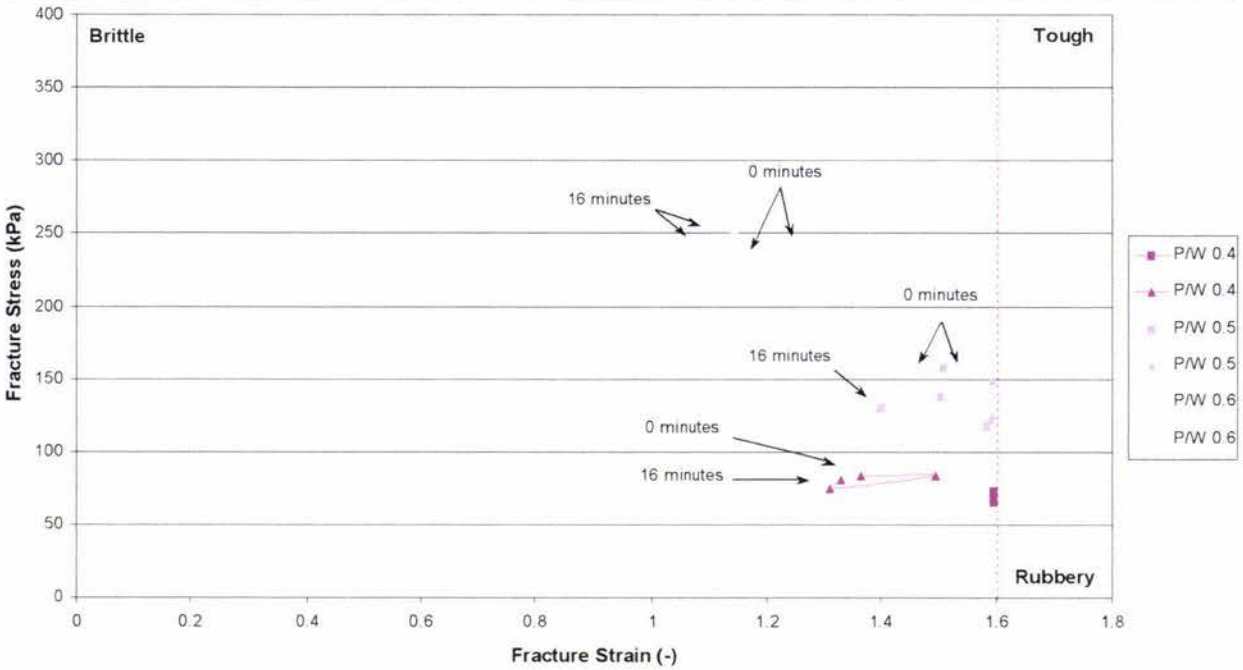

Figure 4.13: Fracture stress and fracture strain for SMC composite gel samples.

Table 6: Fracture properties of SMC composite gel sample (n = 2).

P/W	Processing Time (min)	Fracture Stress (kPa)	Fracture Strain (-)
0.6	0	-	-
	4	235[a]	1.231[a]
	8	230[a]	1.179[a]
	16	243[a]	1.130[a]

For each parameter, superscripts with no letters in common denote significant differences between samples at $\alpha = 0.05$.

The general trend with increasing processing time was a decrease in fracture strain, but the changes were not significant. There were no significant changes in fracture stress with time. The SMC P/W 0.60 samples did fracture during 80% uniaxial compression. The fact that these samples fractured suggests that there are structural differences between the P/W 0.6 and the lower protein samples.

Using the fracture property definition of overcreaming (Bowland and Foegeding, 1999), it appears that the P/W 0.6 samples may have been approaching an overcreamed state as the fracture properties start to move towards the brittle indicator.

4.3.3.1 Sensory Detection

The SMC P/W 0.6 samples showed little change in fracture stress and fracture strain with time: the changes would not be picked up by sensory evaluation using the method outlined by Pereira (2000).

4.3.4 Milk Protein Concentrate 85

The fracture stress and fracture strain results for MPC 85 composite gels in Table 6 are the averages for duplicate samples. The significant differences between samples at different processing times were determined by using ANOVA for each P/W ratio. Figure 4.14 illustrates the changes in fracture stress and fracture strain with increased processing time for both duplicates at each P/W ratio. The fracture stress increased with increasing P/W ratio, and the fracture strain appeared to increase. The overall trend with P/W was quite evident, although the change with increased processing time was less consistent.

The increase in fracture stress agreed with the Rennet Casein results (Section 4.3.2) and the increase in SMC stress and fracture strain results (Section 4.3.3).

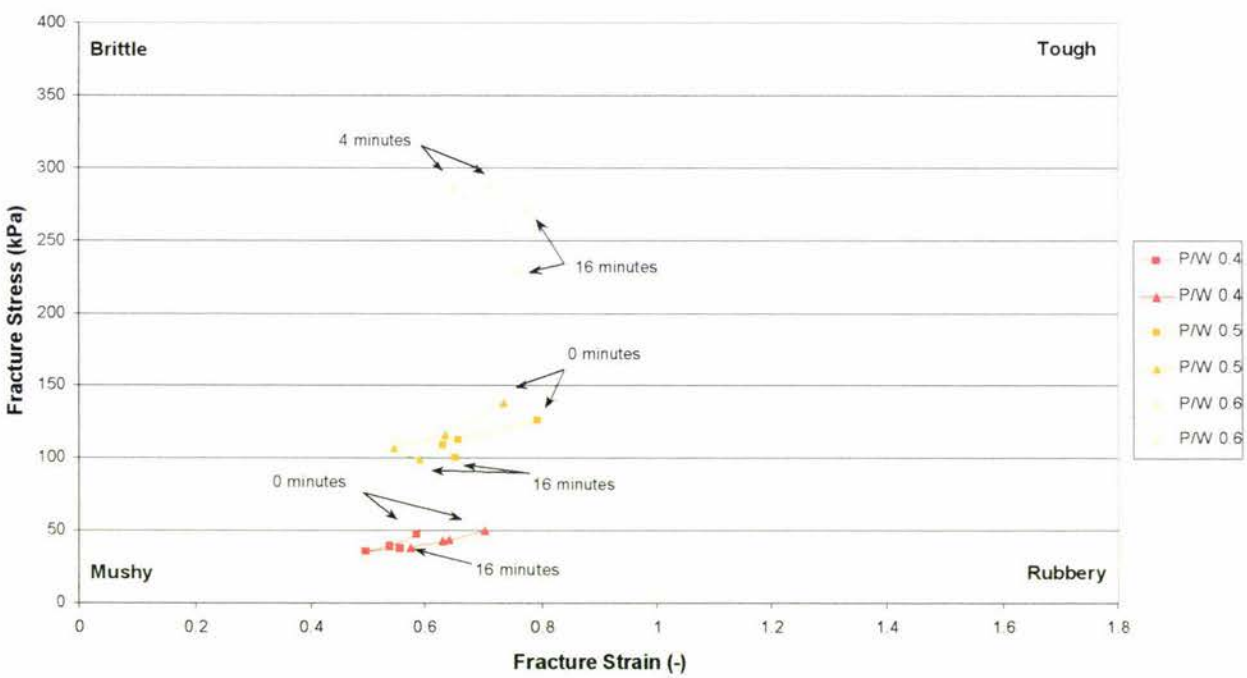

Figure 4.14: Fracture stress and fracture strain for MPC 85 composite gel samples.

Table 7: Fracture properties of MPC 85 composite gel samples (n = 2).

P/W	Processing Time (min)	Fracture Stress (kPa)	Fracture Strain (-)
0.4	0	49^{a}	0.654^{a}
	4	41^{a}	0.585^{ab}
	8	39^{a}	0.563^{b}
	16	38^{a}	0.564^{b}
	All	**42^{a}**	**0.591^{a}**
0.5	0	132^{a}	0.764^{a}
	4	115^{b}	0.647^{b}
	8	108^{bc}	0.587^{b}
	16	100^{c}	0.622^{b}
	All	**114^{b}**	**0.655^{b}**
0.6	4	287^{a}	0.679^{a}
	8	271^{b}	0.703^{ab}
	16	250^{c}	0.768^{b}
	All	**269^{c}**	**0.717^{c}**

For each parameter, superscripts with no letters in common denote significant differences between samples at $\alpha = 0.05$.
Significant differences were calculated within each P/W ratio.

Fracture stress decreased with increasing processing time, while fracture strain appeared to be dependent on the P/W ratio. Fracture stress and fracture strain increased significantly with increased P/W ratio.

The fracture strain for the P/W 0.4 samples decreased, the P/W 0.5 samples decreased except for the last processing time sample, and the P/W 0.6 samples increased in fracture strain with increasing processing time.

The duplicates appeared to agree. Strain was the main difference between samples. The Rennet Casein samples also increased in fracture strain but to a lesser degree, resulting in differences that were not statistically significant.

Relative to the textural indicators, the samples became mushier with increased processing time, consistent with the breakdown of the structure. However, the P/W 0.6 sample moved towards a more rubbery texture. This was not seen in the confocal microscopy, which showed increased emulsification with increased processing time. All P/W ratio samples showed

duplicates fracturing at higher strains. Using the fracture property definition of overcreaming (Bowland and Foegeding, 1999), it appears that the MPC 85 samples were not overcreamed as the fracture properties did not shift towards the brittle indicator.

4.3.4.1 Sensory Detection

The changes in fracture stress and fracture strain for the P/W 0.4 samples were within the ranges in which Pereira (2000) found no detectable sensory differences.

The change in fracture stress from 0- to 4-minutes processing time for the P/W 0.5 samples was just below the change that was detected by Pereira (2000) and may be detectable. The change between 0-minutes and the remaining processing time samples would be detectable but the change from 4- to 16-minutes processing time would not be distinguishable.

The difference between the 4- and 8-minute processing time samples was within the range in which Pereira (2000) found no detectable sensory differences. The difference between these samples and the 16-minute sample was outside that range and would probably be detectable by sensory methods.

4.3.5 Ion-Exchanged Milk Protein Concentrate 85

The fracture stress and fracture strain results for IX MPC 85 composite gels in Table 8 are the averages for duplicate samples. The significant differences between samples at different processing times were determined by using ANOVA for each P/W ratio. Figure 4.15 illustrates the changes in fracture stress and fracture strain with increased processing time for both duplicates at each P/W ratio. The fracture stress increased and the fracture strain did not change significantly with increasing P/W ratio. Similar trends appeared to be occurring in the duplicates, which are close together. The overall trend with P/W was quite evident, although the change with increased processing time is less consistent.

The increase in fracture stress agrees with the Rennet Casein results (Section 4.3.2) and the increase in SMC stress and fracture stress results (Section 4.3.3).

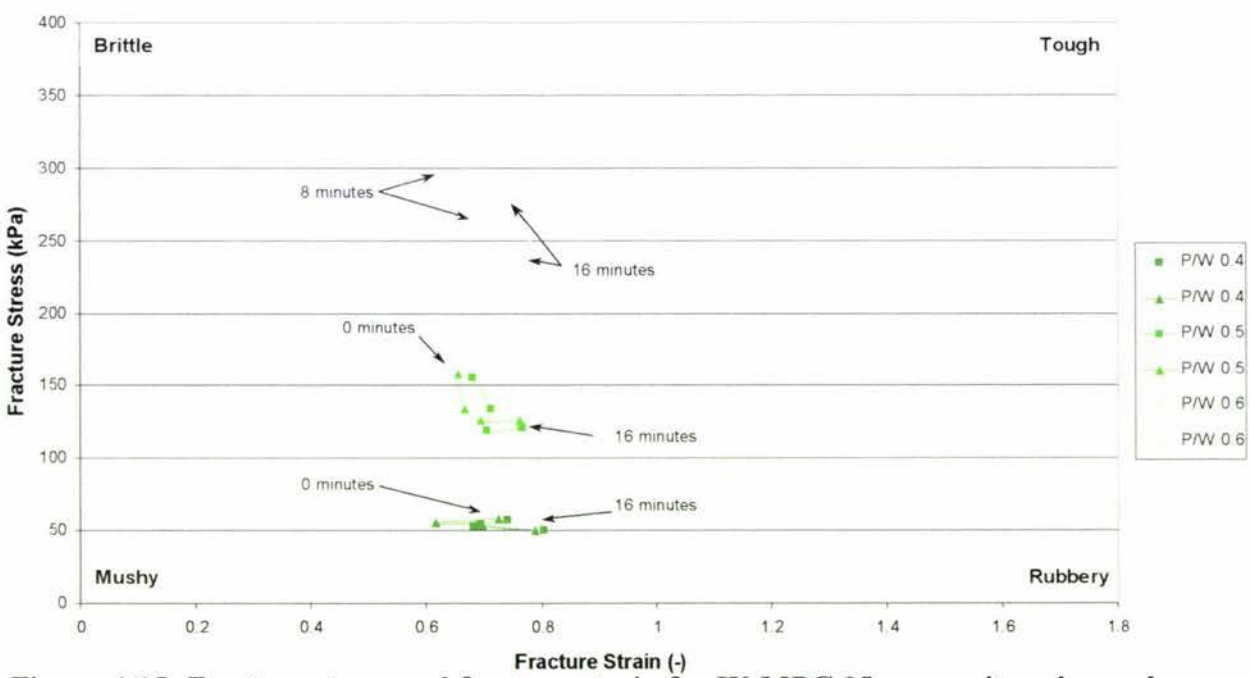

Figure 4.15: Fracture stress and fracture strain for IX MPC 85 composite gel samples.

Table 8: Fracture properties of IX MPC 85 composite gel samples (n = 2).

P/W	Processing Time (min)	Fracture Stress (kPa)	Fracture Strain (-)
0.4	0	58^{a}	0.736^{b}
	4	55^{a}	0.656^{a}
	8	53^{a}	0.689^{ab}
	16	50^{a}	0.795^{c}
	All	**54^{a}**	**0.718^{a}**
0.5	0	157^{a}	0.668^{a}
	4	134^{ab}	0.689^{a}
	8	123^{b}	0.700^{a}
	16	124^{b}	0.764^{b}
	All	**135^{b}**	**0.704^{a}**
0.6	8	280^{a}	0.684^{a}
	16	262^{b}	0.757^{b}
	All	**271^{c}**	**0.719^{a}**

For each parameter, superscripts with no letters in common denote significant differences between samples at $\alpha = 0.05$.
Significant differences were calculated within each P/W ratio.

In general, fracture stress decreased and fracture strain increased with increased processing time. Increased P/W ratio resulted in increased fracture stress, but no significant changes in fracture strain.

With the exception that the P/W 0.4 0-minute sample showed a higher fracture strain and there was no significant change between the P/W 0.5 8- and 16-minute sample fracture stresses.

The P/W 0.4 samples decreased in fracture stress with increasing processing time, but the changes were not statistically significant.

The fracture stress of the P/W 0.5 samples decreased with increasing processing time with the 0-minute sample being significantly higher than the 8- and 16-minute samples. The fracture strain increased with processing time with the 16-minute sample being significantly higher. The P/W 0.5 samples fractured at higher stresses than the P/W 0.4 samples, indicating a stronger network.

The fracture stress of the P/W 0.6 samples decreased significantly and the fracture strain increased significantly with the change in processing time from 8- to 16-minutes. The P/W 0.6 samples fractured at higher strains than the lower protein/water ratio samples. Using the fracture property definition of overcreaming (Bowland and Foegeding, 1999), it appears that the IX MPC 85 samples were not overcreamed as the fracture properties did not shift towards the brittle indicator.

4.3.5.1 Sensory Detection

For the P/W 0.4 samples, the changes in fracture properties were within the range where Pereira (2000) found no differences detectable by sensory evaluation. The fracture stress changes for the P/W 0.5 samples were within the range that may not be detected by sensory means. The 0-minute sample had a higher fracture strain than the other samples and the difference could be detected by sensory evaluation. The change in fracture stress for the P/W 0.6 samples was the same as the minimum change in fracture stress detected by sensory in the work done by Pereira (2000). The change in fracture strain may not be detected.

4.3.6 Comparison Between Protein Sources

Interaction plots generated using Minitab are useful for identifying interactions between variables.

- If the lines are parallel to each other, there is no interaction between the two factors.
- If the lines are not parallel to each other, then there is an interaction.

While interaction plots do not show quantitative differences well, trends can easily be distinguished and anomalies identified. The interaction plots were formed by pooling the data and isolating, a pair at a time, the two input variables being investigated. All the combinations are then plotted as in Figure 17.

Figure 17 showed the interactions for fracture strain between the input variables; processing time, P/W ratio, duplicates and protein source. The interaction plot displays the following features:

- each column (C) and row (R) in the plot represented one of the input variables,
- each cell represented the interaction between two of the input variables,
- the right hand side axis displayed the scale of the response (fracture strain) for each input variable,
- the horizontal axis at the top of the plot displayed the level of each input variable, and
- the legends in the plot refered to the lines in that row.

Every interaction was represented twice. For example, the interaction between processing time and protein source was represented in two cells (R1 C2 and C1 R2).

- C2 R1 shows how each protein source changed with increasing processing time
- C1 R2 shows how each processing time changed with different protein sources

Some trends were easier to distinguish in one cell than the corresponding cell, for example, the difference between MPC 85 and IX MPC 85 with increasing processing time could be clearly seen in C1 R2 but not as easily in C2 R1.

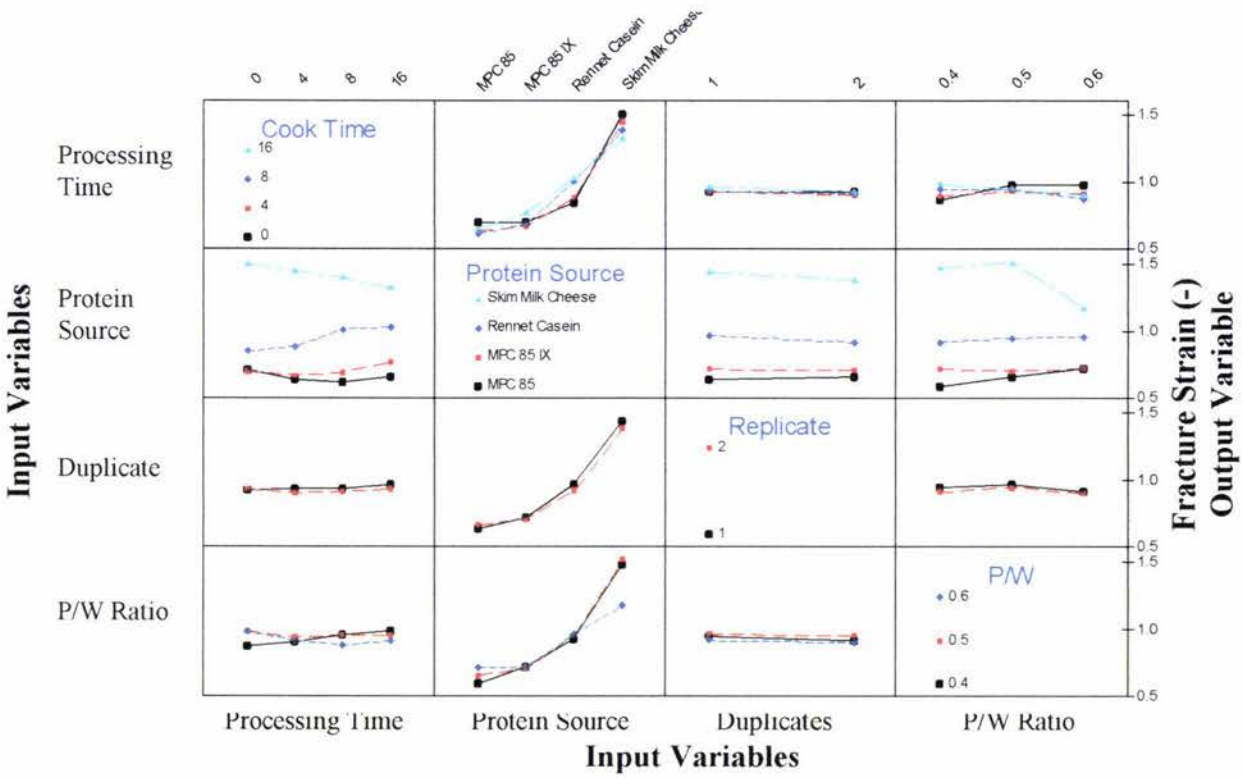

Figure 4.16: Interaction plot for fracture strain.

The SMC P/W ratio 0.4 and 0.5 samples should be disregarded, but as they constituted part of the pooled data their effect must be considered on the SMC responses.

The following variables displayed interactions for fracture strain:

- processing time and protein source (C1 R2 & C2 R1)
- processing time and P/W ratio (C1 R4 & C4 R1)
- P/W ratio and protein source (C2 R4 & C4 R2)

The interaction seen in C2 R4 was due to the P/W 0.6 SMC samples being lower than the other data for that protein source. This was due to the lower P/W ratio samples not fracturing, giving high strain results. The interaction seen in R2 C4 was due to MPC 85 increasing in fracture strain more than the other protein sources. The reason for this is unknown. The SMC results should be disregarded as mentioned.

There appears to be little interaction between the duplicates and the other processing variables (C3 & R3), which is expected.

In addition to interactions, it was also possible to determine the general trends.

- fracture strain increased in the following order: MPC 85 < IX MPC 85 < Rennet Casein < SMC. (Only the SMC P/W 0.6 sample was considered)
- fracture strain did not appear to change with increasing P/W ratio for Rennet Casein and IX MPC 85. MPC 85 appeared to increase in fracture strain with increased P/W ratio.
- the effect of processing time on fracture strain was different for each protein source. Fracture strain increased with processing time (Figure 17) for Rennet Casein while MPC 85 and IX MPC 85 appeared to decrease initially and then increase in fracture strain (C1 R2). The MPC 85 samples increased in fracture strain with increasing P/W ratio to a greater extent than the other protein sources (C4 R2).
- MPC 85 behaved differently with increasing P/W ratio to the other protein sources.

The possible causes of these trends will be discussed later in this section.

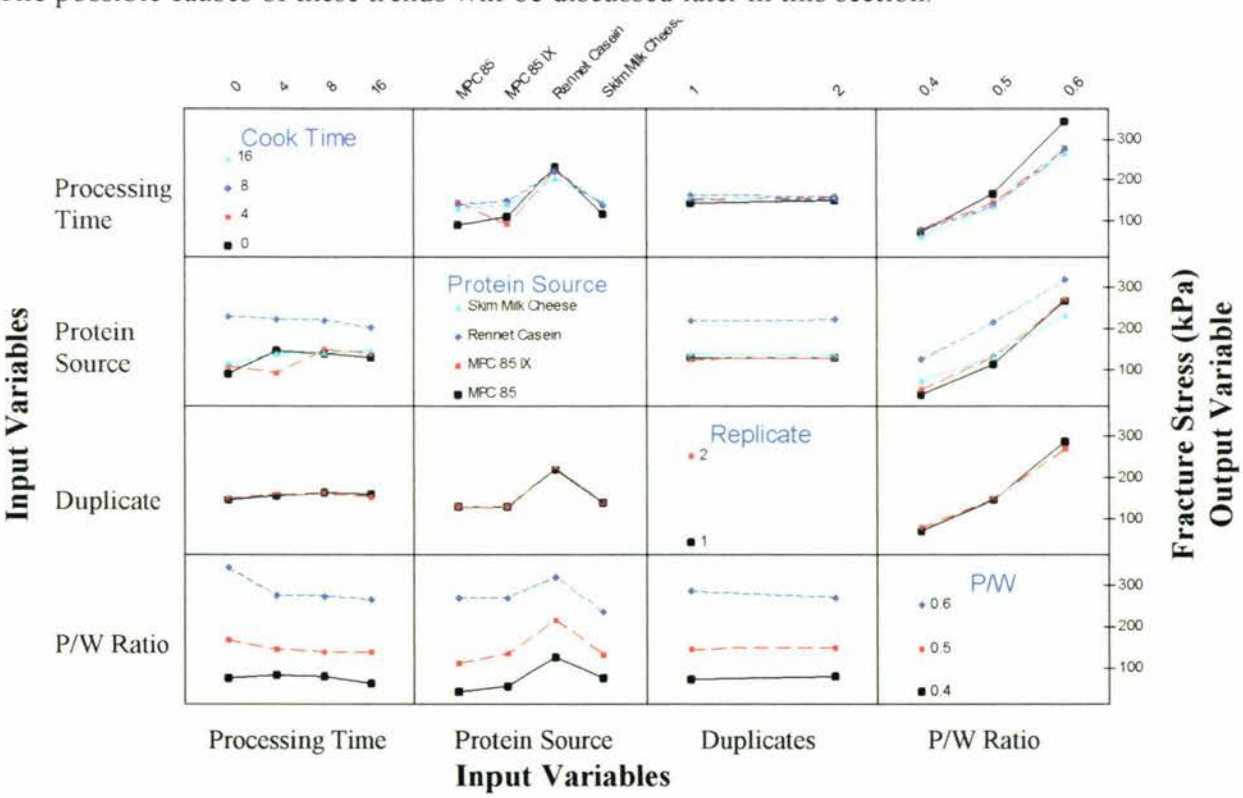

Figure 4.17: Interaction plot for fracture stress.

The following variables displayed interactions for fracture stress:

- processing time and protein source (C1 R2 & C2 R1)
- processing time and P/W ratio (C1 R4 & C4 R1)

The P/W 0.6 0-minute processing time samples seemed to be slightly higher than expected (C1 R4). The IX MPC 85 samples appeared to have a lower 4-minute processing time results than expected (C1 R2 & R1 C2). There appeared to be little interaction between the duplicates and the other processing variables (C3 & R3), which is expected.

In addition to interactions, it was also possible to determine the general trends.

- fracture stress increased in the following order: MPC 85 ≈ SMC ≈ IX MPC 85 < Rennet Casein
- fracture stress increased significantly with increasing P/W ratio for all protein sources
- fracture stress appeared to decrease slightly with increased processing time

There appeared to be a general trend towards decreasing fracture stress with increasing processing time (Figure 18) for Rennet Casein (C1, R2). MPC 85 appeared to increase in fracture stress from 0- to 4-minutes processing time and then decrease. The IX MPC 85 appeared to decrease from 0- to 4-minutes processing time, increase to 8-minutes and then decrease again. The fracture stress clearly increased with increasing P/W ratio (C4) and there appeared to be a general decrease in fracture stress with increased processing time (C1, R4). By looking at R3, it can be seen that Rennet Casein had a higher fracture stress than the remaining protein sources. The duplicates did not appear to interact with any of the other process variables (C3 & R3). The 0-minute processing time sample behaved differently to the others with increasing P/W ratio as the P/W ratio 0.6 samples appeared much higher. This was probably caused by the Rennet Casein results, as the 0-minute samples were much higher than the other samples.

Table 9: Fracture stress and fracture strain for all protein sources (n = 6)

Protein Source	P/W	Fracture Stress (kPa)	Fracture Strain (-)
Rennet Casein	0.4	127^{cd}	0.921^{c}
	0.5	218^{e}	0.952^{c}
	0.6	322^{h}	0.960^{c}
SMC	0.4	75^{b}	1.480^{e}
	0.5	134^{d}	1.521^{e}
	0.6	236^{f}	1.177^{d}
MPC 85	0.4	42^{a}	0.591^{a}
	0.5	114^{c}	0.655^{ab}
	0.6	269^{g}	0.717^{b}
IX MPC 85	0.4	54^{a}	0.718^{b}
	0.5	135^{d}	0.704^{b}
	0.6	271^{g}	0.719^{b}

Fracture stress increased significantly with increasing P/W ratio. Fracture strain showed a change for the SMC but as explained earlier, the results were not fracture properties for the P/W 0.4 and 0.5. The only conclusion that can be drawn is that the P/W 0.6 was more brittle than the lower P/W ratio samples. The MPC 85 samples showed that the P/W ratio 0.4 was mushier than the two higher P/W ratio samples.

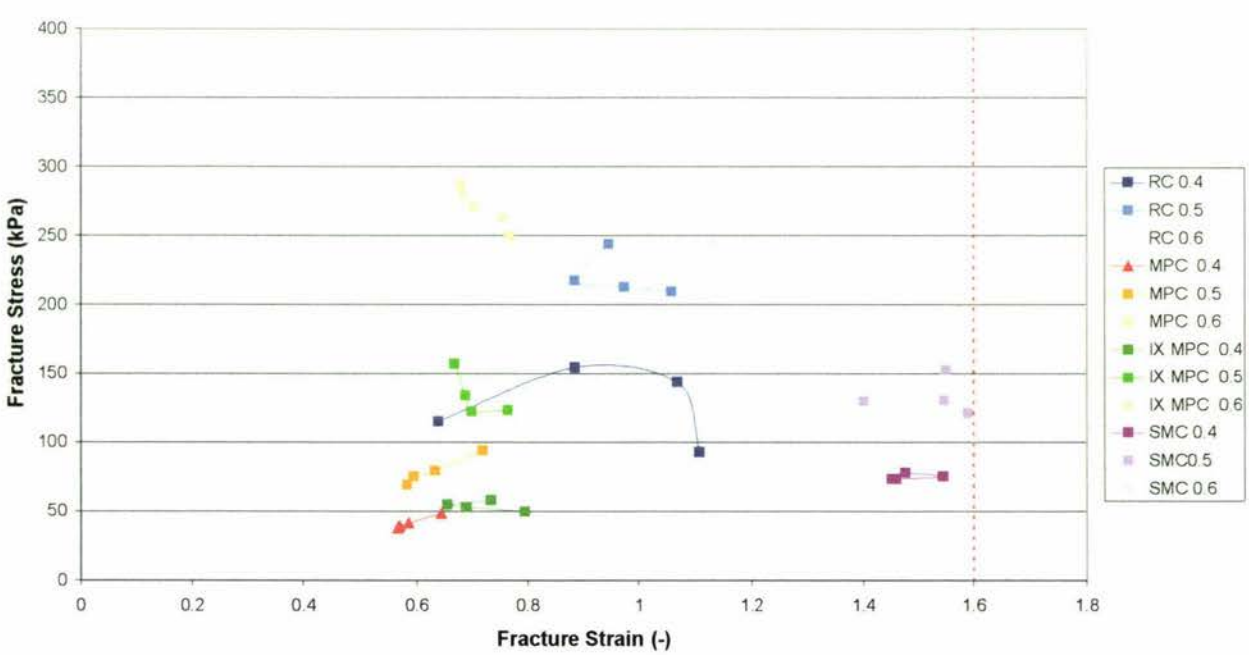

Figure 4.18: Fracture properties of samples for all protein sources (n = 2).

Low P/W ratio SMC gels did not fracture at 80% compression, so the values obtained are the stress and strain at 80% compression, not fracture properties. If the samples did fracture at some point, the fracture strain would be much higher than for Rennet Casein but no conclusions can be drawn as to what the stress at fracture might be. There was no shift in fracture strain of the Rennet Casein gels with increasing P/W ratio, while the SMC P/W 0.6 samples clearly shifted towards a more brittle network than the lower P/W ratio samples. The fracture stress of the P/W 0.6 SMC gels was approximately the same as the P/W 0.5 Rennet Casein gels. The SMC formed a softer, more deformable gel than Rennet Casein. The removal of calcium means that fewer linkages between proteins can form.

At each P/W ratio, the MPC 85 samples showed lower fracture stresses and fracture strains than the Rennet Casein samples. This may have been due to a combination of the following factors relating to MPC 85:

- the presence of whey proteins disrupting the casein network
- a lower casein content (samples were formulated based on total protein)
- intact κ-casein
- differences in mineral content, particularly Ca^{2+}

The presence of whey proteins is generally reported to reduce firmness and in some cases decrease elasticity due to the inert filler theory. Lower casein levels result in fewer stress-bearing linkages, so the fracture stress and fracture strain theoretically decrease.

Intact κ-casein in MPC 85 can play a role in gels such as these due to interaction with β-lactoglobulin. The interaction of these two proteins is thought to impart a more open structure in gels containing micelles by inhibiting renneting and creating steric hindrance preventing aggregation (Fox *et al.*, 2000). As no intact micelles could be seen by electron microscopy (Figure 4.9), this particular effect will not occur, however, β-lactoglobulin and κ-casein may still interact.

The whey containing products are generally significantly softer than the casein-based products. This agrees with several authors (Delbeke, 1987; Spangler *et al.*, 1990; Everett and Jameson, 1993; Chang and Lloyd-Voss, L., 1994; Kaminarides and Stachtiaris, 2000).

IX MPC 85 gels showed slightly higher fracture stress and fracture strain results than standard MPC 85 at each P/W ratio, except P/W 0.6 where the two protein sources were not significantly different. Calcium removal is expected to improve hydration of the powder and produce a weaker gel structure due to less calcium linkages between proteins. The increase in strain between MPC 85 and IX MPC 85 is much smaller than the increase between Rennet Casein and SMC. This may be due to the fact that MPC powders have less casein, which is very sensitive to calcium concentration, in addition to the presence of whey proteins, which are thought to disrupt structure, resulting in weaker networks. The increase in stress between MPC 85 and IX MPC 85 is contradictory to the change observed between Rennet Casein and SMC. This may also be due to less casein and interference of whey proteins. Contradictory reports of the effect of calcium on whey protein gels have been reported by several authors (Schmidt *et al.*, 1979; Johns and Ennis, 1981; Dunkerley and Zadow, 1984; Kohnhorst and Mangino, 1985; Mulvihill and Kinsella, 1988; Kuhn and Foegeding, 1991). The effect of calcium depends on pH and varies depending on how the whey protein and the gels are prepared. The extent to which the whey proteins are affected by the decrease in calcium concentration is unknown.

As the samples were tested at 5°C, the fat could be expected to have an effect on fracture properties when comparing samples at different processing times. At this temperature, the fat is solid and the ratio of fat to protein in the samples was high (fat to protein ratio = 1) an wdould contribute to the gel strength of the product.

4.4 Small Strain Rheology

While large-strain testing may correlate better to sensory evaluation, small-strain behaviour is easier to describe on a theoretical basis. Different information is gathered from each method and a complete rheological evaluation should include both small-strain and failure properties (Ziegler and Foegeding, 1990). The storage and loss moduli (G' and G") show power law dependencies on frequency: G' or G" $\propto \omega^p$ (Ziegler and Foegeding, 1990; Lapasin and Pricl, 1995).

Plotting log (G') versus log (ω) gives a straight line with the slope, p, an indication of how frequency dependant the gel is and the intercept, k, the storage modulus at a frequency of 1 Hz (Egelandsdal *et al.*, 1986). Gels can be classified as strong gels, weak gels and entanglement gels. Strong gels have a permanent covalent network and have a G' that is only slightly frequency dependent (low p value). Entanglement network gels do not have strong cross-links, the gels flow like a liquid at low frequencies and G' and G" are highly frequency dependent (changes over several magnitudes resulting in a high p value) with a crossover occurring at some intermediate point. Weak gels have weak cross-links, are less frequency dependent than the entanglement network (changes within a magnitude) and do not have a crossover point (Clark and Ross-Murphy, 1987; Bowland and Foegeding, 2001).

Statistical analysis showed that while the Rennet Casein and SMC P/W 0.6 samples were not normally distributed, the remaining samples were. Few statistically significant differences were seen within P/W ratios of each protein source.

As with large-strain testing, it was difficult to reach meaningful conclusions about the trends with increased processing time. The small-strain results showed few statistically significant changes with changes in processing time. Accordingly, the trends with increasing processing time are not discussed in detail.

Table 10: Small-strain properties of composite gels samples (G': n = 2; p-value: n = 4).

		Rennet Casein		SMC		MPC 85		IX MPC 85	
P/W	Processing Time (min)	G' at 1 Hz (kPa)	p – value	G' at 1 Hz (kPa)	p - value	G' at 1 Hz (kPa)	p - value	G' at 1 Hz (kPa)	p – value
0.4	0	129^{a}	0.166^{a}	38^{a}	0.204^{a}	87^{a}	0.144^{a}	79^{a}	0.153^{a}
	4	103^{a}	0.180^{a}	38^{a}	0.205^{a}	90^{a}	0.146^{a}	97^{a}	0.153^{a}
	8	90^{a}	0.178^{a}	37^{a}	0.205^{a}	100^{a}	0.147^{a}	95^{a}	0.167^{a}
	16	85^{a}	0.189^{a}	39^{a}	0.202^{a}	98^{a}	0.160^{a}	74^{a}	0.154^{a}
	All	**102^{a}**	**0.178^{b}**	**38^{a}**	**0.204^{c}**	**94^{a}**	**0.149^{b}**	**86^{a}**	**0.157^{c}**
0.5	0	158^{a}	0.167^{a}	86^{a}	0.194^{a}	123^{a}	0.134^{a}	133^{a}	0.136^{a}
	4	133^{a}	0.174^{a}	77^{a}	0.194^{a}	172^{ab}	0.128^{a}	174^{a}	0.135^{a}
	8	125^{a}	0.162^{a}	75^{a}	0.196^{a}	225^{b}	0.129^{a}	171^{a}	0.131^{a}
	16	122^{a}	0.172^{a}	82^{a}	0.196^{a}	141^{ab}	0.130^{a}	149^{a}	0.129^{a}
	All	**135^{a}**	**0.169^{b}**	**80^{b}**	**0.195^{b}**	**165^{b}**	**0.130^{a}**	**157^{b}**	**0.133^{b}**
0.6	0	314^{a}	0.148^{ab}	206^{a}	0.171^{a}	303^{a}	0.129^{a}	216^{a}	0.121^{a}
	4	169^{b}	0.112^{b}	233^{a}	0.172^{a}	310^{a}	0.125^{a}	261^{a}	0.119^{a}
	8	214^{b}	0.147^{ab}	194^{a}	0.163^{a}	314^{a}	0.128^{a}	**239^{c}**	**0.120^{a}**
	16	178^{b}	0.152^{a}	**211^{c}**	**0.169^{a}**	**309^{c}**	**0.127^{a}**		
	All	**219^{b}**	**0.140^{a}**						

For each parameter, superscripts with no letters in common denote significant differences between samples at $\alpha = 0.05$.
Significant differences were calculated within each P/W ratio.

All the composite gels increased in gel strength (increased storage modulus and decreased frequency dependence) with increasing P/W ratio (Table 10), which agrees with the stress-strain data in Section 4.3.4. This result also agrees with results for β-lactoglobulin gels and emulsions where increasing protein content increased G' and decreased the slope (Dickinson and Hong, 1995; Dickinson and Yamamoto, 1996). The behaviour with increased processing time was less clear and dependent on both protein source and P/W ratio.

There were no significant changes in G' with increasing processing time for any samples except Rennet Casein P/W 0.6 and MPC 85 P/W 0.5 composite gel samples. The SMC and IX MPC 85 composite gels showed no significant changes for G' with increasing processing time. There was no obvious trend for G' with increasing processing time. There were no significant changes in p-value with processing time in any of the samples except Rennet Casein P/W 0.6. No trends for p-values could be determined for increasing processing time.

The storage modulus for the P/W 0.6 0-minute processing time sample was significantly higher than the longer processing times. This may not be due to changes during processing but due to one high reading – one of the duplicates gave a reading of 240kPa and the other gave 387kPa, which is not consistent with the other data. The reason for the difference could not be determined. The p-value for the 4-minute sample was significantly lower than the 16-minute processing time sample. The first duplicate gave an extremely low p-value, while the second duplicate gave a p-value of 0.160, which is more consistent with the other samples.

4.4.1 Comparison Between Proteins

All the gels can be classified as weak gels, with some frequency dependence but no crossover of G' and G".

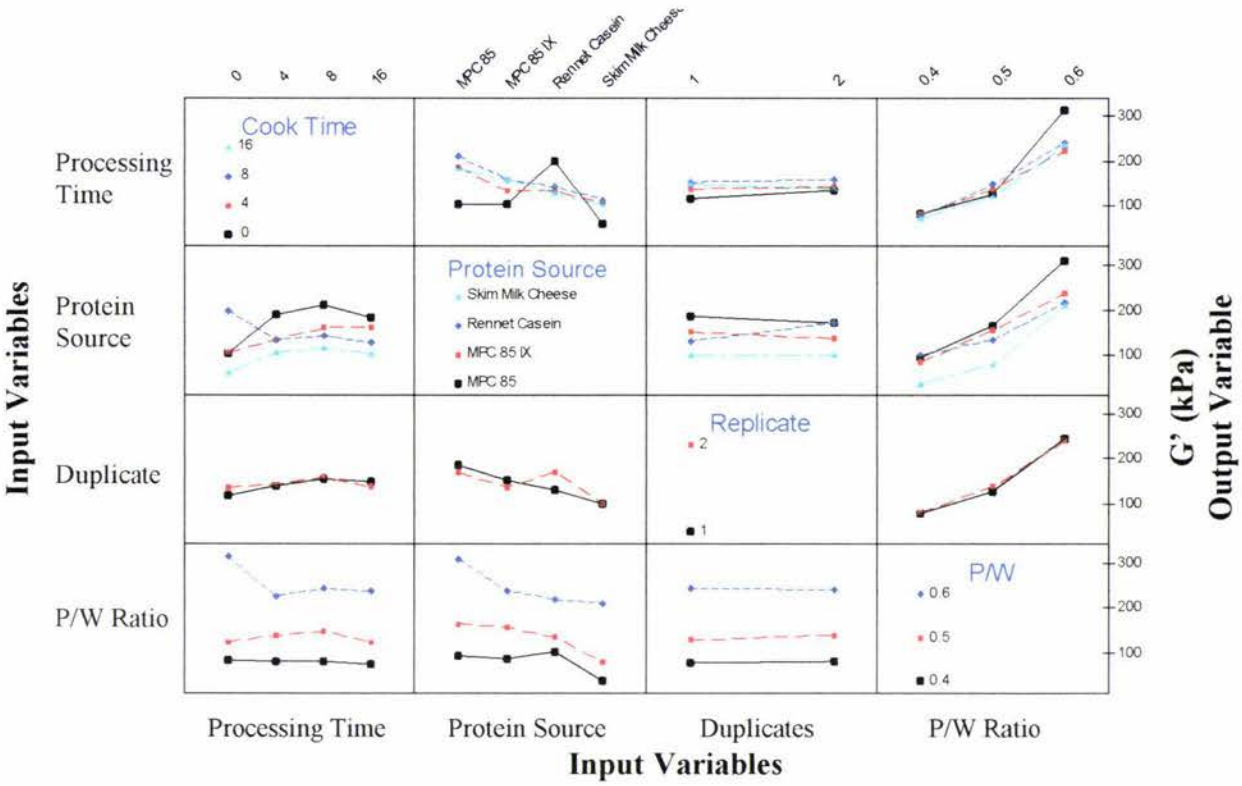

Figure 4.19: Interaction plot for Storage Modulus.

The following variables displayed interactions for G':

- processing time and protein source (C1 R2 & C2 R1)
- processing time and P/W ratio (C1 R4 & C4 R1)
- P/W ratio and protein source (C2 R4 & C4 R2)
- duplicates and protein source (C2 R3 & C3 R2)

The interaction seen in C2 R3 is probably due to the P/W 0.6 0-minutes processing time Rennet Casein duplicates not agreeing as discussed in Section 4.4. This will also have an impact on the 0-minute processing time sample with respect to protein source (C1 R2 & C2 R1) and P/W ratio (C1 R4 & C4 R1).

In addition to interactions, it is also possible to determine the general trends.

- G' increases in the following order: SMC < Rennet Casein < IX MPC 85 < MPC 85.
- G' increases with increasing P/W ratio for all protein sources.

G' increases with processing time to 8-minutes processing time and then decreases (C1 R2) for SMC, MPC 85 and IX MPC 85. The Rennet Casein results are affected by the problem with the duplicate.

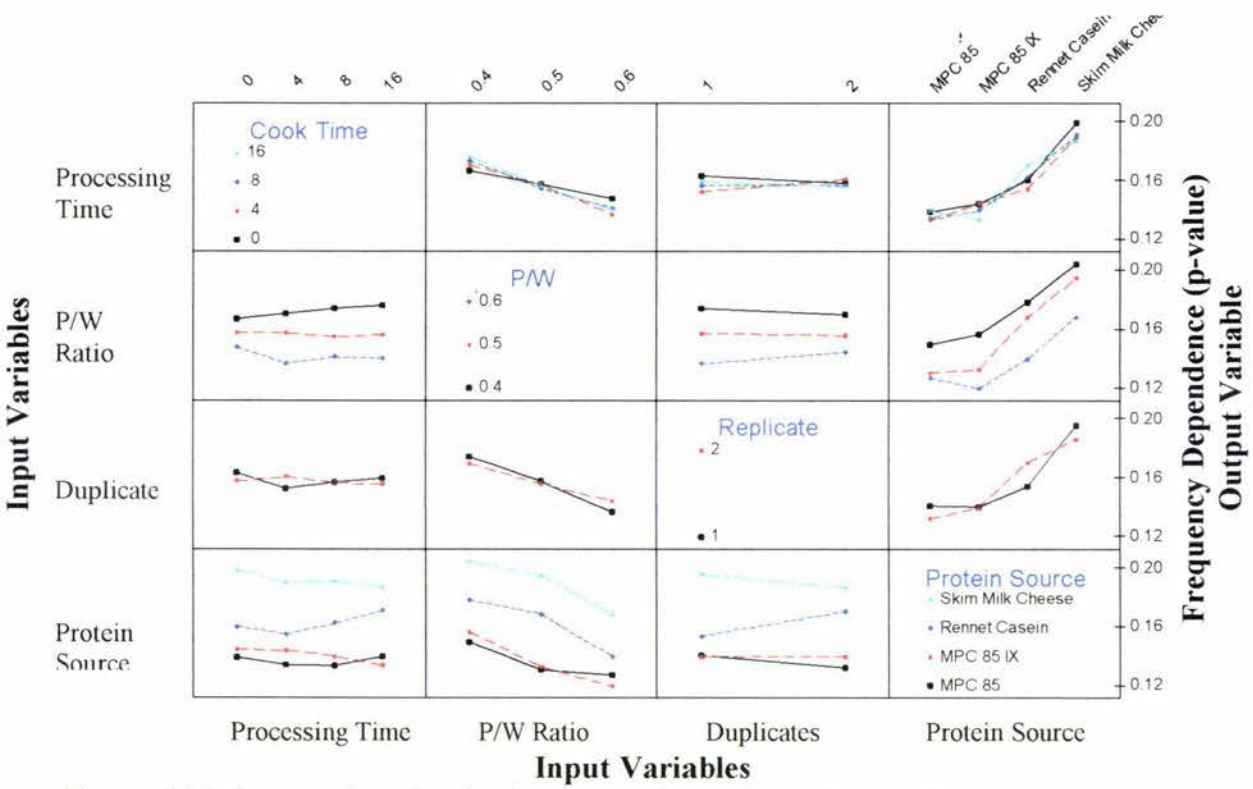

Figure 4.20: Interaction plot for frequency dependence (p-value).

The following variables displayed interactions for p-value:

- processing time and protein source (C1 R4 & C4 R1)
- processing time and P/W ratio (C1 R2 & C2 R1)
- P/W ratio and protein source (C2 R4 & C4 R2)
- duplicates and other variables (C3& R3)

The interaction seen in C1 R3 is due to the P/W 0.6 4-minutes processing time Rennet Casein result being much lower than expected as discussed in Section 4.4. This will also have an

impact on the 4-minute processing time sample with respect to protein source (C1 R4 & C4 R1) and P/W ratio (C1 R2 & C2 R1).

In addition to interactions, it is also possible to determine the general trends.

- p-values decrease in the following order: SMC > Rennet Casein > IX MPC 85 > MPC 85, indicating increasing gel strength as seen in the G' results
- p-value decreases with increasing P/W ratio for all protein sources, which indicates increasing gel strength as seen in the G' results
- p-values are inconsistent with processing time

The slope (extent of frequency dependence) indicates the type of protein network formed. As the slope decreases, the network changing from an entanglement network, to a weak gel, to a strong gel.

Table 11: Small-strain properties of samples for all proteins sources (n = 8).

Protein	P/W	G' at 1 Hz (kPa)	p -value
Rennet	0.4	102^{bc}	0.178^{f}
Casein	0.5	135^{cd}	0.169^{ef}
	0.6	219^{f}	0.140^{bc}
SMC	0.4	38^{a}	0.204^{g}
	0.5	80^{ab}	0.195^{g}
	0.6	211^{ef}	0.169^{ef}
MPC 85	0.4	94^{bc}	0.149^{de}
	0.5	165^{de}	0.130^{ab}
	0.6	309^{g}	0.127^{ab}
IX MPC 85	0.4	86^{b}	0.157^{cd}
	0.5	157^{d}	0.133^{ab}
	0.6	239^{f}	0.120^{a}

For each parameter, superscripts with no letters in common denote significant differences between samples at $\alpha = 0.05$.

For each protein source, the storage modulus decreased with increasing P/W ratio reflecting the increase in gel strength seen in the fracture property results discussed in Section 4.3.6.

The p-values also decreased with increased P/W ratio for each protein source, indicating a shift towards a more ordered network (entanglement network → strong gel).

The order in which the protein source increase gel strengths as determined by small-strain testing does not correlate with the large strain testing results. As has been noted by Ziegler and Foegeding (1990), phase-separated gels may exhibit greater dynamic shear moduli but lower stress and strain at failure.

The SMC samples are weaker gels than the Rennet Casein, which agrees with the fracture properties that indicated SMC formed a softer, more elastic gel. However, the MPC 85 and IX MPC 85 gels, which were softer and more brittle when tested using fracture properties, appeared to be stronger than the Rennet Casein gels.

The MPC 85 formed the most highly structured gels of all the protein sources. The IX MPC 85 formed a weaker gel than MPC 85 (as SMC did with respect to Rennet Casein). The reduction in calcium may have lowered the number of rigid cross-links and the resultant gel became more like an entanglement network.

Rennet Casein and SMC samples produced lower G' and higher p-values than either of the whey protein-containing samples. The lower frequency dependence of the MPC 85 and IX MPC 85 samples indicates a more rigid network structure, possibly due to the presence of disulphide-linked whey protein aggregates.

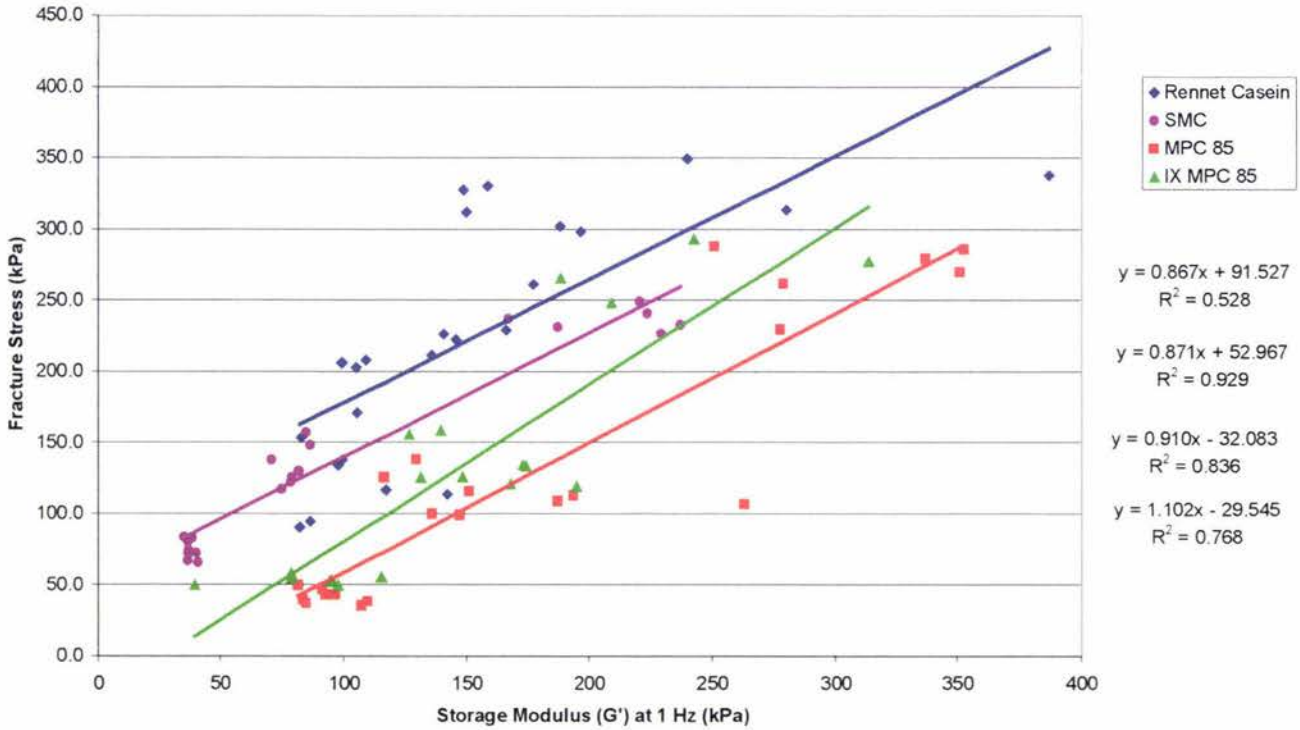

Figure 4.21: Comparisons of Large-Strain and Small-Strain Hardness Parameters.

Figure 4.21 shows correlations between two measures of strength of the samples, large strain (fracture stress) and small strain (storage modulus). Drake *et al.* (1999a) correlated TPA parameters with the loss and storage moduli for commercial and experimental cheeses, and found a correlation coefficient of 0.86 for hardness. From Figure 4.21, it appears that the correlation depends on the protein source used.

Table 12: Regression Coefficients for fracture stress and storage modulus.

Protein Source	Regression Coefficient
Rennet Casein	0.867[a]
SMC	0.871[b]
MPC 85	0.910[c]
IX MPC 85	1.102[d]

The regression coefficients were tested for equality using the method by Sachs (1984). It was found that the regression coefficients are all significantly different, despite Rennet Casein and SMC being apparently quite similar.

The only samples to show a significant correlation between fracture strain and storage modulus at 1 Hz were those of SMC ($R^2 = 0.929$). The lack of fracture for the SMC P/W 0.4 and 0.5 samples means that the fracture stress is actually Stress at 80% Compression and as

such, there would be expected to be less variation (higher correlation). Fracture of the samples would be expected to lower the stress that is recorded as fracture stress, hence if the P/W 0.4 and 0.5 samples had fractured, they would have produced lower fracture stress data, giving a flatter slope. Due to the fracture strain reaching the test maximum, the actual nature of the SMC fracture strain-storage modulus relationship cannot be investigated. It is proposed that this relationship should be investigated in future work, given that the samples do fracture at a higher compression level.

Ziegler and Foegeding (1990) noted that phase-separated gels may exhibit greater dynamic shear moduli but lower stress and strain at failure, so it is not unexpected that the fracture stress vs G' relationship is dependent on the protein source.

4.5 Temperature Dependence

Temperature sweeps have been carried out by other authors to assess the meltability of cheese. The loss tangent, tan δ (Rüegg *et al.*, 1991), and minimum complex modulus, G* (Ustanol *et al.*, 1994), have been suggested as a predictors for meltability. The UW Meltmeter has been used by Wang *et al.* (1998) for cheese meltability assessment and is used at FRC for cheese characteristics evaluation.

The meltability of the MPCG samples was determined by two methods: small strain rheology and using the UW Meltmeter (Wang *et al.*, 1998). Unfortunately during small-strain rheological analysis, the samples behaved differently depending on the composition, with some drying and others melting quickly. Some authors have used the temperature at which G' and G" cross (tan δ = 1) as a measure of meltability (Rao, 1999; Petley-Hibbs, 2001). This was not possible due to some samples never reaching tan δ = 1 as a result of the sample drying out despite being coated in paraffin oil prior to the beginning of the test. Petley-Hibbs (2001) found similar problems, some processed cheese samples made in a Stephan cheese kettle never reached tan δ = 1 during a temperature sweep.

The complex modulus, G*, at a temperature of 60°C was initially chosen to provide comparison between the small-strain method and the UW meltmeter method, but due to a large number of samples producing erratic results at 60°C, the highest temperature at which consistent results could be obtained was used instead - 45°C. Comparing graphs of G' and G" vs temperature was considered as an option, in an analogous way to Petley-Hibbs (2001) who used tan δ vs temperature, but due to the qualitative nature and the large number of samples (96), this was discarded as a method of analysis.

In addition to the difficulties experienced with the small-strain temperature sweep, the software that calculates the biaxial strain rate for the UW Meltmeter was unavailable at the time of analysis as it was being re-written to correct the calculations. Therefore, the empirical determination of final height/initial height was used with final height being the height at 230 seconds after the beginning of the test (Watkinson, P., 2002, personal communication). Some problems were encountered with the execution of the UW Meltmeter test. Care was taken to ensure that the circular plate (Figure 4.22) was centred over the sample well. When the moveable outer ring was lowered the circular plate sometimes slid across the highly lubricated

sample surface and into the outer ring. It was difficult to prevent this from occurring and also difficult to tell which samples were affected.

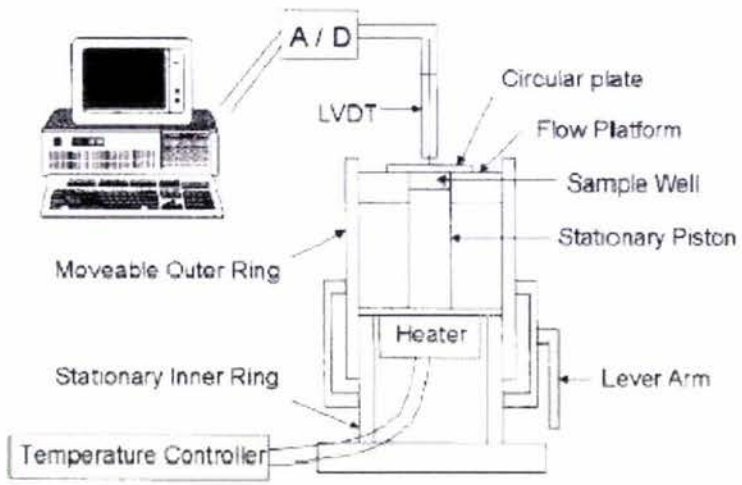

Figure 4.22: UW Meltmeter apparatus. [Taken from Kuo *et al.* (2000)]

Table 13: Melt property trends with increasing processing time for all protein source samples (G*: n = 2; h_f/h_i: n = 4).

P/W	Processing Time	Rennet Casein		SMC		MPC 85		IX MPC 85	
		G* at 45°C	h_f/h_i	G* at 45°C	h_f/h_i	G* at 45°C	h_f/h_i	G* at 45°C	h_f/h_i
0.4	0	9^{a}	0.38^{ab}	2^{a}	0.07^{a}	7^{a}	0.54^{a}	6^{a}	0.62^{b}
	4	13^{a}	0.53^{b}	1^{a}	0.09^{a}	7^{a}	0.53^{a}	6^{a}	0.46^{ab}
	8	9^{a}	0.40^{b}	1^{a}	0.07^{a}	7^{a}	0.54^{a}	5^{a}	0.45^{ab}
	16	4^{a}	0.18^{a}	2^{a}	0.09^{a}	5^{a}	0.49^{a}	2^{a}	0.26^{a}
0.5	0	22^{b}	0.66^{c}	2^{a}	0.09^{a}	19^{a}	0.59^{a}	19^{ab}	0.78^{b}
	4	20^{b}	0.52^{bc}	2^{a}	0.08^{a}	21^{a}	0.56^{a}	22^{b}	0.71^{b}
	8	27^{b}	0.34^{ab}	2^{a}	0.08^{a}	20^{a}	0.55^{a}	16^{ab}	0.58^{ab}
	16	9^{a}	0.29^{a}	2^{a}	0.09^{a}	13^{a}	0.45^{a}	8^{a}	0.41^{a}
0.6	0	27^{ab}	0.57^{a}	-	-	-	-	-	-
	4	42^{c}	0.51^{a}	9^{a}	0.20^{a}	38^{a}	0.77^{a}	-	-
	8	37^{bc}	0.42^{a}	9^{a}	0.14^{a}	43^{a}	0.68^{a}	31^{a}	0.74^{a}
	16	17^{a}	0.36^{a}	10^{a}	0.19^{a}	34^{a}	0.60^{a}	32^{a}	0.56^{a}

For each parameter, superscripts with no letters in common denote significant differences between samples at $\alpha = 0.05$.
Significant differences were calculated within each P/W ratio and for each Protein Source individually.

Decreases in G* at 45°C and h_f/h_i values (Table 13) indicate increases in meltability. SMC and MPC 85 showed no statistically significant changes with processing time for either test

method. For the Rennet Casein and IX MPC 85 samples, the overall trends were towards increased meltability with increasing processing time. In general, the last sample was significantly more meltable than the first. The data from the two test methods (Table 13) showed a general trend but were not well correlated ($R^2 = 0.446$), which was expected due to the difference in nature of the methods and the problems encountered with both methods.

Several authors have found lack of correlation between meltability methods. The Schreiber and Arnott tests have been found not to correlate (Park *et al.*, 1984; Mleko and Foegeding, 2001). Park *et al.* (1984) stated that there are at least two material properties controlling meltability, which Watkinson (2002, personal communication) described as skin formation and casein flow. As found by Thompson and Hewitt (2000), skin formation was a major problem associated with meltability determination of MPCG samples using the Schreiber test.

Most authors report decreased lipid droplet size with increased processing time (Cavalier-Salou and Cheftel, 1991; Saunders *et al.*, 1996c) or shear (Petley-Hibbs, 2001) and a corresponding decrease in meltability. One theory that has been proposed is that the protein matrix holds the smaller lipid droplets more tightly, preventing the molten lipid from escaping. While the results in Section 4.2 show that there was a decrease in lipid droplet size with increased processing time, the meltability appeared to increase rather than decrease. As there are few significant changes and no definite trends in firmness (both small- and large-strain), the changes in meltability cannot be attributed to softening of the protein matrix with increased processing time.

Petley-Hibbs (2001) increased processing shear rate by increasing the stirrer speed while Saunders *et al.* (1996c) increased processing time for MPCGs. Petley-Hibbs (2001) found that an increase in stirrer speed in a Stephan cheese kettle resulted in much larger changes than samples made in a Blentech cheese cooker. The author also found that the Blentech slice formulation was harder than the Stephan slice samples (small-strain and TPA hardness) despite having larger fat globules. This observation was attributed to the high shear in the Stephan dispersing CSAs to a greater extent, leading to greater extent of ion-exchange. As a result, casein fragments may not have reformed bonds producing a softer product. It was also proposed that the low shear in the Blentech may not have broken as many calcium phosphate bonds in the raw cheese, leading to stronger network.

Petley-Hibbs (2001) found that the meltabilty was inversely related to firmness in agreement with Cavalier-Salou and Cheftel (1991) and Saunders *et al.* (1996c). The current experimental work found a trend of decreasing firmness with increasing processing time for large-strain (Section 4.3) (although small-strain testing (Section 4.4) showed no definite trends) and a corresponding increase in meltability. Although the inverse relationship is in agreement with previous authors, the trend with time is reversed.

4.5.1 Comparison Between Protein Sources

The interaction plot for the measurement of the UW Meltmeter parameter, h_f/h_i (Figure 4.23), shows that there is an interaction between protein source and processing time that affects meltability. In most cases meltability increases in the order MPC 85 < IX MPC 85 < Rennet Casein < SMC. The UW Meltmeter results (Table 14) show there are no significant differences between the MPC 85, IX MPC 85 and Rennet Casein at each P/W ratio and that SMC is significantly more meltable than the other protein source-based samples. The general trend with increased processing time is a decrease in meltability. There is some interaction between P/W ratio and protein source, as seen by the divergence of the lines. Meltability increases significantly with decreasing P/W ratio. The duplicates show little interaction with any of the other process variables.

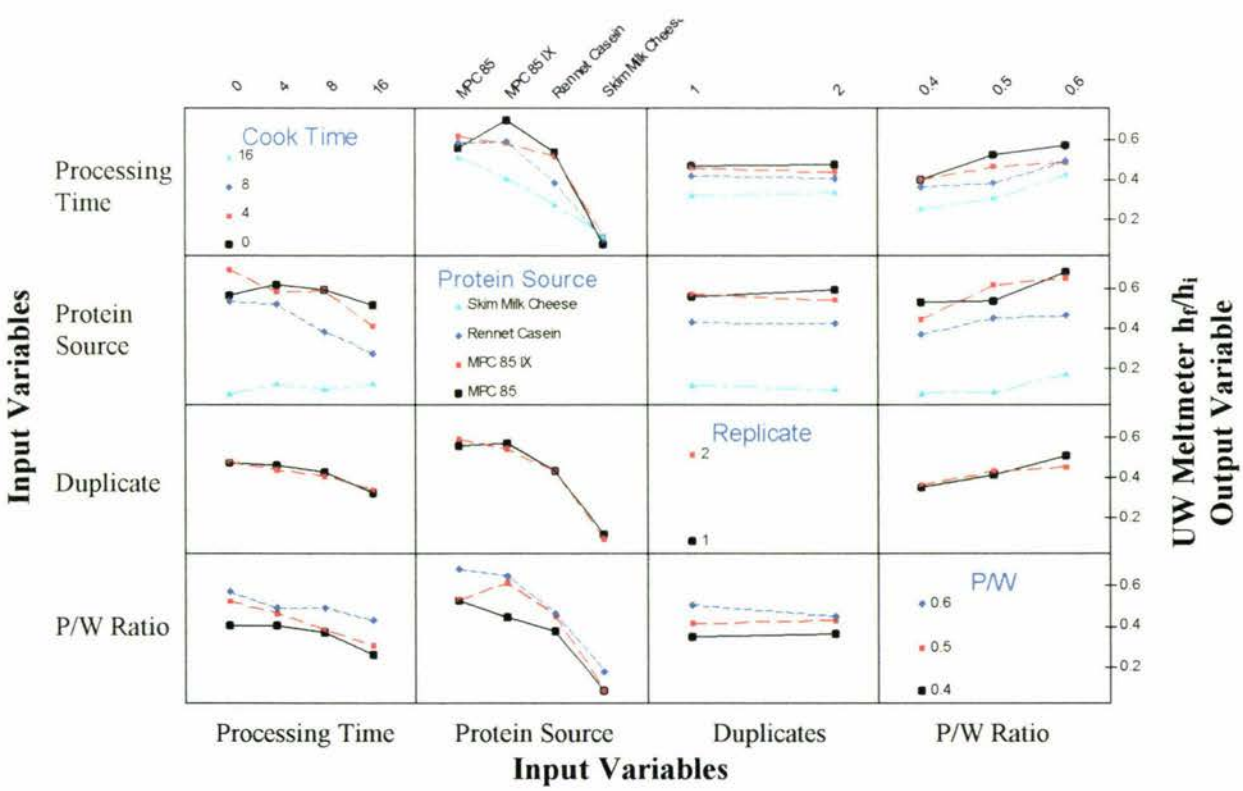

Figure 4.23: Interaction plot for h_f/h_i.

The following variables displayed interactions for h_f/h_i:

- processing time and protein source (C1 R2 & C2 R1)
- processing time and P/W ratio (C1 R4 & C4 R1)
- P/W ratio and protein source (C2 R4 & C4 R2)

There appeared to be little interaction between the duplicates and the other processing variables (C3 & R3), which is expected.

In addition to interactions, it was also possible to determine the general trends.

- meltability increased in the following order: MPC 85 < IX MPC 85 < Rennet Casein < SMC
- meltability decreased with increased processing time
- meltability decreased with increased P/W ratio

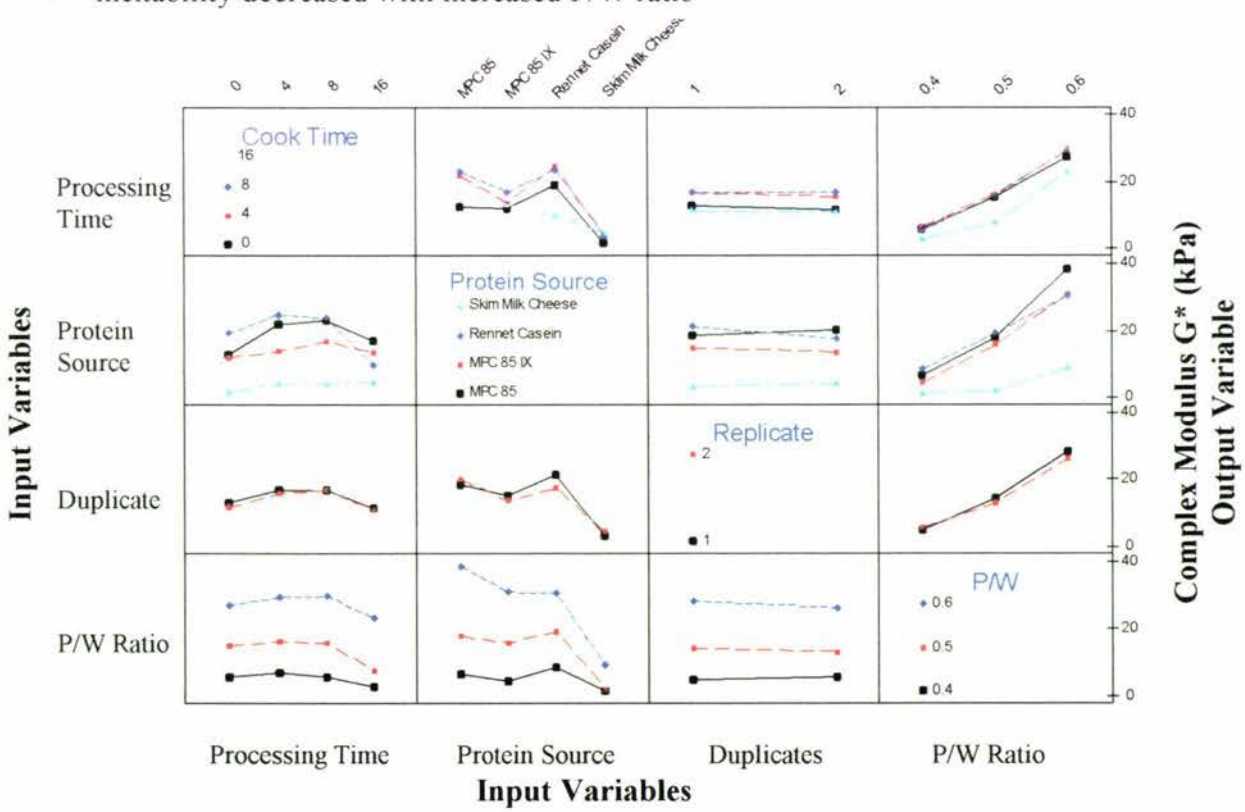

Figure 4.24: Interaction plot for G* at 45°C.

The following variables displayed interactions for G* at 45°C:

- processing time and protein source (C1 R2 & C2 R1)
- P/W ratio and protein source (C2 R4 & C4 R2)

There appeared to be little interaction between the duplicates and the other processing variables (C3 & R3), which was expected.

In addition to interactions, it was also possible to determine the general trends.

- meltability increased in the following order: Rennet Casein ≈ MPC 85 < IX MPC 85 < SMC
- meltability initially increased and then decreased with increased processing time
- meltability decreased with increased P/W ratio

The small-strain results did not agree with the UW Meltmeter results with respect to processing time. However, the trend of decreasing meltability with increasing P/W ratio remained the same. SMC was again found to be the most meltable using this test method.

Table 14: Meltability values for small-strain and UW Meltmeter methods of samples for all protein sources.

Protein	P/W	G* at 45°C	hf/hi
Rennet	0.4	9^{ab}	0.37^{b}
Casein	0.5	19^{c}	0.45^{bc}
	0.6	31^{d}	0.47^{bc}
SMC	0.4	2^{a}	0.08^{a}
	0.5	2^{a}	0.08^{a}
	0.6	9^{ab}	0.17^{a}
MPC 85	0.4	7^{ab}	0.52^{cd}
	0.5	18^{c}	0.53^{cde}
	0.6	39^{d}	0.68^{e}
IX MPC 85	0.4	5^{a}	0.45^{bc}
	0.5	16^{bc}	0.62^{de}
	0.6	31^{d}	0.65^{de}

Superscripts with no letters in common denote significant differences between samples.

Decreases in meltability with P/W ratio (Table 14) are in agreement with results of Mleko and Foegeding (2000) and Taneya *et al.* (1979). Moisture decreases the strength of bonds between the casein fragments, which leads to the product softening sooner when heated (Taneya *et al.*, 1979).

Lee *et al.* (1998) found that the meltability (Arnott test) of the samples increased as follows: calcium caseinate < Rennet Casein = calcium caseinate/MPC70 < MPC 70 < sodium caseinate/Rennet Casein < sodium caseinate/MPC 70 < sodium caseinate and that sodium caseinate was much more meltable than the other samples. The differences were attributed to the calcium levels of the different protein sources. The order of decreasing calcium levels is: calcium caseinate > Rennet Casein > MPC 70 > sodium caseinate.

Similarly to the work of Lee *et al.* (1998), the lower calcium level casein (SMC) was much more meltable than Rennet Casein. The effect of calcium reduction in MPCs may be counteracted by the presence of whey proteins inhibiting the flow of the protein network. Many authors have found whey proteins to inhibit melting of milk protein based products, such as cheese (Savello *et al.*, 1989), and processed cheese (Ernstrom *et al.*, 1980; Abou El-Nour *et al.*, 1996; Abou El-Nour *et al.*, 1998). The effect of MPC was attributed to the

binding of the denatured whey protein to the casein during the melting process particularly to para-κ-casein and possibly α_{s1}-casein, which induces a decrease in the meltability. Mleko and Foegeding (2001) also found increasing whey protein content decreased melt in processed cheese analogues.

In contrast to the results of this experimental work, Lee *et al.* (1998) found an MPC 70-based analogue to be more meltable than Rennet Casein-based analogue. However Lee *et al.* (1998) did not compare protein sources on a total protein basis but on a powder weight basis. As Rennet Casein has approximately 10% more protein on a weight basis, the higher meltability of the MPC 70 samples may be due to lower protein levels (c.f. trends seen in the current work of increased meltability with decreased protein content).

5.0 CONCLUSIONS

This study investigated MPCG manufacture using four protein sources (Rennet Casein, skim milk cheese (SMC), milk protein concentrate (MPC 85), calcium-depleted milk protein concentrate (IX MPC 85)), three protein to water (P/W) ratios (0.4, 0.5, 0.6) and four processing times (0, 4, 8, 16 minutes). The properties of the products were investigated using confocal and transmission electron microscopy, as well as rheological and functional tests.

Increased processing time resulted in a decrease in fat droplet size. The heat and shear during mixing help hydrate the protein and reduce the size of the fat droplets, with the hydrated protein stabilising the smaller fat droplets and preventing coalescence. There were few significant changes in firmness (both small- and large-strain) with increased processing time. In general, there was a trend towards a softer product, which does not agree with most literature. Increased processing time resulted in an increase in meltability. This is also contrary to most of the literature although the inverse relationship between firmness and meltability has been discussed in the literature.

Increased P/W ratio resulted in higher viscosity during manufacture. The higher levels of protein result in more protein:protein contact and an increase in the process viscosity. A decrease in fat droplet size was observed with increasing P/W ratio. At a constant shear rate, which is a function of the auger speed, the increase in viscosity results in an increase in shear stresses thus producing smaller fat droplets. Firmness increased with increasing P/W ratio. Moisture decreases the strength of bonds between the casein fragments (Taneya *et al.*, 1979), so decreasing moisture content results in increased product strength. Meltability decreased with increasing P/W ratio. As decreasing moisture strengthens the bonds between proteins, the product becomes less meltable.

The main differences between the protein sources are outlined as follows:

Processing: the SMC samples demonstrated the unique ability to be stretched for several metres from the cooker during packing at 85°C. This may have potential in the analogue Mozzarella market. Several samples were not completely emulsified at early cook times: both the SMC and MPC 85 P/W 0.6 0-minute processing time samples and the IX MPC 85 P/W 0.6 0- and 4-minutes processing time samples.

Microstructure: there appeared to be 3 phases of different protein concentrations for Rennet

Casein, MPC 85 and IX MPC 85: a dilute, homogenous phase; a concentrated protein phase, and; an intermediate phase, which tends to enclose regions of the two former phases. Rennet Casein displayed a large amount of the intermediate protein concentration phase, which appeared to be associated with the lipid phase. MPC 85 and IX MPC 85 showed the presence of whey protein aggregates and displayed aggregation of fat droplets, which was attributed to the presence of whey proteins. Calcium reduction in both the renneted-casein system and the MPC system resulted in lower levels of emulsification (larger lipid droplets).

Fracture properties: the SMC P/W 0.4 and 0.5 gels did not fracture at 80% compression, indicating that the gels are very elastic.

The order of increasing fracture stress was:

MPC 85 ≈ SMC ≈ IX MPC 85 < Rennet Casein.

The order of increasing fracture strain was:

MPC 85 < IX MPC 85 < Rennet Casein < SMC (P/W 0.6).

Small-strain properties: all samples were weak gels with some frequency dependence, but no crossover of G' and G".

G' increased in the order:

SMC < Rennet Casein < IX MPC 85 < MPC 85.

p-value decreased in the order:

SMC > Rennet Casein > IX MPC 85 > MPC 85.

Meltability: SMC was significantly more meltable than the other protein sources. The UW meltmeter and small-strain temperature sweep did not agree on the order of meltability except for the SMC samples.

Correlations between large- and small-strain testing showed that the correlation coefficient was dependent on the protein source being used. The two meltability tests were only loosely correlated ($R^2 = 0.446$).

Protein source had the greatest impact on product characteristics, followed by P/W ratio with processing time having little, and often inconsistent, effects.

6.0 RECOMMENDATIONS FOR FUTURE WORK

Future work should follow similar manufacturing and testing procedures to investigate the following areas:

- **Processing**

  Preliminary investigations into different processing equipment showed that the different mixer configurations had a large impact on the range of products able to be produced. The effect of shear needs to be investigated with respect to the following aspects:

  - mixing chamber configuration
  - mixing blade

  As part of the preliminary work, it was found that processing conditions could be optimised for different protein sources. The following areas should be investigated further:

  - cook temperature
  - temperature profile

- **Composition**

  As a result of the changes found between the protein sources in this work, it is recommended that the composition of MPCGs should be investigated further, with specific emphasis on:

  - levels of whey protein
  - levels of calcium removal

  The preliminary work also showed that the order in which the ingredients were added, affected how easily the product formed, so it is recommended that the following be investigated:

  - order of addition of ingredients
  - rate of addition of ingredients

Better methods need to be developed to assess the meltability of a wide variety of MPCGs as this characteristic is as important as texture to the consumer. Also, the detectable sensory limits for fracture stress, fracture strain and small-strain properties need to be determined.

The point at which changes in a product become detectable to the consumer is important for both product development and quality control.

SMC was identified as a very elastic gel with potential in the analogue mozzarella market. The fracture properties of SMC should be investigated at higher strains to determine if and at what stress and strain the gels fracture.

REFERENCES

Anon. (1995) Dairy Processing Handbook. Tetra Pak Processing Systems AB. Sweden.

Abd El-Salam, M.H.; Al-Khamy, A.F.; El-Garawany, G.A.; Hamed, A., and Khader, A. (1996) Composition and rheological properties of processed cheese spread as affected by the level of added whey protein concentrates and emulsifying salt. *Egyptian Journal of Dairy Science.* 24:309-322.

Abou El-Nour, A.; Scheurer, G.J., and Buchheim, W. (1998) Use of rennet casein and milk protein concentrate in the production of spread-type processed cheese analogue. *Milchwissenschaft.* 53(12):686-690.

Abou El-Nour, A.; Scheurer, G.J.; Omar, M.M., and Buchheim, W. (1996) Physicochemical and rheological properties of block-type processed cheese analogue made from rennet casein and total milk protein. *Milchwissenschaft.* 51(12):684-687.

Aguilera, J.M. and Kessler, H.G. (1988) Physico-chemical and rheological properties of milk fat globules with modified membranes. *Milchwissenschaft.* 43(7):411-415.

Aguilera, J.M. and Kessler, H.G. (1989) Properties of mixed and filled-type dairy gels. *Journal of Food Science.* 54(5):1213-1221.

Aguilera, J.M. and Kinsella, J.E. (1991) Compression strength of dairy gels and microstructural interpretation. *Journal of Food Science.* 56(5):1224-1228.

Aguilera, J.M.; Kinsella, J.E., and Liboff, M. (1993) Structure-compressive stress relationships in mixed dairy gels. *Food Structure.* 12:469-474.

Ak, M.M. and Gunasekaran, S. (1995) Evaluating rheological properties of Mozzerella cheese by the squeezing flow method. *Journal of Texture Studies.* 26:695-711.

American Public Health Association. (1985) Standard methods for examination of dairy products. APHA. Washington D.C., USA.

Aoki, T.; Umeda, T., and Nakano, T. (1999) Effect of sodium chloride on the properties of casein micelles. *Milchwissenschaft.* 54:91-93.

Arnott, D.R.; Morris, H.A., and Combos, C.A. (1957) Effect of certain chemical factors on the melting quality of process cheese. *Journal of Dairy Science.* 40:957-959.

Baldwin, K.A.; Baer, R.J.; Parsons, J.G.; Seas, S.W.; Spurgeon, K.R., and Torrey, G.S. (1986) Evaluation of yield and quality of Cheddar cheese manufactured from milk with added whey protein concentrate. *Journal of Dairy Science.* 69:2543-2550.

Banks, J.M. and Muir, D.D. (1985) Effect of incorporation of denatured whey protein on the yield and quality of Cheddar cheese. *Journal of the Society of Dairy Technology.* 38(1):27-32.

Berger, W., Klostermeyer, H., Merkenich, K., and Uhlman, G. (1989) Processed cheese manufacture: A JOHA® Guide. Klostermeyer, H. (ed.). BK Ladenburg GmbH. Wurzberg, Germany.

Bhaskar, V. (2002) personal communication.

BK Ladenburg, (1993) JOHA emulsifying salts. BK Ladenberg, Germany.

Bourne, M.C. (1982) Food texture and viscosity: concept and measurement. Academic Press, New York. pp. 45-117.

Bowland, E.L. and Foegeding, E.A. (1999) Factors determining large-strain (fracture) rheological properties of model processed cheese. *Journal of Dairy Science.* 82:1851-1859.

Bowland, E.L. and Foegeding, E.A. (2001) Small strain oscillatory shear and microstructural analyses of a model processed cheese. *Journal of Dairy Science.* 84:2372-2380.

British Standards (1976) BS 770; Part 5.

Buwalda, R. (2001) personal communication.

Campanella, O.H.; Poppelwell, L.M.; Rosenau, J.R., and Peleg, M. (1987) Elongational viscosity measurements of melting american process cheese. *Journal of Food Science.* 52(5):1249-1251.

Caric, M. and Kalab, M. (1993) Processed cheese products. *In* Cheese: Chemistry, Physics and Microbiology. Chapman and Hall, London. pp. 467-505.

Cavalier-Salou, C. and Cheftel, J.C. (1991) Emulsifying salts influence on characteristics of cheese analogs from calcium caseinate. *Journal of Food Science.* 56(6):1542-1547, 1551.

Chang, R. and Lloyd-Voss, L. (1994) Unpublished work.

Chen, J. and Dickinson, E. (1998a) Viscoelastic properties of heat-set whey protein emulsion gels. *Journal of Texture Studies.* 29(3):285-304.

Chen, J. and Dickinson, E. (1998b) Viscoelastic properties of protein-stabilized emulsions: effect of protein-surfactant interactions. *Journal of Agricultural and Food Chemistry.* 46:91-97.

Chen, J., Dickinson, E., and Edwards, M. (1999) Rheology of acid-induced sodium caseinate stabilized emulsion gels. *Journal of Texture Studies.* 30:377-396.

Clark, A.H. and Ross-Murphy, S.B. (1987) Structural and mechanical properties of biopolymer gels. *Advances in Polymer Science.* 83:57-192.

Conaghan, E. (2002) personal communication.

Cooney, M.J.; Rosenberg, M., and Shoemaker, C.F. (1993) Rheological properties of whey protein concentrate gels. *Journal of Texture Studies.* 24(3):325-334.

Cox-Smith, T. (1987) Unpublished work.

Crawford, R. (2002) personal communication.

Creamer, L.K.; Iyer, M., and Lelievre, J. (1987) Effect of various levels of rennet addition on characteristics of Cheddar cheese made from ultrafiltered milk. *New Zealand Journal of Dairy Science and Technology.* 22:205-214.

Dalgleish, D.G.; Goff, H.D.; Brun, J.M., and Luan, B. (2002) Exchange reactions between whey proteins and caseins in heated soya oil-in-water emulsion systems - overall aspects of the reaction. *Food Hydrocolloids.* 16:303-311.

Delbeke, R. (1987) Experiments on making Saint-Paulin by full concentration of milk with ultrafiltration. *Milchwissenschaft.* 42(4):222-225.

Dickinson, E. and Hong, S.-T. (1995) Influence of water-soluble nonionic emulsifier on the rheology of heat set protein stabilised emulsion gels. *Journal of Agricultural and Food Chemistry.* 45(10):2560-2566.

Dickinson, E. and Yamamoto, Y. (1996) Rheology of milk protein gels and protein-stabilised emulsion gels cross-linked with transglutaminase. *Journal of Agricultural and Food Chemistry.* 44(6):1371-1377.

Drake, M. A., Gerard, P. D., Truong, V. D., and Daubert, C. R. (1999a) Relationship between instrumental and sensory measurements of cheese texture. *Journal of Texture Studies.* 30:451-476.

Drake, M.A.; Truong, V.D., and Daubert, C.R. (1999b) Rheological and sensory properties of reduced-fat processed cheeses containing lecithin. *Journal of Food Science.* 64(4):744-747.

Dunkerley, J.A. and Zadow, J.G. (1984) The effect of calcium and cysteine hydrochloride on the firmness of heat coagula formed from Cheddar whey protein concentrates. *Australian Journal of Dairy Technology.* 3:44.

Egelandsdal, B.; Fretaheim, K., and Harbitz, O. (1986) Dynamic rheological measurements on heat-induced myosin gels: an evaluation of the method's suitability for filamentous gels. *Journal of the Science of Food and Agriculture.* 37:944-954.

Elgar, D. (2002) personal communication.

Elston, P. (2002) personal communication.

Ennis, M. P., O'Sullivan, M. M, and Mulvihill, D. M. (1998) The hydration behaviour of rennet caseins in calcium chelating salt solution as determined using a rheological approach. *Food Hydrocolloids*. 12:451-457.

Ernstrom, C.A.; Sutherland, B.J., and Jameson, G.W. (1980) Cheese base for processing: a high yield product from whole milk by ultrafiltration. *Journal of Dairy Science*. 63:228-234.

Everett, D.W. and Jameson, G.W. (1993) Physicochemical aspects of Cheddar cheese made from ultrafiltered milk. *The Australian Journal of Dairy Technology*. 48:20-29.

Everett, D. W. and Olson, N. F. (2000) Dynamic rheology of renneted milk gels containing fat globules stabilized with different surfactants. *Journal of Dairy Science*. 83:1203-1209.

Eymery, O. and Pangborn, R.-M. (1988) Influence of fat, citric acid and sodium chloride on texture and taste of cheese analog. *Sciences Des Aliments*. 8:15-32.

Foegeding, E.A., Lee, S. K., and Buwalda, R. (1996) Unpublished work.

Fox, P.F., Guinee, T. P., Cogan, T. M., and McSweeney, P. L. H. (2000) Fundamentals of cheese science. Aspen Publishers Inc. Maryland, USA.

Gezimati, J.; Singh, H., and Creamer, L.K. (1996) Heat-induced interactions and gelation of mixtures of bovine β-lactoglobulin and serum albumin. *Journal of Agricultural and Food Chemistry*. 44(3):804-810.

Green, M.L. (1985) Effect of milk pretreatment and making conditions on the properties of Cheddar cheese from milk concentrated by ultrafiltration. *Journal of Dairy Research*. 52:555-564.

Green, M.L.; Turvey, A., and Hobbs, D.G. (1981) Development of structure and texture in Cheddar cheese. *Journal of Dairy Research.* 48:343-355.

Guinee, T.P. (1987) Processed cheese products: physico-chemical aspects. *Proceedings of the Symposium on Industrial Aspects of Milk Proteins.* Moorepark Research Centre. Ireland. pp. 111-178.

Gupta, S.K.; Karahadian, C., and Lindsay, R.C. (1984) Effect of emulsifier salts on textural and flavor properties of processed cheese. *Journal of Dairy Science.* 67:764-778.

Gupta, V.K. and Reuter, H. (1993) Firmness and melting quality of processed cheese foods with added whey protein concentrates. *Lait.* 73:281-288.

Harvey, C.D.; Morris, H.A., and Jenness, R. (1982) Relation between melting and textural properties of process Cheddar cheese. *Journal of Dairy Science.* 65:2291-2295.

Harwalker, V.R. and Kalab, M. (1988) The role of β-lactoglobulin in the development of the core-and-lining structure of casein particles in acid-heat-induced milk gels. *Food Microstructure.* 7:173-179.

Haylock, S.J. and Avery, G. A. (1984) Unpublished work.

Hemar, Y. (2002) personal communication.

Hirst, R. (2002) personal communication.

Hort, J. and Le Grys, G. (2000) Rheological models of Cheddar cheese texture and their application to maturation. *Journal of Texture Studies.* 31:1-24.

Hsieh, Y.L. and Regenstein, J.M. (1992) Modelling protein gelation and application of entropy elasticity to understand protein gel properties. *Journal of Texture Studies.* 23(4):379.

International Dairy Federation (1964) IDF Standard 29.

International Dairy Federation (1986) IDF Standard 5B.

International Dairy Federation (1988) IDF Standard 88A.

International Dairy Federation (1993) IDF Standard 20B; Part 2, 4.

International Dairy Federation (2000) IDF Standard 185.

Johns, J.E.M. and Ennis, B.M. (1981) The effect of replacement of calcium with sodium ions in acid whey on the fundamental properties of whey protein concentrates. *New Zealand Journal of Dairy Science and Technology.* 16(1):79-86.

Jost, R.; Baechler, R., and Masson, G. (1986) Heat gelation of oil-in-water emulsions stabilized by whey proteins. *Journal of Food Science.* 51:440-444, 449.

Kalab, M.; Yun, J., and Yiu, S.H. (1987) Textural properties and microstructure of process cheese food rework. *Food Microstructure.* 6(2):181-192.

Kaminarides, S. and Stachtiaris, S. (2000) Production of processed cheese using kasseri cheese and processed cheese analogues incorporating whey protein concentrate and soybean oil. *International Journal of Dairy Technology.* 53(2):69-74.

Kohnhorst, A.L. and Mangino, M.E. (1985) Prediction of the strength of whey protein gels based on composition. *Journal of Food Science.* 50:1403-1405.

Korolczuk, J. and Mahaut, M. (1991) Effect of whey proteins and heat treatment of milk on the consistency of UF fresh cheese. *Milchwissenschaft.* 46(7):435-437.

Kosikowski, F. (1977) Cheese and Fermented Milk Foods. F.V. Kosikowski & Assoc., Brooktondale, New York. pp. 337-340.

Kuhn, P.R. and Foegeding, E.A. (1991) Factors influencing whey protein gel rheology: Dialysis and calcium chelation. *Journal of Food Science.* 56(3):789.

Kuo, M.-I.; Wang, Y.-C., and Gunasekaran, S. (2000) A viscoelasticity index for cheese

meltability evaluation. *Journal of Dairy Science.* 83:412-417.

Lapasin, R. and Pricl, S. (1995) Rheology of industrial polysaccharides: theory and applications. Blackie Academic and Professional. London, UK.

Lawrence, R.C. (1989) The use of ultrafiltration technology in cheesemaking. *Bulletin of the IDF.* 240:2-15.

Lee, S.K., Buwalda, R., Bracey, K., Hirst, R., Thresher, W., and Grant, D. (1999a) Unpublished work.

Lee, S.K., Buwalda, R. J., Bracey, K. M., Hirst, R., and Euston, S. R. (1999b) Unpublished work.

Lee, S.K. and Klostermeyer, H. (1994a) Unpublished work.

Lee, S.K. and Klostermeyer, H. (1994b) Unpublished work.

Lee, S.K. and Klostermeyer, H. (1994c) Unpublished work.

Lee, S.K.; Klostermeyer, H.; Schrader, K., and Buchheim, W. (1996) Rheological properties and microstructure of model processed cheese containing low molecular weight emulsifiers. *Nahrung.* 40(4):189-194.

Lee, S.K., McKenna, A. B., and Buwalda, R. J. (1995) Unpublished work.

Lee, S.K., Moore, I. P. T., Bracey, K., Hirst, R., Buwalda, R., McKenna, A. B., and Euston, S. R. (1998) Unpublished work.

Mahaut, M. and Korolczuk, J. (1992) Effect of whey protein addition and heat treatment of milk on the viscosity of UF fresh cheeses. *Milchwissenschaft.* 47(3):157-159.

Marchesseau, S.; Gastaldi, E.; Lagaude, A., and Cuq, J.-L. (1997) Influence of pH on protein interactions and microstructure of processed cheese. *Journal of Dairy Science.* 80:1483-1489.

Marshall, R.J. (1990) Composition, structure, rheological properties, and sensory texture of processed cheese analogues. *Journal of Food Science and Agriculture.* 50:237-252.

McClements, D.J.; Monaham, F.J., and Kinsella, J.E. (1993) Effect of emulsion droplets on the rheology of whey protein isolate gels. *Journal of Texture Studies.* 24(4):411-422.

McMahon, D.J. and McManus, W.R. (1998) Rethinking casein micelle structure using electron microscopy. *Journal of Dairy Science.* 81:2985-2993.

McMahon, D.J. and Oberg, C.J. (1998) Influence of fat, moisture and salt on functional properties of mozzarella cheese. *The Australian Journal of Dairy Technology.* 53:98-101.

Mleko, S. and Foegeding, E.A. (2000) Physical properties of rennet casein gels and processed cheese analogs containing whey proteins. *Milchwissenschaft.* 55(9):513-516.

Mleko, S. and Foegeding, E.A. (2001) Incorporation of polymerized whey proteins into processed cheese analogs. *Milchwissenschaft.* 56(11):612-615.

Mulvihill, D.M. and Donovan, M. (1987) Whey proteins and their thermal denaturation - a review. *Irish Journal of Food Scence and Technology.* 11:43-75.

Mulvihill, D.M. and Kinsella, J.E. (1988) Gelation of β-lactoglobulin: effects of sodium chloride and calcium chloride on the rheological and structural properties of gels. *Journal of Food Science.* 53(1):231-236.

Munro, P.; Watkinson, P., and Lucey, J. (2000) The rheology equation. *Pharmaceutical and Biotech Daily.* 35(2):23-27.

Muthukumarappan, K.; Wang, Y.-C., and Gunasekaran, S. (1999) Short communication: modified Schreiber test for evaluation of Mozzerella cheese meltability. *Journal of Dairy Science.* 82:1068-1071.

New Zealand Dairy Industry (2001) Unpublished work.

New Zealand Dairy Research Institute (2001) Unpublished work.

Newstead, D. (2002) personal communication.

Nolan, E.J.; Holsinger, V.H., and Shieh, J.J. (1989) Dynamic rheological properties of natural and imitation Mozzerella cheese. *Journal of Texture Studies.* 20(2):179-189.

Olson, N.F. and Price, W.V. (1958) A melting test for pasteurized process cheese spreads. *Journal of Dairy Science.* 41:999-1000.

Park, J.; Rosenau, J.R., and Peleg, M. (1984) Comparison of four procedures of cheese meltability evaluation. *Journal of Food Science.* 49:1158-1170.

Parnell-Clunies, E.M.; Kakuda, Y., and Humphrey, R. (1986) Electron dense granules in yoghurt: characterization by x-ray microanalysis. *Food Microstructure.* 5:295-302.

Paulson, A.T. and Tung, M.A. (1989) Dynamic shear and puncture probe measurements of canola protein isolate gels. *Journal of Texture Studies.* 19:389-396.

Pearce, R.J. (1989) Thermal denaturation of whey protein. *Bulletin of the IDF.* 238:17-23.

Peleg, M. (1977) Operational conditions and the stress strain relationships of solid foods - theoretical evaluation. *Journal of Texture Studies.* 8:283-295.

Pereira, R.B. (2000) Sensory, rheology and microstructural characteristics of model emulsified dairy systems. *Doctor of Philosophy of Technology Thesis.* Massey University, Palmerston North, New Zealand.

Petley-Hibbs, T. (2001) Influence of processing conditions on the microstructural and physical properties of processed cheese. *Master of Engineering Thesis.* The University of Auckland, Auckland, New Zealand.

Rao, A. M., (1999) Rheology in fluid and semisolid foods. G.V. Barbosa-Canovas (ed.) Chapman & Hall Inc., Maryland.

Rayan, A.A.; Kalab, M., and Ernstrom, C.A. (1980) Microstructure and rheology of process cheese. *Scanning Electron Microscopy.* III:635-643.

Rosenberg, M. (2000) Applications for fractionated milkfat in modulating rheological properties of milk and whey composite gels. *The Australian Journal of Dairy Technology.* 55:56-60.

Rosenthal, A. J., (1999) Food texture: measurement and perception. Aspen Publishers Inc., Maryland.

Rüegg, M.; Eberhard, P.; Poppelwell, L., and Peleg, M. (1991) Melting properties of cheese. *Bulletin of the IDF.*(268):36-43.

Sachs, L. (1984) Applied Statistics. A handbook of techniques. 2nd ed. Springer-Verlag New York Inc., New York. pp. 440-442.

Saunders, A., Haisman, D., Johnson, W., Hall, C., Tamehana, M., Zanker, M.-A., and Aird, R. (1997) Unpublished work.

Saunders, A., Haisman, D., Sharma, M., Duizer, L., Hall, C., Johnson, W., and Aird, R. (1996a) Unpublished work.

Saunders, A., Haisman, D., Sharma, M., Hall, C., and Aird, R. (1996b) Unpublished work.

Saunders, A., Haisman, D., Sharma, M., Hall, C., Tamehana, M., Zanker, A.-M., and Aird, R. (1996c) Unpublished work.

Saunders, A., Haisman, D., and Tamehana, M. (1995) Unpublished work.

Savello, P.A.; Ernstrom, C.A., and Kalab, M. (1989) Microstructure and meltability of model process cheese made with rennet and acid casein. *Journal of Dairy Science.* 72(1):1-11.

Schmidt, R.H.; Illingsworth, B.L.; Deng. J.C., and Cornell, J.A. (1979) Multiple regression and response surface analysis of the effects of calcium chloride and cysteine on heat-

induced whey protein gelation. *Journal of Agricultural and Food Chemistry.* 27:529-532.

Sharma, M., Hall, C., Haisman, D., Saunders, A., and Aird, R. (1997a) Unpublished work.

Sharma, M., Hall, C., Rowe, S., Haisman, D., Saunders, A., and Aird, R. (1997b) Unpublished work.

Shimp, L.A. (1985) Process cheese principles. *Food Technology.* 39:63-69.

Spangler, P.L.; Jensen, L.A.; Amundson, C.H.; Olson, N.F., and Hill, C.G. (1990) Gouda cheese made from ultrafiltered milk: effects of concentration factor, rennet concentration, and coagulation temperature. *Journal of Dairy Science.* 73(6):1420-1428.

Swiatek, A. (1964) Einfluß der Art und Menge des Schmelzsalzes auf die Konsistenz von Scmelzkäse. *Milchwissenschaft.* 19:409-417.

Tamime, A.Y.; Muir, D.D.; Shenana, M.E.; Kalab, M., and Dawood, A.H. (1999) Processed cheese analogues incorporating fat-substitutes 2. Rheology, sensory perception of texture and microstructure. *Lebensmittel-Wissenschaft Und-Technologie.* 32:50-59.

Taneya, S.; Izutsu, T., and Sone, T., (1979) Dynamic viscoelsticity of natural cheese and processed cheese. *In* Food Texture and Rheology. P. Sherman (ed.) Academic Press Inc., London. pp. 369-383

Tang, Q.; McCarthy, O.J., and Munro, P.A. (1995) Effects of pH on whey protein concentrate gel properties: comparisons between small deformation (dynamic) and large deformation (failure) testing. *Journal of Texture Studies.* 26(3):255.

Texture Technologies Corp., (2002) Texture Profile Analysis Explained & Annotated [Web Page]. Available at: www.texturetechnologies.com/texture_profile_analysis.html.

Thomas, M.A.; Newell, G.; Abad, G.A., and Turner, A.D. (1980) Effect of emulsifying salts on objective and subjective properties of processed cheese. *Journal of Food Science.*

45:458-459, 466.

Thompson, C.J. and Hewitt, S. A. (2000) Unpublished work.

Truong, V.D. and Daubert, C.R. (2001) Textural characterization of cheeses using vane rheometry and torsion analysis. *Journal of Food Science.* 66(5):716-721.

Tunick, M.H.; Nolan, E.J.; Shieh, J.J.; Basch, J.J.; Thompson, M.P.; Maleeff, B.E., and Holsinger, V.H. (1990) Cheddar and Cheshire cheese rheology. *Journal of Dairy Science.* 73:1671-1675.

Ustanol, Z.; Kawachi, K., and Steffe, J. (1994) Arnott test correlates with dynamic rheological properties for determining Cheddar cheese meltability. *Journal of Food Science.* 59:90-97.

van Vliet, T. and Dentener-Kikkert, A. (1982) Influence of the composition of the milk fat globule membrane on the rheological properties of acid milk gels. *Netherlands Milk and Dairy Journal.* 36(3):261-265.

van Vliet, T.; Lucisano, M., and Casirighi, E. (1991) Inventory of test methods. *Bulletin of the IDF.* 268:17-25.

van Vliet, T. and Peleg, M. (1991) Effects of sample size and preparation. *Bulletin of the IDF.* 268:26-29.

Walstra, P. and van Vliet, T. (1982) Rheology of cheese. *Bulletin of the IDF.* 153:22-27.

Wang, Y.-C.; Muthukumarappan, K.; Ak, M.M., and Gunasekaran, S. (1998) A device for evaluating melt/flow characeristics of cheeses. *Journal of Texture Studies.* 29:43-55.

Watkinson, P. (2002) personal communication.

Watkinson, P.J. (1993) Unpublished work.

Watkinson, P.J.; Boston, G.; Campanella, O.; Coker, C.; Johnston, K.; Luckman, M., and

White, N. (1997) Rheological properties and maturation of New Zealand Cheddar cheese. *Le Lait.* 77:109-120.

Watkinson, P.J. and Jackson, F.L. (1999) A new procedure for estimating the modulus of deformability of cheese from uniaxial compression tests. *Journal of Texture Studies.* 30(5):563-580.

Yost, R.A. and Kinsella, J.E. (1992) Microstructure of whey protein isolate gels containing emulsified butter fat droplets. *Journal of Food Science.* 57(4):892-897.

Zehren, V.L. and Nusbaum, D.D. (1992) Process cheese. D. Cooley & Co. Inc. Green Bay, Wisconsin.

Zhou, N. and Mulvaney, S.J. (1998) The effect of milkfat, the ratio of casein to water, and temperature on the viscoelastic properties of rennet casein gels. *Journal of Dairy Science.* 81(10):2561-2571.

Ziegler, G.R. and Foegeding, E.A. (1990) Gelation of proteins. *Advances in Food and Nutrition Research.* 34:203-298.

Zoon, P. (1991) The relation between instrumental and sensory evaluation of the rheological and fracture properties of cheese. *Bulletin of the IDF.* 268:30-35.

Zuber, F.; Mégard, D., and Cheftel, J.C. (1987) Continuous emulsification and gelation of dairy ingredients by HTST extrusion cooking: production of processed cheeses. *International Journal of Food Science and Technology.* 22:607-626.

APPENDIX 1.0 COMPRESSION TESTING SOFTWARE

Force-distance data collected using the TA-HD during compression was initially analysed using XTRAD software (Version 3.7, Stable Micro Systems) and the appropriate data were exported into J4.02 software (Master Work Software, Tawa, New Zealand). This software calculated Hencky strain as suggested by Peleg (1977).

$$\dot{\varepsilon}_0 = v / h_0$$

$$\varepsilon_c = \Delta h_t / h_0$$

$$\varepsilon_H = -\ln (1 - \varepsilon_c)$$

$$\sigma = (1000 F_t / \pi r_0^2)(1 - \varepsilon_c)$$

Where:

$\dot{\varepsilon}_0$ = Initial strain rate (s^{-1})

v = Compression rate (mm/s)

h_0 = Initial sample height (mm)

Δh_t = Distance sample is compressed (mm)

ε_c = Cauchy Strain (-)

ε_H = Hencky Strain (-)

σ = Stress from lubricated compression test (kPa)

F_t = Force during compression (N)

r_0 = Initial radius of sample (m) (Watkinson *et al.*, 1997)

It is assumed that there is negligible change in sample volume during compression and follows the guidelines outlined by Zoon (1991); where fracture stress indicates firmness (force required to crack the sample), and fracture strain indicates longness (resistance to crumbling).

The data were compared in Microsoft Excel 97 on texture plots by graphing fracture stress against fracture strain (Watkinson and Jackson, 1999). Minitab ANOVA was used to determine which samples were significantly different at the 95% confidence level, and to determine interactions between the experimental variables.

APPENDIX 2.0 MANUFACTURING EQUIPMENT COMPARISON

Summary

The Blentech cheese cooker was the apparatus that was found to give the most reliable results, was easy to use and provided a product that was easily removed from the apparatus.

Introduction

Initial exploratory investigations into possible equipment were conducted to assess which apparatus was most suited to producing the products required for an investigation into protein source, P/W ratio and processing time.

Materials and Methods

Processing Equipment

Several possible pieces of equipment were proposed for sample manufacture:

- Brabender Farinograph (Brabender Instruments Inc., NJ, USA)
- Blentech Cheese Cooker (5 kg capacity, model # CC10, Blentech Corporation, Rohnert Park, CA, USA)
- Stephan Mixer (2 L capacity, Model UMC 5 Electronic, A. Stephan u Sohne GmbH & Co, 3250 Hamein, Germany)

Brabender Farinograph

The Brabender Farinograph was investigated first. Several P/W ratios and batch sizes of MPC 85-based composite gels were made to determine the limitations of the equipment.

Several methods off addition were trialled but generally there was little mixing between chambers, the firmer products sat above the blades and did not become mixed and liquid fat leaked out of the metal seals. Order of addition was found to have a large impact on the ability of the equipment to mix the ingredients into a gel. The samples were difficult to remove from the apparatus and it was difficult to obtain accurate heating curves. Due to the

significant difficulties involved in sample production, process control and the small sample size (300 g), the Brabender Farinograph was not investigated further.

Blentech Cooker

The Stephan experimental procedure was designed according to the results of the Blentech work.

At a speed setting of 165 rpm, the Blentech was only able to make gels between the P/W ratios of 0.4 and 0.5 (target values). Trials showed that the amount of water introduced from the steam was 25% of the total water in the product and this was included in the formulation. One of the contributing factors for variability in the final product was the steam quality which was inconsistent.

Figure A2.1: Lab-scale Blentech Cheese Cooker.

Table 15: Formulations for Blentech Cheese Cooker.

P/W ratio	0.40	0.45	0.50
Rennet Casein (g)	1049.1	1115.5	1175.0
Anhydrous Milk Fat (g)	821.8	873.4	920.0
Water (g)	1986.9	1862.3	1750.6
Salt (g)	32.9	34.9	36.8
Citric Acid (g)	40.0	40.0	40.0
Potassium Sorbate (g)	4.0	4.0	4.0
Disodium Phosphate (DSP) (g)	65.7	69.9	73.6

The Rennet Casein, emulsifying salts, sodium chloride and AMF were mixed at 165 rpm for 5 minutes at ambient before the water was added and direct steam injection initiated. The temperature was taken up to 83°C and the MPCG was allowed to mix for 5 minutes at this temperature to ensure that all the free fat was incorporated. The sample was then poured into 500 g containers and allowed to cool to ambient before being chilled at 5°C.

Stephan Cooker

The formulation for the Stephan cooker was based on the formulations for the Blentech samples taking into account moisture contents tested as discussed in the Materials and Methods Section (p 35).

Figure A2.2: Lab-scale Stephan Cheese Kettle.

Table 16: Formulations for Stephan Cheese Cooker.

P/W Ratio	0.430	0.466	0.474	0.520
Rennet Casein (g)	435.1	454.1	457.6	478.7
Anhydrous Milk Fat (AMF) (g)	341.1	355.5	358.3	374.8
Water (g)	764.2	730.0	723.1	683.2
Salt (g)	13.7	14.7	14.3	15.0
Citric Acid (g)	16.6	16.3	16.4	16.3
Potassium Sorbate (g)	1.7	1.6	1.6	1.6
Disodium Phosphate (DSP) (g)	27.3	28.4	28.7	30.0

The Rennet Casein, emulsifying salts, sodium chloride and water were mixed for 1 minute at 2100 rpm with water circulating through the jacketed bowl at a temperature of 85°C. The AMF was added and the MPCG was mixed while heating to a final temperature of 83°C. The

gel was poured into butter containers and allowed to cool to ambient before being chilled at 5°C.

Sample Testing and Data Analysis

The samples were stored at 5°C for 6 days. Six cylindrical samples were cut from the gels in the 500 g containers using a 20 mm internal diameter cork borer mounted on a drill press. The cylindrical samples were then sliced to a length of 25 mm using a wire cutter and a template. The cut samples were wrapped in polyethylene film, placed in airtight containers and held at 5 ± 1°C overnight. The samples were compressed twice to 80% using a TA-XT2 (Stable Micro Systems, Haslemere, UK) using a load cell of 250 N. The 60 mm diameter upper plate and the (95 x 105 mm) lower plate were made of Teflon and lubricated with paraffin oil (high viscosity) to minimise friction. Samples were tested at 5 ± 1°C and at a compression rate of 0.83 mm s^{-1}. The resulting force-displacement data were converted to fracture stress, strain, area and modulus using J402 software. The data were analysed using the one-way ANOVA function in the statistical software package Minitab (Version 12.21, Minitab Inc.).

Results and Discussion

Fracture Properties

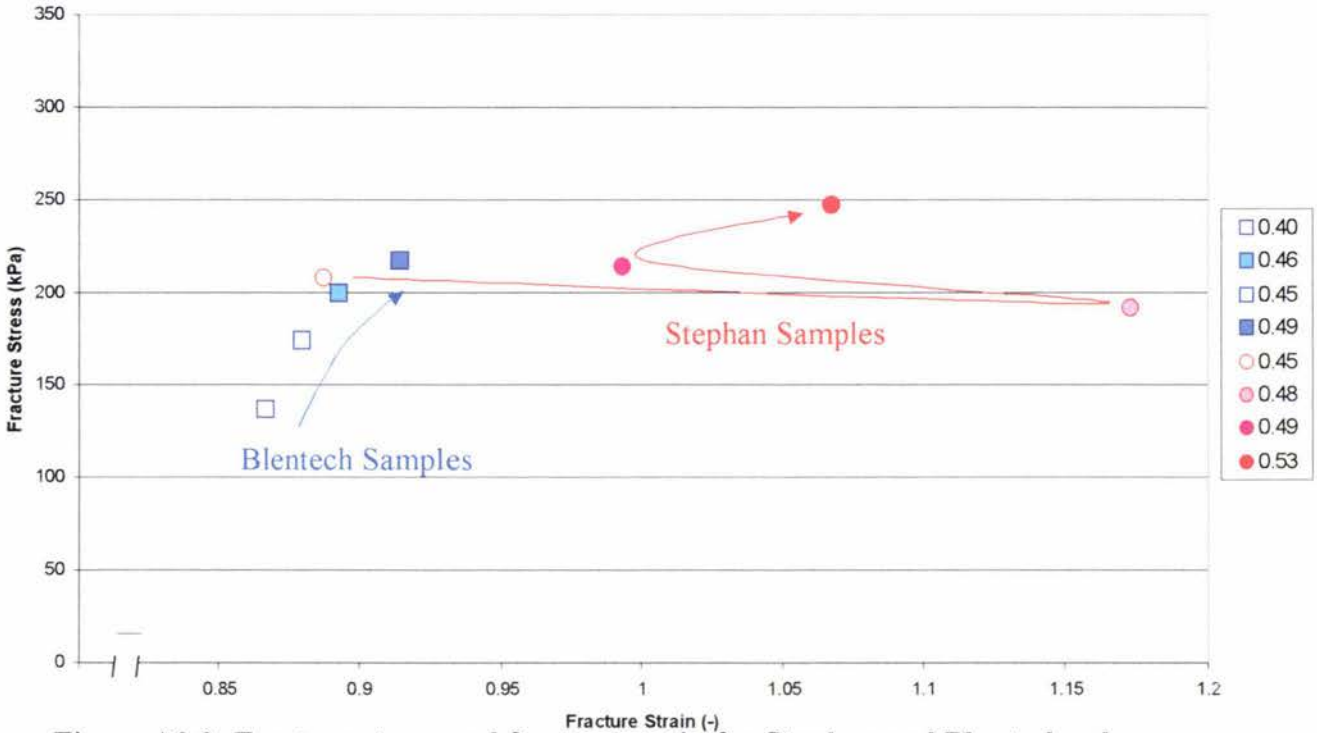

Figure A2.3: Fracture stress and fracture strain for Stephan and Blentech gels.

The duplicates (P/W 0.45 samples) were close in terms of P/W ratio but there were large differences with respect to fracture properties. There were large changes for the Stephan samples, which may have been due to the difference in processing times as a result of poor process control. The Stephan gave products with a wide variation in fracture strain and a relatively low variation in fracture stress, while the Blentech gave opposite results.

Table 17: P/W variation in samples.

Equipment	Target P/W ratio	Variation from Target	Actual P/W ratio	Probable causes
Blentech	0.40	0.1	0.40	Variability in steam supply or evaporation
	0.45	-0.4	0.46	
	0.45	-0.2	0.45	
	0.50	0.4	0.49	
Stephan	0.40	-1.3	0.45	Evaporation
	0.45	-0.9	0.48	
	0.45	-0.7	0.49	
	0.50	-0.7	0.53	

Microstructure

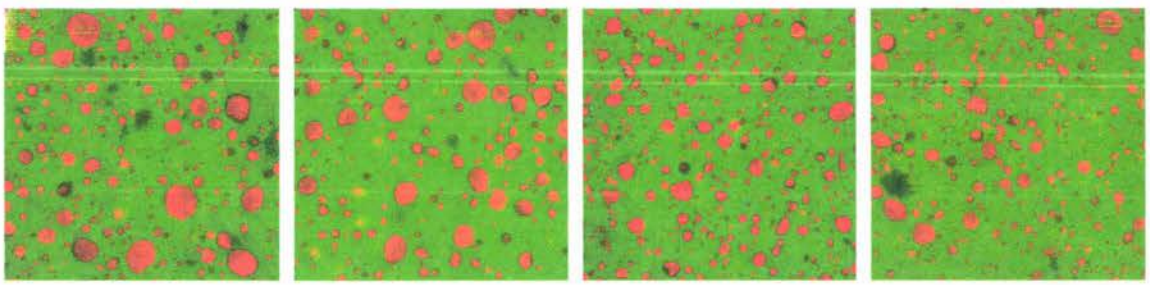

P/W 0.40 P/W 0.46 P/W 0.45 P/W 0.49

Figure A2.4: Blentech samples.

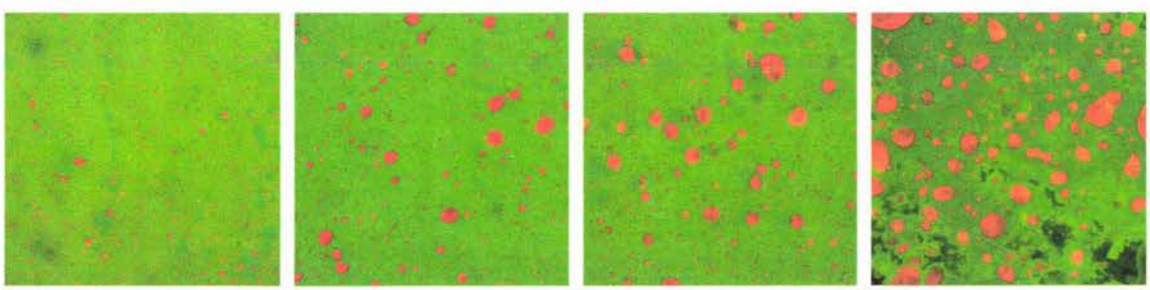

P/W 0.45 P/W 0.48 P/W 0.49 P/W 0.53

Figure A2.5: Stephan samples.

Manufacturing Problems

The Stephan had difficulty making the high P/W ratio samples and it was difficult to remove the product from the equipment when the samples became viscous. The Blentech made the high P/W ratio samples easily and the product was easy to discharge from the equipment.

APPENDIX 3.0 TA-XT2 AND INSTRON COMPARISON

Summary

The distinct differences between the Instron and TA-XT2 do not allow comparison of past work carried out by FTRC with the work done in this study. It is proposed that the differences are a result of systematic errors involved in using two different pieces of equipment for testing and the effect of different compression levels combined with the lesser effects of temperature and sample dimensions.

Texture profile analysis (TPA) results are imitative of the mastication process that takes place in the mouth and are appropriate for the work done in the past by FTRC, which was predominantly product development work. The fundamental method of fracture property analysis was found to be a more suitable textural analysis method for research work.

Introduction

Initial exploratory investigations into possible large-strain rheology testing equipment were conducted. Two methods were investigated initially: the standard New Zealand Dairy Research Institute (NZDRI) (Munro *et al.*, 2000) method utilising the TA-XT2 Texture Analyser and the Food Technology Research Centre (FTRC, Massey University) method utilising the Instron Universal Testing Machine (Saunders *et al.*, 1996c). These two methods use different sample dimensions, compression levels and testing conditions but the extent to which the results from the two methods were different was not known. These two methods were compared to determine whether future work could be compared with composite gel work already carried out by the FTRC for the New Zealand Dairy Board.

Materials and Methods

One gel formulation and manufacturing method were used in these comparisons for consistency. The formulation was adapted from an FTRC pilot-plant scale Stephan cheese kettle formulation (Saunders *et al.*, 1995).

The ingredients used were Rennet Casein (Alaren 799 edible Rennet Casein 90 mesh) - New Zealand Dairy Board (NZDB), (Wellington, New Zealand), fresh frozen milk fat for recombining (FFMR) - New Zealand Dairy Board (NZDB), (Wellington, New Zealand),

sodium chloride (food grade) - Dominion Salt Ltd. (Blenheim, New Zealand), sodium citrate, disodium hydrogenphosphate (food grade) - Interchem Agencies (Auckland, New Zealand), and potassium sorbate.

The protein, potassium sorbate, citric acid, disodium phosphate, salt and water were placed in the Stephan cheese kettle bowl at ambient temperature and mixed for 1 minute at 2100 rpm. The anhydrous milk fat was added and the mixture was heated indirectly to 72°C using a waterbath set at 80°C.

The processing time from fat addition to final temperature was 7 minutes ± 30 seconds. The samples were then poured into 500 g containers and allowed to cool at ambient for 15 minutes before being stored at 5 ± 1°C. Three replicates were made and stored for 3 days and all the samples were tested on the same day using the different methods.

All the methods involved double compression of the samples.

Table 18: Formulation for texture analysis method comparison.

Ingredient	Amount (g)
Rennet casein	389.0
Anhydrous Milkfat (AMF)	320.0
Water	825.4
Salt	16.0
Citric Acid	16.0
Potassium Sorbate	1.6
Disodium Phosphate (DSP)	32.0
Total Mass	1600.0

TA-XT2 Texture Analyser Method

Six cylindrical samples were cut using a 20 mm diameter cork borer mounted on a drill press and sliced to a length of 25 mm using a wire cutter and template. The samples were wrapped in polyethylene film, placed in airtight containers and held at 5°C overnight. The samples were compressed to 80% of their original height using a TA-XT2 Texture Analyser with a load cell of 250 N. The circular diameter upper and rectangular lower plates were made of Teflon and lubricated with heavy paraffin oil. Samples were tested at 5 ± 1 °C with a crosshead speed of 0.83 mm s^{-1}. This method is that used in previous MPCG research by

(Saunders *et al.*, 1996a; Saunders *et al.*, 1996b; Saunders *et al.*, 1996c; Saunders *et al.*, 1997; Sharma *et al.*, 1997a; Sharma *et al.*, 1997b).

Instron Universal Testing Machine Method

Six cylindrical samples were cut using a 22 mm diameter hand-held cork borer and sliced to 30 mm length using a wire cutter. The cut samples were wrapped in polyethylene film, placed in airtight containers and stored in a fridge at 5°C. The samples were removed from the fridge immediately prior to testing in a 20°C room. The top plate was made from high-density polyethylene and the square base plate was made from stainless steel, both were greased using vegetable oil (canola oil). The samples were compressed twice to 75% using a universal testing machine with a cross-head speed of 0.83 mm s^{-1} and 100 or 1000 N load cells, depending on sample properties.

Mixed Method

This method was the same as the NZDRI method with the exception that the sample dimensions and compression level was the same as the Instron method described above.

Data Analysis

Two methods of analysis were used to compare the TA-XT2 method with the Instron method as the FTRC used TPA in previous work while the NZDRI standard method calculates fracture properties.

Texture Profile Analysis (TPA)

For the investigation of compression methods, the following standard TPA parameters were obtained:

- hardness (the peak force during the first compression cycle),
- cohesiveness (the ratio of the positive force area during the second compression to that in the first),
- adhesiveness (the negative force area for the first bite), and
- springiness (the height that the sample recovers between the first and second bites).

The force time data were extracted using XTRAD (Stable Micro Systems, Halsemere, UK) and processed using Microsoft Excel to obtain the TPA parameters. Other parameters extracted included failure stress and displacement (when they occurred). The point of failure was seen as a distinct peak, at a compression of less than the maximum. The gradient from time zero to the failure point was recorded.

Fracture Properties Analysis

Force–distance data from the compression were extracted using XTRAD (Stable Micro Systems). The force-distance data from the start (time = 0) to the maximum of the first compression was imported into software (Master Work Software, Tawa, New Zealand) written in J, a functional programming language (Iverson Software Inc, Toronto, Canada) as a text file. The sample diameter and the distance the sample was compressed were entered manually. The sample diameter used in calculations was the average of two measurements taken using a Digimatic micrometer (Mituoyo Corporation, Tokyo, Japan) prior to the beginning of the test and the distance compressed was extracted using XTRAD software.

The Master Work software was used to calculate the fracture stress (Pa), fracture strain and modulus of deformability (Pa). It uses the assumption of constant volume during compression to properly standardise the measurements for force (stress), distance (strain) and stiffness (maximum stress/strain). This method follows similar guidelines as those outlined in Zoon (1991) where fracture stress indicates firmness (force required to crack the sample), fracture strain indicates longness (resistance to crumbling) and modulus indicates stiffness (force required to dent the sample surface).

The XTRAD software also calculated the negative area under the force-time graph following the first compression and when multiplied by the compression speed (0.83 mm s^{-1}) in Microsoft Excel 97 resulted in the Adhesion Area (mJ). This is a measure of work done to lift the plate off the sample surface.

The data were compared in Microsoft Excel 97 on texture plots by graphing fracture stress against fracture strain and modulus of deformability (stiffness) against adhesion area (adhesiveness).

Statistical Analysis

The TPA parameters and fracture properties were analysed using the one-way ANOVA function in the statistical software package Minitab (Version 12.21, Minitab Inc.). A one-way analysis of variance (ANOVA) tests the hypothesis that the means of several populations are equal and assumes that the population variances are equal. The null hypothesis is that the population means are the same, the alternative hypothesis is that one or more population means differ from the others.

Results and Discussion

Texture Profile Analysis (TPA)

The FTRC used texture profile analysis in their composite gel research and as much of the data produced are inaccessible, the reports written for the New Zealand Dairy Board (using TPA parameters) provide the only database for the work.

It must be noted that the different sample dimensions, compression levels and testing conditions will have an impact on the results, the purpose of this investigation was to determine to what extent the results were affected and if the results are in some way comparable between test methods.

Table 19: Hardness values at full compression.

Method	Mean Hardness (N) (Compression Level)	Cohesiveness	Adhesiveness (mJ)	Springiness
TA-XT2	(80%) 84.1[a] (75%) 63.7[a]	0.147[a]	3.34[a]	0.263[a]
Instron	(75%) 83.5[a b]	0.128[b]	2.20[b]	0.195[b]
Mixed	(75%) 64.6[b a]	0.141[a]	2.49[b]	0.306[a]

Groups with a superscript in common are not significantly different ($\alpha = 0.05$).

The TPA measurements for hardness at maximum compression, which are given in Table 19 in black font, show that the TA-XT2 and Instron methods appear to be similar while the mixed method gives lower results. The TA-XT2 method was expected to give higher results because the hardness increases as the level of compression increases.

The hardness results for the TA-XT2 samples were adjusted to 75% compression and compared again to the other two methods as shown in Table 19 in red font. The mixed

method produced significantly lower results (20 N) than the Instron method despite the test being carried out at a lower temperature. The samples were tested in a 20°C room and should, in theory, be softer than the samples tested at 5°C. The sample dimensions were the same for the mixed method but the tests were carried out on the TA-XT2 as opposed to the Instron. It is proposed that the observed difference is due to systematic errors involved with using a different instrument.

The TA-XT2 sample had a significantly higher adhesiveness. It is thought that this is due to more surface area contacting the plate as a result of a higher level of compression increasing the radius beyond the radius of the compressed Instron and mixed method samples.

The Instron method had significantly lower cohesiveness and springiness results than the TA-XT2 method which was thought to be due to the combination of a lower compression level and the sample being softer (~10°C) and hence more deformable.

Future work, using TPA, will not be able to be compared to past work carried out by FTRC for the New Zealand Dairy Board because the different compression levels, temperatures and sample dimensions affect the results to a high degree.

Fracture Analysis

Table 20: Fracture properties for compression method comparison.

Method	Mean Strain (-)	Mean Stress (kPa)	Mean Adhesiveness (mJ)	Mean Modulus (kPa)
TA-XT2	0.522^{a}	92.5^{a}	3.4^{a}	455.3^{a}
Instron	0.461^{b}	76.0^{b}	2.2^{b}	353.8^{b}
Mixed	0.517^{a}	86.5^{c}	2.4^{b}	410.1^{c}

Groups with a superscript in common are not significantly different ($\alpha = 0.05$).

The results of this analysis are given in Table 20. The TA-XT2 sample was adjusted to 75% compression to allow a better comparison between methods. The fracture strain for the Instron method was significantly lower than the TA-XT2 and mixed methods, indicating that equipment may have a large impact on strain. In principle, if a well-defined fundamental rheological property is measured by different methods, the result is independent of the method used, providing the time scale is the same (van Vliet *et al.*, 1991). The stress was significantly lower for the Instron method than the other methods due to the combined effects of a higher temperature and a larger height to diameter ratio. Again, instrumentation may

have a large, unquantified impact on the results. The mixed method fracture stress was lower than the TA-XT2 method fracture stress, although not significantly lower and may be attributed to the higher height to diameter ratio. The TA-XT2 samples had a higher adhesiveness and the modulus followed the same trend as fracture stress and fracture strain.

Future results, using fracture property analysis, cannot be compared to past work done by FTRC because the instrumentation gives significantly different results in addition to the fact that the raw data for the FTRC work would be required.

APPENDIX 4.0 TA-XT2 AND TA-HD COMPARISON

In prior work (Appendix 3.0), samples of high P/W ratios overloaded the TA-XT2. As a result, those samples were analysed using a third method utilising the TA-HD Texture Analyser. It was assumed at NZDRI that the two methods gave the same results (Watkinson, P., 2002, personal communication) but this assumption had not been tested.

Summary

The TA-XT2 and TA-HD exhibited significantly different results and it was concluded that future work should be carried out only on the TA-HD to avoid overloading the equipment.

Materials and Methods

A TA-XT2 Texture Analyser (Stable Micro Systems, Surrey, England) using a 250 N load cell with a cross-head speed of 0.83 mm s^{-1} was compared to a TA-HD Texture Analyser (Stable Micro Systems, Surrey, England) using a 500 N load cell with a cross-head speed of 0.8 mm sec^{-1}. The comparison with the TA-HD used the standard NZDRI method of fracture property analysis as described in Appendix 3.0. The samples were tested at 5°C.

The ingredients used were Rennet Casein (Alaren 799 edible Rennet Casein 90 mesh) - New Zealand Dairy Board (NZDB), (Wellington, New Zealand), fresh frozen milk fat for recombining (FFMR) - New Zealand Dairy Board (NZDB), (Wellington, New Zealand), sodium chloride (food grade) - Dominion Salt Ltd. (Blenheim, New Zealand), sodium citrate, disodium hydrogenphosphate (food grade) - Interchem Agencies (Auckland, New Zealand), and potassium sorbate.

One gel formulation was used in this investigation as described in earlier work (Appendix 3.0). Three replicates were made by mixing the protein, potassium sorbate, citric acid, DSP, salt and water for 1 minute at 2100 rpm before adding the AMF and heating to 83°C using a waterbath set at 85°C. The processing times were varied by altering the initial temperature of the Stephan bowl and the water being added.

Results and Discussion

Table 21 shows that the TA-XT2 and TA-HD are significantly different except with respect to adhesiveness. The TA-XT2 produced a lower fracture strain and a higher fracture stress and

modulus. The samples demonstrated little adhesiveness and as a result, may not be representative of any differences between the two methods.

Table 21: Fracture properties for TA-XT2 and TA-HD.

Method	Stress (kPa)	Strain (-)	Adhesiveness (mJ)	Modulus (kPa)
TA-XT2	329^{a}	0.71^{a}	0.39^{a}	901^{a}
TA-HD	273^{b}	0.87^{b}	0.26^{a}	724^{b}

Groups with a superscript in common are not significantly different ($\alpha = 0.05$).

It has been incorrectly assumed in the past that the TA-XT2 and TA-HD produced the same results (Watkinson, P., 2002, personal communication). To facilitate analysis of future results, one of the two machines must be used exclusively. As the samples being used in this experimental work may overload the TA-XT2, it was decided that the TA-HD should be used exclusively for future work.

APPENDIX 5.0 PROCESSING REGIME INVESTIGATION

Summary

There appeared to be some changes in fracture properties with increasing processing time. The trends were different for Rennet Casein and MPC 85 and it was proposed that these be explored further in the main body of the work. It was decided as a result to take samples at 0-, 4-, 8- and 16-minutes processing times.

Introduction

Klostermeyer and Buchheim (1988) reported that 4 minutes processing was insufficient to obtain optimal structure formation, which took a further 5 minutes. Pereira (2000) found that processing beyond 8 minutes produced a viscous mixture that was hard to pour while processing for times less than 8 minutes resulted in insufficient protein hydration and fat emulsification. As the protein source may behave differently, it was important to decide which processing times were suitable for further investigation. Initial exploratory investigations into possible sampling times was conducted.

Methods and Materials

Two protein sources, MPC 85 and Rennet Casein, were formulated to obtain a P/W ratio of 0.4. The fat, salt and disodium phosphate levels were kept constant on a protein basis while the lactic acid was adjusted to achieve the desired pH of 5.7. A 3-minute pre-mixing stage was included to allow sufficient time for protein hydration prior to cooking. The emulsifying salts were included in the pre-mixing stage to decrease the amount of calcium phosphate cross-linking, which inhibits the emulsifying ability of the proteins.

Table 22: Processing formulations.

Ingredient	Rennet Casein Amount (g)	MPC 85 Amount (g)
Protein source	4667.6	4534.7
Water	8818.2	9045.1
AMF	3795.4	3723.9
DSP	264.0	215.9
Salt	301.7	300.4
Lactic Acid	153.0	180.0

The amount of water expected to be added via direct steam injection was estimated at 9% of the total mass.

The water and salt, DSP and acid were placed in the pilot plant scale Blentech and mixed at a speed of 56 rpm. The protein source was added over a period of 2 minute, after which the solid fat was added and the speed increased to 127 rpm for 3 minutes. The speed was then increased to 155 rpm and heating started via direct steam injection until product temperature of 85°C was achieved. The heating curve was kept constant for all MPCGs by controlling the initial temperature of the cooker and raw ingredients and by controlling the steam pressure used for direct steam injection. The maximum temperature of 85°C was reached in 6.0 ± 0.5 minutes. The MPCGs were processed at 85°C for 0, 2, 4, 6, 8, 10, 14, 18 and 20 minutes at a mixing speed of 155 rpm while the maximum temperature was maintained via indirect steam.

Results and Discussion

The moisture contents of the samples were lower than expected due to less water entering the product via steam than calculated. However, the results were similar: 44.4% for Rennet Casein and 44.6% for MPC 85.

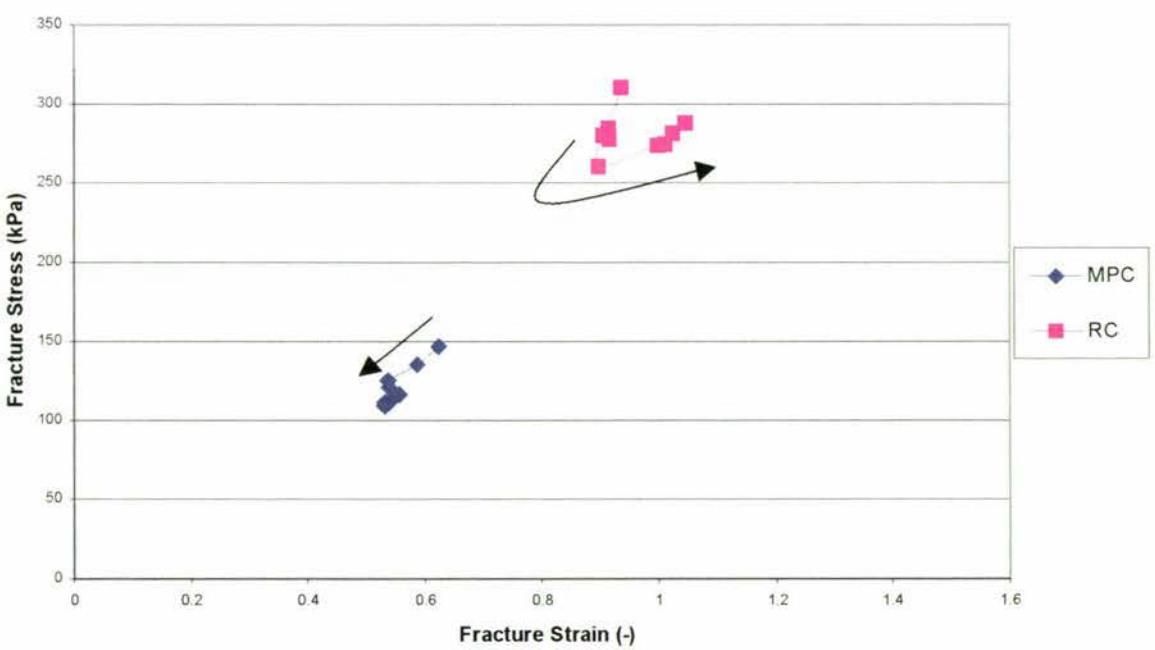

Figure A5.1: Fracture properties of Rennet Casein and MPC samples.

The fracture properties were determined using the method outlined in Section 3.3.1.2 and are represented in Figure A5.. The arrows indicate the trend with increasing processing time.

The two protein sources behave differently and show distinctly different fracture properties. The Rennet Casein samples do not appear to change much between 14- and 20-minutes processing time, while the MPC 85 samples appear to change little from 4-minutes onwards.

After discussion, it was decided that the processing times to be investigated were 0-, 4-, 8, and 16 minutes.

APPENDIX 6.0 ADDITIONAL EXPLORATORY WORK

Exploratory work was carried out to determine whether an alternative addition method of MPCG manufacture used at NZDRI was as good as or better than that outlined in Appendix 5.0. The method was identical to the method outlined in Appendix 5.0 except that the order of addition of ingredients was altered. The fat, emulsifying salts, acid and the protein source were placed in the Blentech and mixed at a speed of 56 rpm for 2 minutes. The water was then added and the speed increased to 127 rpm for 3 minutes. This method was found to produce a number of undissolved protein lumps and was not used in further work.

Other exploratory work was carried out to determine repeatability of the methods developed. Small-scale trials on the laboratory-scale Blentech were abandoned due to insufficient process control. Direct steam injection gave variable moisture results due to poor steam quality. Indirect heating by running steam through the vessel jacket resulted in protein gelling on the surface of the jacket, which limited heat transfer. Not only did this result in the inability to maintain the desired temperature profile, it also removed protein from the gel and caused browning. In addition to this, the layer of burnt-on whey protein was difficult to remove during cleaning of the vessel. It was decided that the pilot plant scale Blentech (model # CC45) would be better suited for future experimental work as repeatable results could be obtained using direct steam injection (Buwalda, R., 2001, personal communication).

NOMENCLATURE

ℓ	Length (mm)
$\delta\ell$	Change in length (mm)
ε	Strain (-)
σ	Stress (Pa)
γ	Shear strain (-)
τ	Shear stress (Pa)
H	Sample height at any time (mm)
H_o	Initial sample height (mm)
Δh_t	Displacement of crosshead at time *t* (mm)
v	Speed of compression (mm s^{-1})
F_t	Force during lubricated compression at time *t* (N)
r_o	Initial radius of sample (m)
σ_{max}	Maximum stress (Pa)
σ_∞	Infinite stress (Pa)
$\dot{\varepsilon}_o$	Initial strain rate (s^{-1})
ε_{max}	Maximum strain (-)
ε_c	Cauchy strain (-)
ε_H	Hencky strain (-)
σ_o	Maximum stress (Pa)
γ_o	Maximum strain (-)
$\sigma_{el.}$	Elastic material reaction stress (Pa)
$\sigma_{v.}$	Viscous material reaction stress (Pa)
$\dot{\gamma}$	Strain rate/Shear rate (s^{-1})
G'	Storage modulus (Pa)
G"	Loss modulus (Pa)
G*	Complex modulus (Pa)
G^*_{min}	Minimum complex modulus (Pa)
δ	Phase angle (°)
tan δ	Loss tangent
ω	Oscillation frequency (Hz)
η^*	Apparent viscosity

ABBREVIATIONS

AMF	Anhydrous milk fat
Ca	Calcium
C/P ratio	Calcium to protein ratio
CSA	Calcium sequestering agent
DSP	Disodium phosphate
EMC	Enzyme modified cheese
FRC	Fonterra Research Centre Limited
FTRC	Food Technology Research Centre
HPLC	High-performance liquid chromatography
IX MPC	Ion-exchanged MPC (calcium depleted)
MPC	Milk protein concentrate
MPCG	Milk protein composite gel
Na	Sodium
NaCl	Sodium chloride
NCN	Non-casein nitrogen
NPN	Non-protein nitrogen
NZDRI	New Zealand Dairy Research Institute
P/W ratio	Protein to water ratio
SALP	Sodium aluminium phosphate
SMC	Skim milk cheese
SMP	Skim milk powder
TEM	Transmission electron microscopy
TMP	Total milk protein
TN	Total nitrogen
TPA	Texture profile analysis
TSC	Trisodium citrate
TSP	Trisodium phosphate
WPC	Whey protein concentrate
WPI	Whey protein isolate